Old Dominion University

ODU Digital Commons

Summer 2015

Study of Photochemical Formation of Hydroxyl Radical in Natural Waters

Luni Sun
Old Dominion University, lsunx001@odu.edu

Follow this and additional works at: https://digitalcommons.odu.edu/chemistry_etds

Part of the Chemistry Commons

STUDY OF PHOTOCHEMICAL FORMATION OF HYDROXYL

RADICAL IN NATURAL WATERS

by

Luni Sun
B.S. Marine Chemistry, July 2006, Ocean University of China, China
M.S. Marine Chemistry, July 2009, Ocean University of China, China

A Dissertation Submitted to the Faculty of
Old Dominion University in Partial Fulfillment of the
Requirements for the Degree of

DOCTOR OF PHILOSOPHY

CHEMISTRY

OLD DOMINION UNIVERSITY
August 2015

Approved by:

_____
Kenneth Mopper (Director)

_____
Neil V. Blough (Member)

_____
Patrick G. Hatcher (Member)

_____
David J. Burdige (Member)

ABSTRACT

STUDY OF PHOTOCHEMICAL FORMATION OF HYDROXYL RADICAL IN
NATURAL WATERS

Luni Sun
Old Dominion University, 2015
Director: Dr. Kenneth Mopper

This dissertation mainly focuses on the sources of the hydroxyl radical ($\bullet$OH) from photochemical reactions in natural waters, in particular from reactions involving dissolved organic matter (DOM). Firstly, an accurate method for estimating $\bullet$OH formation rate during long-term irradiation was developed. It was observed that previous methods for measuring $\bullet$OH formation rates in the natural waters, which were based upon sequentially determined cumulative concentrations of probe photoproducts, significantly underestimated actual $\bullet$OH formation rates. It was found that the underestimation was mainly due to the degradation of the probe photoproducts and that only 'instantaneous' formation rates were appropriate for accurately estimating $\bullet$OH photochemical formation rates. 'Instantaneous' $\bullet$OH formation rates were obtained by adding probes to a sub-sample at each time point during the long-term irradiation and irradiating the sub-sample for a short time. By employing this approach, $\bullet$OH formation rates were measured during a photoflocculation study in natural waters. In addition to $\bullet$OH formation, hydrogen peroxide concentration, dissolved organic carbon, total dissolved nitrogen, water optical properties, and iron speciation were measured. The results showed that in iron- and DOM-rich water samples $\bullet$OH appears to be mainly produced from the Fenton reaction initially, but subsequently from other sources, in particular DOM photoreactions. In order to elucidate possible photoreaction sites and mechanisms of $\bullet$OH photoformation

from DOM, phenolic compounds were used as model DOM chromophores. •OH quantum yields (Φs) at 280~340 nm were measured by •OH trapping reaction with benzene. It was found that many phenolic acids are capable of producing •OH, especially those with para hydroxyl and carboxyl groups (especially 2,4-dihydroxybenzoate and 4-hydrodroxybenzoate), which have markedly high •OH Φs. By conducting methane trapping and competition kinetics experiments, it was confirmed that free •OH was produced from these compounds. The results suggest that hydroxybenzoic acid moieties within DOM play an important role in the photoproduction of •OH. Finally, it was hypothesized that a quinoid enol tautomer present as a water cluster was responsible for •OH production from phenolic compounds with para hydroxyl and carboxyl groups.

Phenolic acids with para hydroxyl and carbonyl groups are common components of lignin, which is a major source of DOM in freshwaters. In order to examine the lignin phenolic composition of natural samples, a simplified method using alkaline copper oxide oxidation coupled with solid-phase extraction and high performance liquid chromatography (HPLC) was developed. In this study, an interlaboratory comparison of the simplified HPLC approach with the conventional, but much more complex and expensive, high pressure reaction vessel GC-MS method was also conducted. The agreement between the two different methods was generally very good. A major benefit of this simplified HPLC method is that it allows any investigator with standard HPLC equipment to analyze lignin components, whereas previously only a small number of specialized labs were able to perform these analyses.

This dissertation is dedicated to all who encouraged, supported and helped me, especially my family members and friends.

ACKNOWLEDGMENTS

I would like to thank my advisor Dr. Kenneth Mopper for the guidance, education, encouragement, and support through my six years of graduate career. His scientific knowledge and his guidance on scientific writing are appreciated and have greatly improved my skills. I also thank the members of my committee, Dr. Patrick Hatcher, Dr. Neil Blough, and Dr. David Burdige for their advice and time in my dissertation research. In addition, Dr. Patrick Hatcher and his group helped me by making their facilities, including HPLC, available. Dr. Blough gave me lots of critical scientific advice which improved my knowledge and my results.

I would like to thank Dr. Elizabeth Minor for the support of my research and her guidance during a research cruise. I thank Dr. Bala Ramjee for his advice on hydroxyl radical formation mechanisms. I would like to thank Dr. Hongmei Chen and Dr. Hussain Abdulla for their help in the sample collection, experiment setup, and discussions of the results. I also thank my former group member Dr. John Helms for his training in the lab and for discussions of results. I thank Xiaoyan Cao for her help on my writing skills. I would like to thank the faculty and staff of the Department of Chemistry and Biochemistry and Department of Ocean Earth and Atmospheric Science for providing facilities and resources. I especially thank Alicia Herr and Tammy Subotich, who have helped me with the lab organization and my teaching assistance experience.

I would also thank Dr. Mopper's family. Their friendship and help have made my life in this country much easier and enjoyable. I also thank Dr. Hatcher's group, who not

only helped me with my research, but also invites me to their activities and holiday parties.

Finally, I would like to thank my family, especially my husband Haibo Ma in China for their unconditional support. I also thank all my friends for their help through my life.

TABLE OF CONTENTS

Page

LIST OF TABLES

LIST OF FIGURES

CHAPTER I

INTRODUCTION

Reactive transient species, such as hydrogen peroxide (H_2O_2), singlet oxygen, superoxide ion (O_2^-), excited state dissolved organic matter (DOM) and hydroxyl radical (•OH), play important roles in photochemical processes in natural waters (Zhou and Mopper, 1990). The •OH is one of the most reactive species and can take a part in many reactions (Buxton et al., 1988; Vaughan and Blough, 1998). Its steady-state concentrations are low in most waters, and vary greatly depending on the sources. The reported steady-state concentration values are from $(2.6 - 4.3) \times 10^{-19}$ M in the Antarctic waters (Qian et al., 2001) to $(3.0-8.5) \times 10^{-16}$ M in rivers (Arakaki and Faust, 1998; Brezonik and Fulkerson-Brekken, 1998).

Photochemical reactions are the major source of •OH in natural waters. The photo-formation of •OH depends on its major sources in sunlit waters, which include nitrate and nitrite photolysis, the photo-Fenton reaction, and DOM photoreactions (Mostofa et al., 2013). Nitrite (NO_2^-)/nitrate (NO_3^-) photolysis involves the formation of O^- (eqs 1, 2, 3) (Mack and Bolton, 1999; Vanghan and Blough, 1998):

$$NO_3^- + h\nu \rightarrow NO_2^- + O^- \tag{1}$$

$$NO_2^- + h\nu \rightarrow NO + O^- \tag{2}$$

$$O^- + H_2O \rightarrow \bullet OH + OH^- \tag{3}$$

Nitrate contributes 1~89 % and 7~75 % •OH production in rivers and seawaters, respectively; while nitrite contributes 2~70 % and 1~8 % in rivers and seawaters (Hoigné et al., 1988; Mostofa et al., 2013).

This dissertation is formatted based on the journal *Marine Chemistry*

The photo-Fenton reaction is predominant in iron-rich freshwaters and estuaries, and can account for more than 70% of total photochemical •OH production (Southworth and Voelker, 2003; White et al., 2003; White, 2000). The photo-Fenton reaction involves the oxidation of Fe(II) by H_2O_2 to form Fe(III) and •OH (eq 4). Long-term irradiation of natural waters results in the recycling of Fe(III) to Fe(II), probably through ligand to metal charge transfer (LMCT) reactions with DOM (eq 5) which produce carboxylic acid radicals that can be subsequently decarboxylated (Scott et al., 1998; Barbeau, 2006; Klapper et al., 2002), and through the reduction by HO_2/O_2^- (eq 6) (Voelker et al., 1997):

$$Fe(II) + H_2O_2 \rightarrow Fe(III) + •OH + OH^- \tag{4}$$

$$Fe(III)L \rightarrow Fe(II) + photoproducts \tag{5}$$

$$Fe(III) + HO_2/O_2^- \rightarrow Fe(II) + O_2 \tag{6}$$
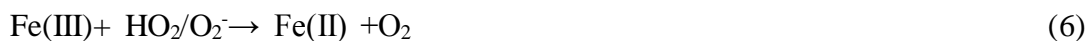
Where Fe(II) and Fe(III) include all inorganic and organic-complexed iron species, and L is the DOM ligand. Both inorganic and organically-complexed Fe(II) are able to participate in the Fenton reaction. In humic substance-rich natural waters, the organically-complexed iron can be formed between iron and phenolic and carboxyl groups (Baruah et al., 1981). Although organically-complexed Fe(II) is less reactive with H_2O_2 than inorganic Fe(II) under circum-neutral conditions (Miller et al., 2012), it is important because •OH may not be produced from the oxidation of inorganic Fe(II) under these conditions (Miller et al., 2012), and the inorganic Fe(II) concentration is a small percentage of total Fe (Emmenegger et al., 2001; Shiller et al., 2006). •OH may also be formed through Fenton-like chemistry involving H_2O_2 and DOM reductants, though the identity of these reductants is unknown (Sharpless and Blough, 2014).

DOM photoreactions are an important source for •OH production in many natural waters. The •OH production sites have been speculated to be quinone moieties within humic substances (Page et al., 2011; Vaughan and Blough, 1998), based on the fact that quinone model compounds are involved in the •OH probe trapping reactions (Alegría et al., 1999; Ononye and Bolton, 1986; Pochon et al., 2002). However, several studies have questioned the importance of quinones in the production of •OH. Firstly, quinone concentrations within DOM are too low in most instances (Sharpless and Blough, 2014; Aeschbacher et al., 2009). Secondly but most importantly, there is strong evidence against the production of free •OH by benzoquinone; instead, existing evidence supports the formation of a reactive oxidizing intermediate, that is responsible for the observed •OH trapping reactions (Clark and Stonehill, 1972; Phillips et al., 1986; Pochon et al., 2002; Gan et al., 2008). Thus, the sources and mechanisms of the •OH from DOM are essentially unknown (Sharpless and Blough, 2014).

Due to its high reactivity, •OH is difficult to measure directly; therefore it is usually quantified either through the loss of a probe or the accumulation of a photoproduct of a probe. The •OH methods include simultaneously and non-simultaneously methods. The simultaneous methods involve the use of diamagnetic compounds, e.g. nitrone or nitroso compound to trap •OH to form stable paramagnetic aminoxyl radicals, which are then detected by electron paramagnetic resonance (EPR) techniques (Burns et al., 2012). In the non-simultaneous methods, there are two broad categories of the probe reactions: 1) •OH addition to probes, with •OH either being added to the carbon atoms in probes such as 4-nitrophenol, nitrobenzene, benzene, benzoic acid, and terephthalate, or being added to the sulfoxide group in probes, e.g. dimethyl-sulfoxide; and 2) abstraction of a

hydrogen atom from the probes such as methanol, formic acid, methane and butyl chloride (Anastasio and McGregor, 2001; Page et al., 2010; Page et al., 2011). In the quantification of •OH through the accumulation of a photoproduct, the probe is added to the sample and the cumulative concentration of the photoproduct is measured after a period of irradiation (al Housari et al., 2010; Mostofa et al., 2013; Nakatani et al., 2007; Zhou and Mopper, 1990). •OH formation rate is then calculated from the cumulative concentration over time.

However, quantification of •OH using some of these probes has two main issues. Firstly, though the product compounds are non- or very weak absorbers of light in the solar irradiance spectrum and thus do not undergo direct photoreaction, they may undergo indirect phototransformation/destruction in the presence of DOM in natural waters. Possible mechanisms include electron or hydrogen atom transfer from reactive excited triplet states of DOM (Canonica et al., 1995; Golanoski et al., 2012), or reaction with reactive oxygen species, such as H_2O_2 (Beltran-Heredia et al., 2001), •OH (Esplugas et al., 2002), and singlet oxygen (Wilkinson et al., 1995). Thus, the cumulative concentrations of photoproducts from the probes (and thus the corresponding •OH photoproduction) can be underestimated if their phototransformation/destruction during long-term irradiations is not taken into account. Since the degradation of the products usually follows pseudo-first order kinetics (Beltran-Heredia et al., 2001; Esplugas et al., 2002), this underestimation is minor when the product concentration is small, e.g., when only initial •OH formation rates are taken into account (al Housari et al., 2010). However, the underestimation may become significant when the concentration is high, when time-course studies of •OH formation rates and steady-state concentrations are required. In this

situation, it usually takes several hours to adequately measure •OH generation (Mostofa et al., 2013; Nakatani et al., 2007; White et al., 2003).

The second issue of •OH quantification arises from the probes themselves, which are not necessarily specific for free •OH, but are also capable of detecting other lower-energy oxidizing species. For example, quinones, which have been speculated to be responsible for •OH production (Page et al., 2012; Gómez-Toribio et al., 2009), have been shown to produce a reactive oxidizing intermediate. This species exhibits reactivity about one order of magnitude lower than free •OH (Pochon et al., 2002), but takes part in some probe trapping reactions (Clark and Stonehill, 1972; Phillips et al., 1986; Pochon et al., 2002; Gan et al., 2008). Vione et al. (2010) showed that the transformation of the probe nitrobenzene or generation of 4-hydroxybenzoic acid from benzoic acid is not selective for free •OH. Therefore, the observed "•OH" measured by some probes usually include both free •OH and reactive oxidizing species. Page et al. (2011) conducted a methane quenching experiment (which is specific for free •OH), and measured the hydroxylbenzoic acid ratio, which involves a comparison of the ratios of the ortho, meta, and para products generated from hydroxylation of benzoic acid. They found the results were not always consistent with free •OH in a set of five DOM isolates.

To address the first issue of underestimation of •OH formation rate during long-term irradiation, it is necessary to establish the stability of both the •OH probe compounds and the quantified product species with respect to direct and indirect photolysis in natural waters (Burns et al., 2012). We estimated the time-course •OH formation rates using two approaches: 1) correcting for product loss, and 2) obtaining near-instantaneous formation rates. The corrected formation rates were obtained by

adding the photodegradation rates of corresponding photoproducts back to their formation rates, and the instantaneous rates were obtained by measuring the photoproducts formation rates for a short irradiation time ($\leq$ 2h). These approaches have been tested in DOM-rich freshwater (Great Dismal Swamp) and DOM-poor estuarine water. The results are shown and discussed in Chapter II.

Using the near-instantaneous approach for measuring •OH formation rates, the source of •OH was studied during photoflocculation of DOM. Photoflocculation may be important in transformation and transportation of DOM and particulate organic matter (POM) in DOM-rich freshwater, estuarine and ocean margin environments (Chen et al., 2014; Helms et al., 2013). The time-course •OH formation rates were estimated in humic-rich Dismal Swamp and wood extracted samples. Total Fe and H_2O_2 concentrations were measured to study the importance of the photo-Fenton reaction, while DOC was measured to elucidate other sources, i.e. DOM, in production of •OH during the photoflocculation process. Furthermore, highly degraded wood was collected at the Dismal Swamp sampling site and extracted by water for studying the sources of •OH in the water soluble fraction. DOM optical properties including slope ratio S_R ($S_{275-295 \text{ nm}}/S_{350-400 \text{ nm}}$), specific UV absorption measured at 254 nm ($SUVA_{254}$) and excitation-emission matrix fluorescence (EEMS) coupled with PARAFAC analysis were performed for the extracted sample, and Fe speciation including particulate Fe, organically-complexed Fe, total free Fe (non-complexed), dissolved Fe(II) and dissolved Fe(III) was measured in the sample with added iron during the photoflocculation process. These results are included in Chapter III.

It has been shown that •OH can be produced from not only the Fenton reaction and nitrate and nitrite photolyses, but also DOM photoreactions (Page et al., 2011; Vaughan and Blough, 1998). In Chapter IV, model compounds were used to study the source and mechanism of •OH formation from DOM photoreactions. In this chapter, it is shown that phenolic acids may be important sources of photochemically produced •OH within DOM. We chose to study these compounds because aromatic moieties (i.e., chromophores) within DOM contain mainly carboxyl and hydroxyl functionalities, especially humic acid, lignin and tannin derived phenolics (Hayes et al., 1989). Secondly, an excited quinoid enol tautomer, similar to quinone structure, has been observed in several hydroxyphenacyl compounds by laser flash spectroscopy (Klíčová et al., 2012; Vulpius et al., 2010). Since the excited triplet state quinone is known to be more reactive than the ketone or acid (Pochon et al., 2002), this tautomer may take part in the •OH probe reactions. I found that most phenolic acids model compounds were capable of photoproducing •OH, and that compounds with para hydroxyl and carboxyl groups, particularly the 2,4- dihydroxybenzoic and 4-hydroxybenzoic acids, exhibited remarkably high •OH photoproduction. We conducted methane trapping and competition kinetics experiments to evaluate the relative importance of free •OH vs. less reactive oxidizing species. Moreover, we hypothesized a mechanism for •OH formation from the compounds with para hydroxyl and carboxyl groups, and examined pH effects with respect to this mechanism.

The above study showed that phenolic compounds, particularly those with para hydroxyl and carboxyl groups, are capable of photochemically producing •OH. These aromatic structures are commonly present in humic substances. For instance, fulvic and

humic acids originating from soil contain a large proportion of benzenecarboxylic and phenolic compounds, which, in turn, are primarily derived from lignin degradation and transformation (McDonald et al., 2004; Geib et al., 2008; Palmqvist and Hahn-Hägerdal, 2000). Lignin is the second most abundant natural polymer (Heitner et al., 2010). It is built from three basic monomers, namely *p*-coumaryl alcohol, coniferyl alcohol, and sinapyl alcohol. Lignin can be partially degraded to form smaller compounds containing carboxyl groups, methoxyl groups and phenols through fragmentation and oxidation. These transformation products are further modified and incorporated into humic substances (Heitner et al., 2010; McDonald et al., 2004). Due to the complexity and nonuniformity of lignin, it is difficult to determine its structure directly. Thus, chemical degradation of lignin to its building block molecules is required. The chemical methods can be classified by the depolymerization pathways which are oxidative, solvolytic, and hydrogenolytic (Heitner et al., 2010). In the oxidative method, the traditional alkaline CuO oxidation method originally developed by Hedges and Ertel (1982) is commonly used. The procedure has been optimized and modified by several groups. These optimizations include utilization of up to twenty reaction vessels to improve sample throughput (Knuutinen and Mannila, 1991; Lobbes et al., 2000); employing a microwave digestion system (Goñi and Montgomery, 2000); glucose addition to low carbon sample (Kaiser and Benner, 2011; Kaiser et al., 2001; Louchouarn et al., 2000), ethyl acetate extraction instead of ethyl ether extraction (Goñi and Montgomery, 2000; Kaiser and Benner, 2011; Kögel and Bochter, 1985), and solid phase extraction (SPE) instead of liquid-liquid extraction (Amelung et al., 1999; Kaiser and Benner, 2011; Kögel and Bochter, 1985).

Chapter V compares the lignin phenolic composition based on a simple HPLC CuO method to that obtained by the conventional high pressure reaction vessel CuO GC-MS procedure (Hernes et al., 2007; Spencer et al., 2010) for a large variety of sample types. The HPLC approach is shown to be substantially simpler and less expensive than the GC method, it does not require strict sample dehydration and derivatization steps, and moreover, it enables compound-specific isotopic analyses. In the HPLC method, inexpensive and commercially available thick-walled Teflon vials were employed. This chapter shows the interlaboratory comparison results of the two methods, in general the agreement between the two methods was very good.

In summary, this dissertation mainly focuses on the source of •OH in natural waters. Firstly, an accurate method was established for estimating •OH formation rate during long-term irradiation by employing near-instantaneous formation rates (Chapter II), which was then applied to water samples during a study of DOM photoflocculation. By examining •OH formation rate, H_2O_2 concentration, DOC, DOM optical properties, and iron speciation, the relationship of •OH formation with these parameters during photoflocculation process was examined for an iron and DOM-rich Dismal Swamp water sample (Chapter III). Since humic substances appear to produce •OH, model DOM chromophoric compounds, in particular phenolic acids, were used to elucidate the source and mechanism of •OH photoformation from DOM (Chapter IV). Chapter V compares the lignin phenolic composition based on a simple HPLC CuO method to that obtained by the conventional high pressure reaction vessel GC-MS procedure for a wide variety of water, sediment and plant samples. Good agreement between these methods was obtained.

CHAPTER II

ESTIMATING HYDROXYL RADICAL PHOTOCHEMICAL FORMATION RATES IN NATURAL WATERS DURING LONG-TERM LABORATORY IRRADIATION EXPERIMENTS

PREFACE

The content of this chapter was published in 2014 in Environmental Science: Processes & Impacts, and below is the full citation. See Appendix A for the copyright permission.

Sun, L., Chen, H., Abdulla, H.A. and Mopper, K. (2014) Estimating hydroxyl radical photochemical formation rates in natural waters during long-term laboratory irradiation experiments. Environmental Science: Processes & Impacts. 16 (4), 757-763.

1. INTRODUCTION

The hydroxyl radical ($\bullet$OH) is one of the most reactive species in natural waters. It not only reacts with a variety of organic and inorganic compounds, resulting in their chemical and structural transformation (Buxton et al., 1988; Vaughan and Blough, 1998), but can also impact aquatic organisms, e.g., damage the macromolecules DNA, proteins and lipids and result in excretion of protective slime (Mague et al., 1980; Zlotnik and Dubinsky, 1989). The $\bullet$OH is mainly produced from the photochemical reactions in natural waters.

Since $\bullet$OH is a highly reactive specie, it occurs with very short lifetime in natural waters. Its lifetime is 2.6~6.0 µs in river, dew, and cloud waters (Arakaki and Faust,

1998; Mostofa et al., 2013). Thus, the photochemical formation rates of •OH are difficult to be measured directly, and are determined indirectly either through the loss of a reagent or accumulation of a product. A probe is added into the system, which should react selectively and unambiguously with •OH and does not alter the chemistry of the system. The electron paramagnetic resonance (EPR) technique can measure •OH simultaneously by using diamagnetic compounds, e.g. nitrone or nitroso to trap •OH to form stable paramagnetic aminoxyl radicals (Burns et al., 2012). In the non-simultaneous methods, the probe reactions can be split into two broad categories: 1) •OH addition to probes, with •OH either being added to the carbon atoms in probes such as 4-nitrophenol, nitrobenzene, benzene, benzoic acid, and terephthalate, or being added to the sulfoxide group in probes, e.g. dimethyl-sulfoxide; and 2) abstraction of a hydrogen atom on the probes such as methanol, formic acid, methane and butyl chloride (Anastasio and McGregor, 2001; Page et al., 2010; Page et al., 2011).

Among these probes, benzene and benzoic acid have been commonly used through •OH addition onto the ring. Typically, the probes are added initially to the samples and the cumulative concentrations of phenolic products are measured after irradiating for several minutes (Arakaki and Faust, 1998) or hours (al Housari et al., 2010; Mostofa et al., 2013; Nakatani et al., 2007; Zhou and Mopper, 1990). These phenolic product compounds are non- or very weak absorbers of light in the solar irradiance spectrum and thus do not undergo direct photoreaction; however, in natural waters, their phototransformation/destruction may be promoted by the presence of DOM, possibly through electron or hydrogen atom transfer from reactive excited triplet states of DOM (Canonica et al., 1995; Golanoski et al., 2012), or reaction with reactive oxygen species,

such as hydrogen peroxide (Beltran-Heredia et al., 2001), •OH (Esplugas et al., 2002), and singlet oxygen(Wilkinson et al., 1995). Thus, during long-term irradiations, this loss may lead to underestimation of the cumulative concentrations of phenolic products. Since the degradation of the phenolic products usually follows the pseudo-first order kinetics (Beltran-Heredia et al., 2001; Esplugas et al., 2002), the degradation rate can be written as:

$$\frac{dc}{dt} = =k\mathrm{c}$$

Where k is the degradation rate constant, and c is the phenolic products concentration.

From this equation, the underestimation is likely minor when the concentration is small, e.g., only initial •OH formation rates are taken into account (al Housari et al., 2010). However, the underestimation may be significant for time-course studies of •OH formation rates or steady-state concentration, in which it usually require several hours to adequately measure the generation of •OH (Mostofa et al., 2013; Nakatani et al., 2007; White et al., 2003). For example, to examine the photo-Fenton reaction in natural waters, the •OH formation rate, H_2O_2, and Fe concentrations are required to be measured hourly under different experimental conditions (White, 2000). Moreover, to study the source and sink of •OH (as well as other reactive species) from DOM, it may require hours to days to measure the DOM photochemical transformation (Helms et al., 2013; Mopper and Kieber, 2000; Moran and Zepp, 1997). Since DOM is an important source and sink of •OH (as well as other reactive species), accurate estimation of •OH can improve our understanding of DOM transformation pathways. Therefore, it is necessary to establish the stability of both the •OH probe compound and the quantified product species with

respect to direct and indirect photolysis in natural waters (Burns et al., 2012).

In this study, we estimated time-course •OH formation rates in DOM-rich freshwater Great Dismal Swamp (DS) and DOM-poor estuarine water by two approaches: 1) correcting for product loss and 2) obtaining near-instantaneous formation rates. The corrected formation rates were obtained by adding the photodegradation rates of corresponding photoproducts to their formation rates, and the instantaneous rates were obtained by measuring the photoproducts formation rates for a short time ($\leq$2h).

2. EXPERIMENTAL SECTION

2.1 Chemicals

Phenol (purity grade >99 %), sodium benzoate (99.5 %), benzene (HPLC grade) were obtained from Sigma; salicylic acid (SA) (99%) were obtained from Fisher; and methanol (HPLC grade) was obtained from Acros. Ultra-pure water (Milli-Q water, >18 MΩcm^{-1}) was used for solution preparation.

2.2 Sample description

Water samples were freshly obtained from the Portsmouth Ditch in the Great Dismal Swamp (near 36.7 ⁰S and 76.4 ⁰W, salinity 0 ppm, pH 3.7) and Elizabeth River estuary (near 36.9 ⁰S and 76.3 ⁰W, salinity 20 ppm, pH 7.5) in spring 2013. Samples were collected by 20 L polyethylene containers which had been previously cleaned with dilute acid and base solutions and filtered within 24 hours of collection through a pre-cleaned 0.1 µm capsule filter (Polycap TC, Whatman). Dissolved organic carbon (DOC) and total dissolved nitrogen (TDN) were 54 ppm and 1.9 ppm for the DS sample, and 3 ppm and 0.9 ppm for the Elizabeth River estuarine sample filtrate.

2.3 Irradiations

Irradiations were conducted using a solar simulator containing UVA340 bulbs (Q-Panel). The solar simulator is described elsewhere (Minor et al., 2007). These lamps have a spectral output nearly identical to natural sunlight from ~295 to ~360 nm (http://www.solarsys.biz/0103.shtml). In a comparison of the light output from the solar simulator to natural sunlight, the solar simulator provided 127% of the photobleaching occurring under winter mid-day sunlight at 36.89 °N latitude (Helms et al., 2008). Consequently, the •OH production rates in this study are likely somewhat higher than in the environment, and thus, during the 15 days experiment, the samples were exposed to an equivalent of about 60 days of natural sunlight in winter. All samples were placed into quartz tubes, which were acid soaked and pre-combusted, and kept oxygenated by periodic shaking in air. Sample controls were irradiated without probes under the same condition. Dark controls with the probes added were wrapped in foil and placed inside the solar simulator. All samples were irradiated at room temperature and at their natural concentrations and pH in order to approximately simulate surface conditions, and to avoid potential contamination.

2.4 Determination of •OH formation rate

Probe compounds sodium benzoate or benzene were added to aliquots of the water sample to final concentrations of 5.0 mM and 3.0 mM respectively. Complete dissolution of benzene was facilitated by vigorous stirring at room temperature. These samples were used to determine the effect of long-term, continuous irradiation of the •OH probes. At each time point, subsamples from irradiated and dark control samples were taken for probe photoproducts determination. Other aliquots of the water sample were placed

under solar simulator and initially without the probes present, which were used for measuring instantaneous •OH formation rates and DOC/TDN. At each time point, subsamples were taken to measure DOC/TDN, and sodium benzoate or benzene probes were added to an aliquot followed by irradiation for ≤2h irradiate for ≤2h. The •OH formation rates during this short time period is defined as the instantaneous •OH formation rates.

Benzoic acid reacts with •OH to form SA and other products, while benzene reacts to form mainly phenol. The fraction of SA (or phenol) formed relative to the other •OH photoproducts is constant (Zhou and Mopper, 1990) thereby enabling the use of SA (or phenol) production to determine the total •OH production, as described below. The SA and phenol photoproducts were measured using HPLC. The HPLC system consist of an E-Lab Model 2020 gradient programmer and data acquisition system (OMS Tech, Miami, FL) installed on an IBM-compatible PC, an Eldex Model AA pump (Eldex Laboratories, Menlo Park, CA), a six-port Valco injector (Valco Instruments, Houston, TX) and a Hitachi model F-1080 fluorescence detector; the excitation/emission wavelengths were 300/400 nm (Qian et al., 2001) for SA and 260/310 nm for phenol(Takeda et al., 2004), respectively. Cumulative SA and/or phenol concentrations were plotted vs. irradiation time. The observed photo-formation rates of SA and phenol (R_{ob}) were determined from the tangent slopes at each time point of the curve using Matlab. R_{ob} was used to evaluate the uncorrected •OH photo-production rate, R_{unc}, which was calculated by the following equation:

$$R_{unc} = \frac{R_{ob} \times F}{Y} \tag{1}$$

Where Y is the yield of photoproduct formed per probe molecule oxidized by •OH.

Since the reaction between probe and •OH forms more than one product (Mezyk et al., 2007; Zhou and Mopper, 1990), this value is always less than 100 % (see Results and Discussion). F is a calibration factor, which is related to the fraction of the •OH flux that reacts with the probe and accounts for competing •OH scavengers in natural waters, such as DOM.

F is evaluated for each sample type by competition kinetics experiments as described in detail by Zhou and Mopper (Mopper et al., 1991). The samples were added a series of different probes concentrations. The concentration for benzoate was from 1~10 mM while for benzene it was 0.5~5 mM. The photoproduct formation rates (R_{SA} and R_{ph}) were obtained at different probe concentrations.

2.5 Determination of photodegradation rates of •OH probe products

Photodegradation rates of SA and phenol were obtained by irradiating 40 μM SA and 180 μM phenol in the DS sample and measuring their concentrations over 24 h. The concentrations of SA and phenol chosen were close to the maximum cumulative concentrations formed in our irradiation experiments.

2.6 Determination of dissolved organic carbon (DOC), total dissolved nitrogen (TDN)

Samples were filtered through pre-combusted GF/F filters to remove the particles formed during irradiation. DOC and TDN were measured for all samples using high temperature (720 °C) catalytic combustion on a Shimadzu TOC-V-CPH carbon analyzer. Potassium hydrogen phthalate (KHP) and KNO_3 were used to make calibration curves to quantify the DOC and TDN concentrations respectively.

3. RESULTS AND DISCUSSIONS

3.1 F values

The probes not only react with •OH, but also natural scavengers in the waters. Thus, the photoproduct formation rate R_{SA} or R_{ph} is as a saturation-type function of added probe concentration ([benzoate] or [benzene]) in the Dismal Swamp sample (Figure 1a, c) and Elizabeth River sample (Figure 1e). From the equation (Zhou and Mopper, 1990):

$$\frac{1}{R_p}=\frac{1}{P_{OH}}+\frac{k_{ns}}{P_{OH}k_p}\times(1/[\text{probe}]) \tag{2}$$

Where R_p is the reaction rate of •OH with the probe; P_{OH} is the total •OH formation rate; k_{ns} is the apparent •OH scavenging rate constant of natural scavengers; k_p is the reaction rate constant of the probe scavenger with •OH. A straight line was obtained by plotting $1/R_p$ against $1/[\text{probe}]$ (Figure 1b, d, f):

$$\text{intercept}=\frac{1}{P_{OH}} \tag{3}$$

$$\text{slope}=\frac{k_{ns}}{P_{OH}k_p}=\text{intercept}\times\frac{k_{ns}}{k_p} \tag{4}$$

$$k_{ns}/k_p=\text{slope/intercept} \tag{5}$$

equation $(2)\times P_{OH}$, and combine with (5):

$$\frac{P_{OH}}{R_p}=1+\text{slope}/(\text{intercept}\times[\text{probe}]) \tag{6}$$

F value was defined as:

$$F=1+\text{slope}/(\text{intercept}\times[\text{probe}]) \tag{7}$$

For our experiments, F was 1.11~1.26, depending on the probe and sample types; i.e., types and concentrations of natural scavengers. The F values are listed in Table 1.
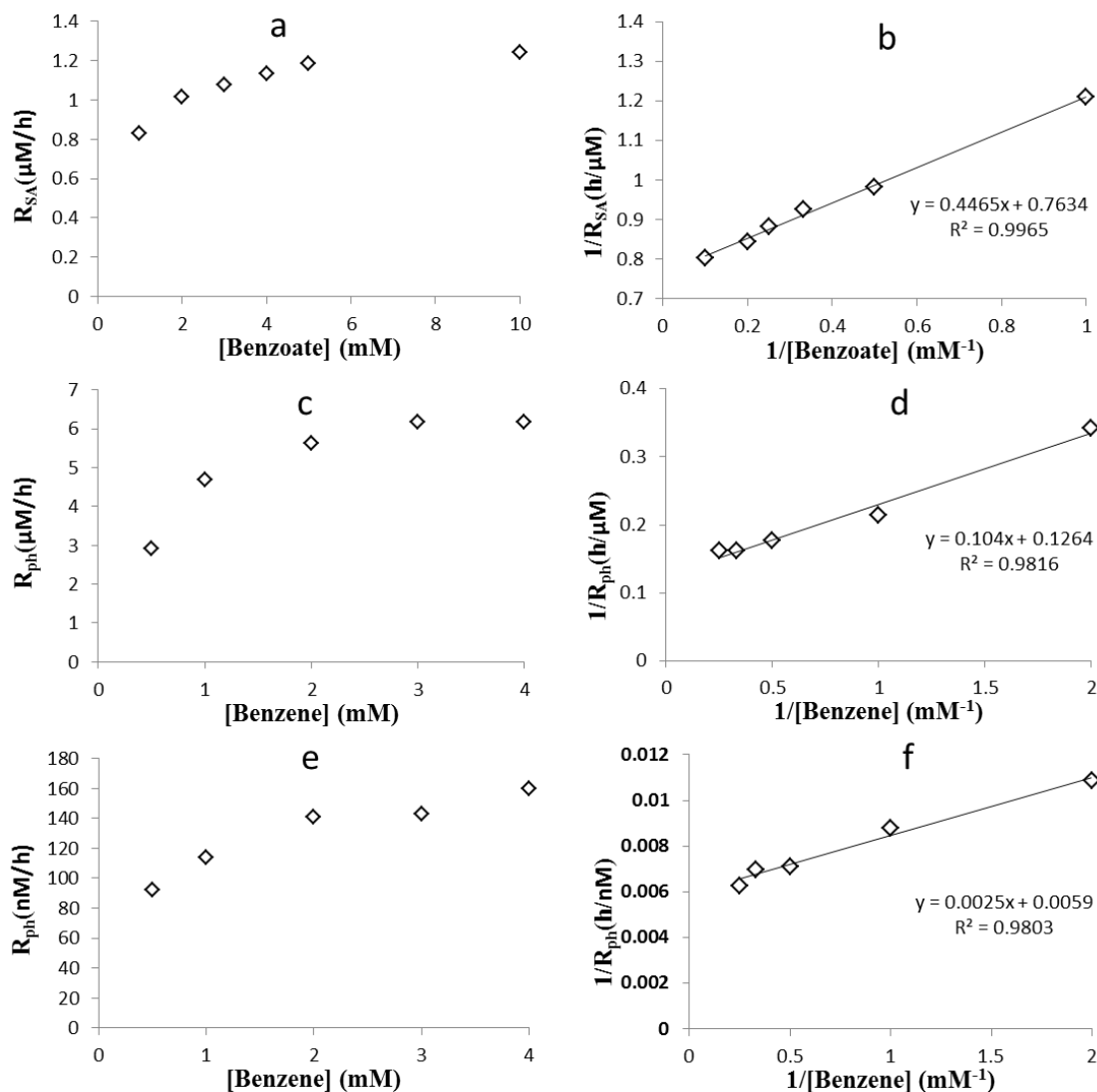
Figure 1. (a) Relationship between the probe concentration [Benzoate] and photoproduct

formation rate R_{SA}; (b) Relationship between 1/[Benzoate] and 1/ R_{SA}; (c) Relationship

between the probe concentration [Benzene] and photoproduct formation rate R_{ph}; (d)

Relationship between 1/[Benzene] and 1/ R_{ph} in the Dismal Swamp sample; (e)

Relationship between the probe concentration [Benzene] and photoproduct formation rate

R_{ph}; (f) Relationship between 1/[Benzene] and 1/ R_{ph} in the Elizabeth River sample.

Table 1

F values by using different probes in different samples. Benzoate was not used for the Elizabeth River sample.

	Great Dismal Swamp	Elizabeth River
3 mM Benzene	1.26±0.03	1.14
5 mM Benzoate	1.11±0.01	Not measured

3.2 Calibration of Y_{ph} value

Y is the yield of photoproduct formed per probe molecule oxidized by •OH. Most Y values of SA (Y_{SA}) from published radiolysis experiments are 17~18% (Anastasio and McGregor, 2001; Matthews and Sangster, 1965; Zhou and Mopper, 1990) while the values of phenol (Y_{ph}) range from 66% to 95% (Anastasio and McGregor, 2001; Balakrishnan and Reddy, 1970; Loeff and Stein, 1963; Minero et al., 2007); the high Y_{ph} of 95% was observed during nitrate photolysis(Minero et al., 2007). Because of the wide range of published Y_{ph} values, we did not select a Y_{ph} value for our system from published data. Instead, we used the much less variable Y_{SA} value 17% (Zhou and Mopper, 1990) to calibrate the Y_{ph} value by using H_2O_2 photolysis as a pure •OH source. H_2O_2 scavenges •OH significantly only at relatively high concentrations ($k_{H2O2} = 3 \times 10^7$ $M^{-1}s^{-1}$) (Haag and Hoigné, 1985). Different concentrations of H_2O_2 ($\leq$200 μM) were added to solutions containing sodium benzoate or benzene and irradiated for 1 h using the same solar simulator. Assuming the degradation of SA and phenol is negligible in this short period, at the same concentrations of H_2O_2, the •OH photoproduction rate R_{unc} should be the same for both probes, that is:

$$R_{unc} = \frac{R_{SA} \times F_{SA}}{Y_{SA}} = \frac{R_{ph} \times F_{ph}}{Y_{ph}} \tag{3}$$

It should be pointed out that H_2O_2 also scavenges •OH, but only significantly at relatively high concentrations due to its low second order rate constant ($k_{H2O2} = 3 \times 10^7$ M^{-1}s^{-1}, one magnitude less than $k_{benzoate}$ and $k_{benzene}$) (Haag and Hoigné, 1985), $F_{SA}=F_{ph}=1$:

$$R_{unc=} \frac{R_{SA}}{Y_{SA}} = \frac{R_{ph}}{Y_{ph}} \qquad (4)$$

Y_{ph} was then calculated as:

$$Y_{ph} = \frac{Y_{SA} \times R_{ph}}{R_{SA}} \qquad (5)$$

In our experiments, Y_{ph} value was calculated as 69.3±2.2 %, which was then used for all calculations. This value is in agreement with most published values (Anastasio and McGregor, 2001; Balakrishnan and Reddy, 1970; Minero et al., 2007).

3.3 Corrections of •OH formation rates

Photodegradation was observed for both SA and phenol, and followed pseudo-first order reaction kinetics (Beltran-Heredia et al., 2001; Esplugas et al., 2002). The loss of the photoproducts may be caused by reactive excited triplet states of DOM (Canonica et al., 1995; Golanoski et al., 2012) and reactive oxygen species including H_2O_2, •OH, and singlet oxygen (Beltran-Heredia et al., 2001; Esplugas et al., 2002). The photodegradation rate at each time point is $k \times$[SA or phenol]$_t$, where k is the slope of the plot of Ln (concentration) vs. the irradiation time; it is -0.0495 h^{-1} for SA and -0.0459 h^{-1} for phenol (Figure 2).
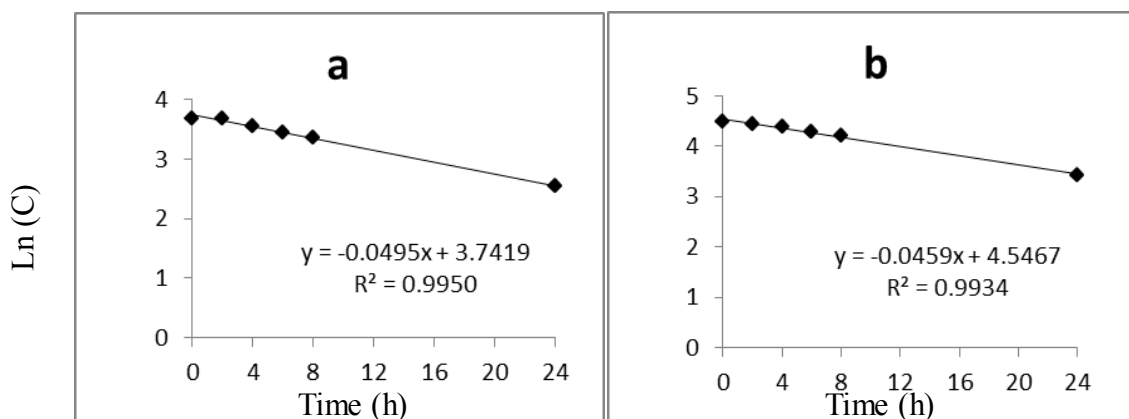
Figure 2. (a) SA and (b) phenol photodegradation in the DS sample over a 24 h irradiation in a UV solar simulator. Subsamples for measuring SA and phenol degradation rates were taken at the same time as the •OH measurements.

The corrected photoformation rate of SA or phenol is the observed SA (or phenol) formation rate (R_{ob}) plus its degradation rate. Therefore, the •OH formation rate (R_{cor}) was corrected and calculated by the following equation:

$$R_{cor} = \frac{(R_{ob} + k \times [\text{SA or phenol}]_t) \times F}{Y} = R_{unc} + \frac{k \times [\text{SA or phenol}]_t \times F}{Y} \tag{6}$$

R_{unc}, R_{cor}, and R_{ins} at each time point during 15 d are shown in Figure 3 and Figure 4. R_{ins} was assumed to be the true •OH formation rate; i.e., the degradation of SA or phenol is negligible for a one hour irradiation (Figure 2). The negative R_{unc} values at the longer irradiation times (Figure 3 and Figure 4) are probably due to the substantial photodegradation of the probe photoproducts upon long-term irradiation.
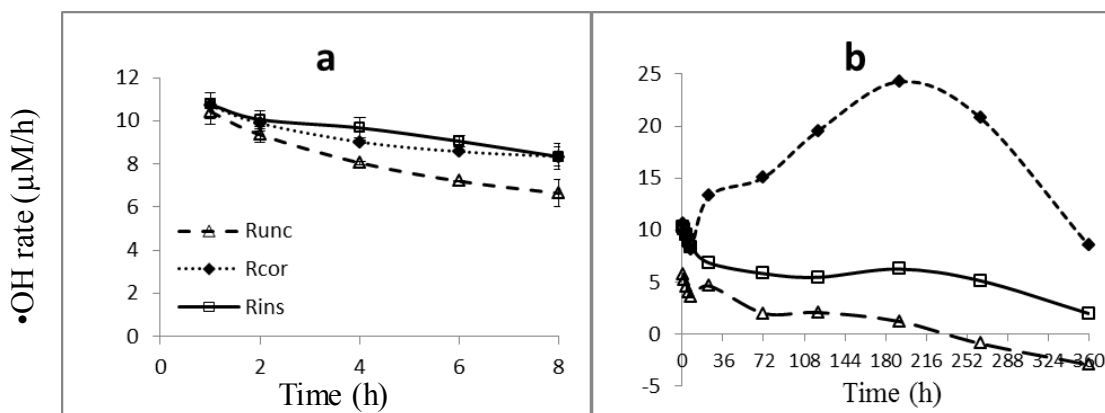
Figure 3. R_{unc}, R_{cor} and R_{ins} using benzoic acid as probe for 8h (a) and 15 day (b) irradiations of DS water. Error bars are within the data points unless otherwise indicated.
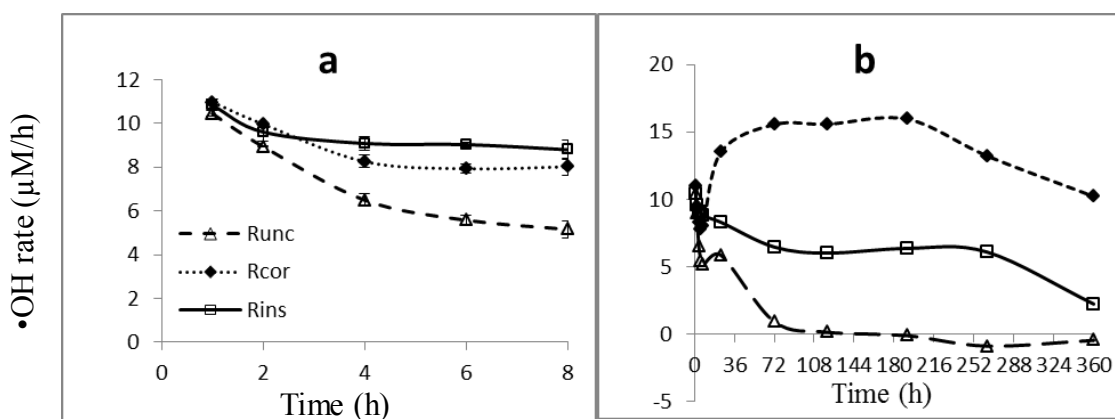
Figure 4. R_{unc}, R_{cor} and R_{ins} using benzene as probe for 8 h (a) and 15 day (b) irradiations of DS water. Error bars are within the data points unless otherwise indicated.

3.4 Comparison of •OH formation rates

Between 2 h and 8 h, R_{unc} values were lower than R_{ins} values (Table 2). The differences averaged 29 % using benzoic acid and 16% using benzene as probes; thus using R_{unc} significantly underestimated •OH formation. By performing corrections for probe product degradation, the agreement to R_{ins} improved. The differences between R_{cor} and R_{ins} averaged 8 % using benzoic acid and 4% using benzene as probes. However, for longer irradiation periods (more than 8 h), neither R_{unc} nor R_{cor} agreed well with R_{ins}, as differences were >30 %. The reason for the large discrepancies might be that the added probes changed DOM photodegradation and •OH production pathways, which only became significant after long-term irradiations containing the probe. Another reason for the discrepancy of R_{cor} and R_{ins} was that the photoproduct photodegradation rate constant k may be overestimated because the photodegradation experiment was conducted in the absence of the probe. In the presence of the probe, since the probe concentration was at least an order of magnitude higher than the photoproduct concentration, it would consume a major fraction of the •OH, while in the absence of the probe, this fraction of the photoproduced •OH would be available for photoproduct degradation. Thus, R_{cor} is expected to be greater than R_{ins}, especially at high photoproduct concentrations during long-term irradiations. From above results, for long-term irradiations (e.g., > ~1 day) only R_{ins} should be used to determine the •OH production rate.

Table 2

Uncorrected •OH formation rate (R_{unc}), corrected formation rate (R_{cor}), and instantaneous

formation rates (R_{ins}) during 8 h (n=2)

Time (h)	•OH formation rates (µM/h) by using					
	Benzoic acid			Benzene		
	R_{unc}	R_{cor}	R_{ins}	R_{unc}	R_{cor}	R_{ins}
1	10.5±0.1	11.0±0.1	10.8±0.1	10.3±0.5	10.6±0.5	10.7±0.1
2	9.0±0.1	9.9±0.1	10.1±0.4	9.3±0.4	9.9±0.5	10.0±0.4
4	6.5±0.3	8.3±0.3	9.6±0.4	8.0±0.1	9.0±0.1	9.6±0.5
6	5.6±0.2	7.8±0.2	9.0±0.3	7.2±0.1	8.6±0.1	9.0±0.3
8	5.2±0.4	8.0±0.4	8.3±0.5	6.6±0.6	8.1±0.6	8.3±0.5

Measurements were also conducted in a low DOC (3 ppm) sample from the

Elizabeth River (salinity of 20). Only benzene was used as the •OH probe because it has

higher Y and, thus a somewhat better selectivity than benzoic acid (Vione et al., 2010);

and its corresponding photoproduct phenol has higher fluorescent intensity than SA. The

photodegradation rate of phenol in the Elizabeth River sample was $0.00443 \, h^{-1}$, which is

only 1/10 of that for the DS water sample. •OH formation rates were also low in the

Elizabeth River sample (< 40 nM/h). However, this is not only due to low DOM, but also

due to competing natural •OH scavengers including CO_3^{2-} and Br^- in saline water

(Mopper and Zhou, 1990; Zepp et al., 1987). The t test showed no significant differences

between R_{unc}, R_{cor} and R_{ins} during 6 h of irradiation (P>0.17) (Figure 5a); thus, use of a

correction or instantaneous rate was not necessary. However, significant differences were

observed for irradiations > ~24h (Figure 5b); thus the measurement of R_{ins} also appears to

be necessary for long-term irradiations, even for this relatively low DOC sample.
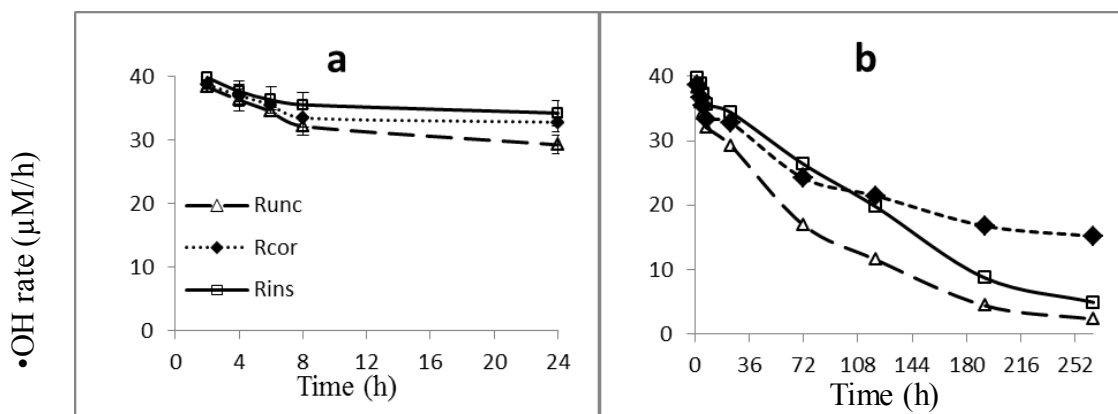
Figure 5. R_{unc}, R_{cor} and R_{ins} for 24 h and 11 day irradiations of Elizabeth River water. Error bars are within the data points unless otherwise indicated.

3.5 Discussion

From above results, in both DOM-rich and DOM-poor natural waters examined in this study, the methods for measuring •OH formation rates by obtaining sequential cumulative concentrations of photoproducts from probes substantially underestimated the actual •OH formation rate during long-term irradiations. Therefore, it is recommended that instantaneous formation rates be used to estimate •OH photochemical formation rates during long-term irradiation experiments, regardless of the probes used. For short-term irradiations of natural waters, it is recommended that photodegradation rates of corresponding probe photoproducts be determined to correct the •OH production rate.

It needs to be pointed out that, in addition to trapping the free •OH, these probes (as well as most other commonly used •OH probes) also react with other highly reactive species (Cooper et al., 1989; Maurino et al., 2008; Page et al., 2011; Pochon et al., 2002);

e.g., excited quinones triplets photochemically produce species capable of some species capable of adding a hydroxyl group to the probe, even though these species exhibit reactivities about one order of magnitude lower than the free •OH (Pochon et al., 2002). It is likely that these species contributed to the formation of hydroxylated compounds from the added probes. Also, these species probably do not reacts with benzoate with the same Y_{sa} as free •OH (Page et al., 2011), therefore, it is recommended that this value be obtained by measuring the ratios of *o*, *p*, *m*-hydroxybenzoic acids produced in natural waters. Moreover, some probes, e.g. benzene, may be more specific than the others, e.g, benzoate, to free •OH (Vione et al., 2010). More evidence and discussion from methane trapping and competition kinetics experiments on DOM model compounds are present in Chapter IV.

During the photo-Fenton reaction, the highly reactive and oxidizing ferryl ion, Fe(IV), can be also formed, although at relatively low rates (Balakrishnan and Reddy, 1970; Bossmann et al., 1998). This species is capable not only of abstraction of a hydrogen atom, even from methane (Yoshizawa et al., 1998), but also of aromatic and benzylic hydroxylation, *e.g.* conversion of benzene to phenol (Bassan et al., 2003; Baxendale and Magee, 1953). Although the ferryl ion is less oxidizing than the hydroxyl radical (Koppenol and Liebman, 1984), we cannot reject its possible minor contribution to probe product formation in our iron-rich system (Vermilyea and Voelker, 2009). Thus, in the •OH formation during long-term irradiation study, all reported •OH production rates include both free •OH and any reactive species capable of reactions with the probe molecules. However, even if part of the probe product signal is due to these other reactive species, they (in addition to •OH) may have played a role in the oxidation of DOM.

CHAPTER III

HYDROXYL RADICAL PHOTOCHEMICAL FORMATION IN NATURAL

WATERS DURING PHOTOFLOCCULATION

PREFACE

The results for the Dismal Swamp water samples discussed in this chapter were

published in 2014 in Environmental Science: Processes & Impacts; below is the full

citation. See Appendix A for the copyright permission.

Sun, L., Chen, H., Abdulla, H.A. and Mopper, K. (2014) Estimating hydroxyl

radical photochemical formation rates in natural waters during long-term laboratory

irradiation experiments. Environmental Science: Processes & Impacts. 16 (4), 757-

763.

1. INTRODUCTION

The hydroxyl radical (•OH) is a highly reactive oxygen species that is formed by

photochemical reactions in natural waters (Buxton et al., 1988; Vaughan and Blough,

1998). There are three major sources for •OH: nitrate and nitrite photolyses, the photo-

Fenton reaction, and dissolved organic matter (DOM) photoreactions (Mostofa et al.,

2013). Nitrate and nitrite photolyses are predominant in fresh waters, where the

contribution of nitrite is predominant (48–80 %) for HO• production in polluted rivers

while nitrate is usually more important (16–49 %) in clean rivers (Hoigné et al., 1988;

Mostofa et al., 2013). In iron-rich waters, the contribution of the photo-Fenton reaction

can account for more than 70% of the total photochemical •OH production (Southworth

and Voelker, 2003; White et al., 2003; White, 2000). The photo-Fenton reaction is the

reaction of Fe(II) with H_2O_2 to yield Fe(III) and •OH; the Fe(III) is then photoreduced to

Fe(II) probably through ligand to metal charge transfer (LMCT) reactions with DOM

(Scott et al., 1998; Barbeau, 2006; Klapper et al., 2002). Not only can inorganic Fe(II)

take part in the Fenton reaction, but also organically-complexed Fe(II), in which the Fe is

usually complexed with the phenolic and carboxyl groups (Baruah et al., 1981). Although

organically-complexed Fe(II) is less reactive with H_2O_2 than inorganic Fe(II), it may be

important in humic-rich waters (Miller et al., 2012). In seawater and high DOM

freshwaters, DOM photoreactions appear to be the main source for •OH. There are two

known •OH production pathways from DOM: a hydrogen peroxide (H_2O_2) dependent

pathway involving the Fenton reaction, where the H_2O_2 is formed from DOM (Vione et

al., 2006), and an H_2O_2 independent pathway (Page et al., 2011). In the later pathway,

hydroquinolic and phenolic moieties within humic substances were thought to be

responsible, at least in part, for •OH photoproduction in early studies (Mopper and Zhou,

1990; Page et al., 2011; Vaughan and Blough, 1998).

    •OH formation has been studied in the presence of iron and DOM under irradiation

(Gao and Zepp, 1998; Zepp et al., 1992), during which photoflocculation can occur (Gao

and Zepp, 1998; Zepp et al., 1992). Photoflocculation may be an important process in

transformation and transportation of DOM and particulate organic matter (POM) from

rivers to the ocean (Chen et al., 2014; Helms et al., 2013a). It has been reported by Gao

and Zepp (1998) that dark-colored particles formed in river samples after 3 days

irradiation, and the particles accounted for 45% of the total iron and 13% of the total

organic carbon. Thorn et al. (2010) found that humic and fulvic isolates became much

less aromatic and soluble after extensive irradiation. Helms et al. (2013a) later employed

nuclear magnetic resonance and Fourier transform infrared spectroscopies to study the process, and found that photochemically flocculated POM was more aliphatic than the residual non-flocculated DOM. Also, all samples containing re-dissolved POM exhibited lower slope ratio (S_R) values, which were calculated as the ratio of spectral slope $S_{275–295}$ to $S_{350–400}$ (Helms et al., 2008), than their particle free counterparts. The POM was enriched in amide functionality, while carbohydrate-like material was resistant to both photochemical degradation and flocculation. Kopáček et al. (2005) proposed the pathway proceeds by iron mediated photodegradation of organic iron-binding ligands causing release of inorganic iron to form insoluble hydroxides. Chen et al. (2014) further confirmed that the DOM-associated Fe is converted to insoluble Fe(III) oxyhydroxides. Also, the photochemically formed particulate condensed aromatic compounds are black carbon-like, which may contribute to the black carbon content of sediments. By using solid-phase extraction to separate free Fe from the organic bound Fe, Shiller et al. (2006) showed that the organically-complexed Fe is released during photo-oxidation of the low molecular-weight DOM, followed by precipitation of the released Fe as colloidal Fe(III) oxyhydroxides. Since •OH may play an important role in the chemical and structural transformation of DOM, and may impact Fe chemistry, its behavior during photoflocculation needs to be further studied.

In this chapter, •OH formation with respect to the Fenton reaction and DOM photoreactions was studied. We estimated time-course •OH photo-formation rates in Great Dismal Swamp (DS) and aqueous wood extract samples using near-instantaneous formation rates, which were obtained by measuring the photoproduct formation rates for a short time (≤2h) at each subsample time point during the irradiation (See Chapter II).

The DS sample was an iron- and DOM-rich freshwater sample, which was previously shown to flocculate during long-term irradiation (Chen et al., 2014; Helms et al., 2013a). Total Fe and H_2O_2 concentrations were measured to study the importance of the photo-Fenton reaction, while DOC was measured to elucidate the role of DOM in production of •OH during the photoflocculation process. S_R data is not shown for the DS sample. Furthermore, since the DS water contained a high concentration of iron, which may have significantly affected the optical properties and •OH photoproduction (Cabaniss, 1992; Manciulea et al., 2009; Pullin et al., 2007), degraded wood, which had a very low iron content was collected at the DS sampling site, was extracted with water to further study the effect of iron. •OH photoproduction, DOM optical properties (S_R, specific UV absorption measured at 254 nm ($SUVA_{254}$) and fluorescence excitation-emission matrices (EEMS)), and Fe speciation (particulate Fe, organically-complexed Fe(II), organically-complexed Fe(III), free Fe(II), and free Fe(III)) were measured.

2. EXPERIMENTAL SECTION

Phenol (purity grade >99%), benzene (HPLC grade), H_2O_2 (35% w/w), p-hydroxyphenyl)-acetic acid (98%), peroxidase type VI horseradish (285 units/mg), catalase from bovine liver (2000~5000 units/mg), trizma (99.9%), ferrozine (97%), hydroxylamine hydrochloride ($H_2NOH \cdot HCl$), ammonium acetate (99%), sodium acetate (99%), desferrioxamine mesylate (DFOM) (92.5%) and ferric chloride (99%) were obtained from Sigma-Aldrich; the iron standard solution was made from of ferric nitrate in 2 % (v/v) nitric acid (1000ppm, Certified, Fisher Chemical), and ferrous ammonium sulfate hexahydrate were obtained from Fisher; methanol (HPLC grade) were obtained

from Acros; and Maxi-Clean 600 mg SCX cation solid phase extraction (SPE) cartridges were obtained from Grace. Ultra-pure water (Milli-Q water, >18 MΩcm^{-1}) was used for solution preparation.

2.2 Sample description

Water samples were obtained from the Portsmouth Ditch in the Great Dismal Swamp (near 36.7 $^\circ$S and 76.4 $^\circ$W, salinity 0 ppm, pH ~3.7). Samples were collected in 20 L polyethylene containers which had been previously cleaned with dilute acid and base and filtered within 24 hours of collection through a pre-cleaned 0.1 μm capsule filter (Polycap TC, Whatman). The wood sample was collected near the water sampling sites. This area is mainly covered by maple gum (http://www.usgs.gov/climate_landuse/land_carbon/default.asp). A high S/V ratio (2.8), defined as the total mass of syringealdehyde, acetosyringone, and sryingic acid divided by the total mass of vanillin, acetovanillone, and vanilic acid produced from CuO HPLC method (described in Chapter V), indicated that the wood sample is angiosperm (Hedges and Mann, 1979). The wood sample was visually highly degraded. The sample was oven-dried at 60 $^\circ$C for 24 hours, crushed into powder by a mortar and pestle to pass through a 600 μm sieve, then 5 g of sample was leached in 1 L Milli-Q water and mixed by magnetic bar overnight at room temperature. The particles were removed by filtration through a pre-combusted 0.7 μm GF/F filter (Whatman) and followed by the 0.1 μm capsule filter. Dissolved organic carbon (DOC) and total dissolved nitrogen (TDN) were 54 ppm and 1.9 ppm for the DS sample, and 12 ppm and 0.5 ppm for the extracted wood filtrate.

To examine the effect of iron on •OH formation rate, 100 μM DFOM, a ligand strongly complex Fe(III), was added to an aliquot of DS sample, which inhibited Fe photochemical reaction through the formation of unreactive Fe(III) complexes (White et al., 2003). In addition, 20 μM $FeCl_3$ was added to an aliquot of wood extracted sample, and the pH was adjusted to the original pH of 4.3. The wood extracted sample was kept in the dark for 24 h to complete organic-iron complex interaction, and then filtered with a GF/F filter.

2.3 Irradiations

All samples were placed into quartz flasks, which were acid soaked and pre-combusted, and kept oxygenated by periodic shaking in air. Irradiations were conducted using a solar simulator containing UVA340 bulbs (Q-Panel). The solar simulator is described elsewhere (Minor et al., 2007). These lamps have a spectral output nearly identical to natural sunlight from ~295 to ~360 nm (http://www.solarsys.biz/0103.shtml). In a comparison of the light output from the solar simulator to natural sunlight, the solar simulator provided 127% of the photobleaching occurring under winter mid-day sunlight at 36.89 °N latitude (Helms et al., 2008). Dark controls were wrapped in foil and placed inside the solar simulator. All samples were irradiated at room temperature and at their natural concentrations and pH in order to approximately simulate surface conditions, and to avoid potential contamination.

At each time point, irradiated and dark control samples were subsampled. •OH formation rates, pH, and DOC/TDN were measured for all samples. Dissolved iron (DFe) and H_2O_2 production were measured for the DS sample, while slope ratio S_R ($S_{275-295 \ nm}/S_{350-400 \ nm}$), $SUVA_{254}$, EEMS and Fe speciation (particulate Fe (PFe), organically-

complexed Fe (OFe), free Fe (FFe), Fe(II) and Fe(III)) were measured for the wood extracted sample. The •OH formation rates, H_2O_2 production, S_R, $SUVA_{254}$, EEMS, pH and Fe speciation were measured immediately after subsampling. The subsamples for DOC/TDN were acidified and stored (4 °C) for later analysis. Acid cleaned Teflon vials were used for Fe subsamples. Acid cleaned and combusted glass vials were used for the other measurements.

2.4 •OH formation rate

Probe compound benzene was added to aliquots of the subsample to final concentrations of 3.0 mM. Benzene was used as the •OH probe because it has a better selectivity than benzoic acid (Vione et al., 2010); and its corresponding photoproduct, phenol, has higher fluorescent intensity than salicylic acid. Complete dissolution of benzene was facilitated by vigorous stirring at room temperature. The instantaneous •OH formation rates were determined by irradiating the subsamples for ≤2h (see Chapter II).

Benzene reacts to •OH to form mainly phenol, which was measured using HPLC. The HPLC system consist of an E-Lab Model 2020 gradient programmer and data acquisition system (OMS Tech, Miami, FL) installed on an IBM-compatible PC, an Eldex Model AA pump (Eldex Laboratories, Menlo Park, CA), a six-port Valco injector (Valco Instruments, Houston, TX) and a Hitachi model F-1080 fluorescence detector; the excitation/emission wavelengths was 260/310 nm (Takeda et al., 2004). Instantaneous •OH formation rate R was calculated by the following equation:

$$R = \frac{R_{ph} \times F}{Y} \tag{1}$$

Where R_{ph} is the observed photo-formation rate of phenol; Y is the yield of photoproduct formed per probe molecule oxidized by •OH; we use 69.3±2.2 % for phenol

(see Chapter II); F is a calibration factor, which is related to the fraction of the •OH flux

that reacts with the probe and accounts for competing OH scavengers in natural waters. F

must be evaluated for each sample type by competition kinetics using a series of different

probes concentrations as described in detail by Zhou and Mopper (Mopper et al., 1991).

For our experiments, F was 1.11~1.26, depending on the probes and sample types (see

Chapter II).

2.5 Dissolved organic carbon (DOC) and total dissolved nitrogen (TDN)

DOC and TDN were measured using high temperature (720°C) catalytic

combustion on a Shimadzu TOC-V-CPH carbon analyzer. Potassium hydrogen phthalate

(KHP) and KNO_3 were used to make calibration curves to quantify the DOC and TDN

concentrations respectively.

2.6 Optical properties (S_R and EEMS)

S_R ($S_{275-295 \; nm}/S_{350-400 \; nm}$), $SUVA_{254}$ were measured by UV absorbance (200-700 nm

in 1-nm intervals) using an Agilent 8453 diode array spectrophotometer with a 1 cm

quartz cuvette (Helms et al., 2008). Strongly absorbing samples were diluted prior to

measurement to ensure linear response.

Fluorescence EEMS was measured as described in Murphy et al. (2010).

Measurements include (1) UV absorbance (200-700 nm in 1-nm intervals) using an

Agilent 8453 diode array spectrophotometer with a 1 cm quartz cuvette; (2) raw EEMS

collected using a Cory Eclipse fluorometer with a 1 cm quartz cuvette at specified

excitation wavelengths (λ_{ex}) of 240-450 nm in 5-nm intervals and emission wavelengths

(λ_{em}) of 300-600 nm in 2-nm intervals; (3) blank EEMS and Raman scans (λ_{ex}=350 nm,

λ_{em}=365-450 nm in 0.5 nm intervals) of Milli-Q water, and (4) emission scans (λ_{ex}= 350

nm) of a quinine sulfate (QS) dilution series (0, 20, 50, 100 ppb) from a 1000 ppb

working solution. If the absorbance at 254 nm was above 0.2, dilution was needed. Data

was processed in MATLAB™ using the FDOMcorr toolbox (Murphy et al., 2010).

EEMS were processed by spectral correction, inner filter correction, Raman correction,

and QS calibration, and then analyzed by PARAFAC using the DOMFluor toolbox

(Stedmon and Bro, 2008).

2.7 H_2O_2 production

H_2O_2 production was measured by a modified (*p*-hydroxyphenyl)-acetic acid

(POHPAA) dimerization method (Miller and Kester, 1988). A fluorometric reagent was

made daily, which contained 200 μL of 25.0 mM POHPAA stock solution, 9.9 ml 0.25 M

Tris buffer (pH 8.8), and 1.2 mg horseradish peroxidase type VI. The fluorometric

reagent was added to sample with 1:50 ratio. Samples were allowed to react for 30 min at

room temperature and measured by a Hitachi model F-1080 fluorescence detector with

313 nm excitation and 400 nm emission. Total blank was obtained by measuring the

natural fluorescence (NAT) blank, catalase (CAT) blank, and reagent (REAG) blank.

NAT blank is the sample fluorescence with no reagents addition; CAT blank was

obtained by adding aqueous catalase stock solution to sample with 1:200 ratio to remove

H_2O_2 and measuring the fluorescence after 8 min; REAG blank was obtained by adding

catalase stock solution to sample for 8 min reaction, and then adding the fluorometric

reagent and measuring the fluorescence after 30 min. Total blank=NAT+(FL-CAT). The

DS water sample was diluted 10~15 times before measurement. Concentrations of H_2O_2

were determined by standard additions of 5-150 nM H_2O_2 stock solution. The

concentration of the stock solution (1.0 mM) was determined by spectrophotometry using the H_2O_2 molar absorptivity of 38.1M^{-1} cm^{-1} at 240 nm (Miller and Kester, 1988).

2.8 Iron speciation

The DS subsamples were filtered through pre-combusted GF/F filters. Dissolved Fe (DFe) was measured using a Hitachi Z8100 polarized Zeeman flame atomic absorption spectrophotometer equipped with an Fe hollow cathode lamp. Fe standards were prepared from the Fe standard stock solution. Standards ranged from 0 to 100 μM. Standards and samples were measured in triplicate.

Fe speciation was measured for the extracted wood sample, which includes particulate total Fe (PTFe), dissolved organically-complexed Fe(II) (OFe(II)), dissolved organically-complexed Fe(III) (OFe(III)), free Fe(II) (FFe(II)), and free Fe(III) (FFe(III)). The subsamples were 0.2 μm filtered (Gelman Sciences). PTFe was measured indirectly by subtracting dissolved total Fe (DTFe) at each time point from the initial DTFe. The FFe and OFe were separated by SCX cation exchange cartridges (Tangen et al., 2002). The SCX cartridges were employed because it is more convenient than loose resin (Shiller et al., 2006; Tangen et al., 2002). The cartridges were conditioned with 14 mL Milli-Q water, followed by 14 mL 0.4 M ammonium acetate buffer pH 4.5, and 4 mL of sample to rinse out the buffer. Since the free Fe is selectively bound to the SCX cartridges, the remaining Fe in eluate solution after SPE extraction was considered as OFe. FFe were calculated by subtracting the Fe concentration after SPE (OFe) from the total dissolved concentration.

Fe(II) and Fe(III) were determined before and after SPE extraction by a modified ferrozine method (Viollier et al., 2000). Non-reduced sample absorbance for Fe(II), was

measured by mixing 5.0 mL of sample, 500 µL 0.01 M ferrozine solution (prepared in 2 M ammonium acetate), 200 µL 5 M ammonium acetate, and standard addition with a range of 0~20 µM. The final pH was 5~6. Reduced sample absorbance for total Fe(II) and Fe(III), was measured after reducing the sample by hydroxylamine hydrochloride (prepared in 2 M HCl). The dissolved Fe(III) concentration was calculated by subtracting Fe(II) from the total dissolved Fe.

3. RESULTS AND DISCUSSION

3.1 •OH formation in DS water

During 15 days of irradiation, flocculation was observed after day 4 in the DS water. The •OH was continuously formed, and the instantaneous •OH formation rates ranged from ~10.5 µM/h on day 1 to ~2 µM/h on day 15 (Figure 6). After day 1, •OH formation rates decreased rapidly until a plateau at ~6 µM/h was reached (from ~day 3 to day 12), after which it dropped to ~2 µM/h on day 15.

During the irradiation, DFe decreased from nearly 20 µM to 3 µM (Figure 6a). The photoproduction of H_2O_2 varied widely over the irradiation (Figure 6c, d). H_2O_2 showed strong initial production, but fell to zero between day 2 and day 4. We hypothesize that the photo-Fenton reaction was the main source of the •OH initially, on the basis of high DFe and high H_2O_2 photoproduction during the first day. Nitrate photolysis was likely a negligible source of •OH as the maximum •OH production from nitrate was only ~2.1 x 10^{-3} µM /h, based on a dissolved nitrogen concentration of 1.9 ppm and assuming all dissolved nitrogen was nitrate and assuming an •OH photo-production rate from nitrate of ~1.1 x 10^{-3} µM •OH per µM nitrate h^{-1} in seawater in sunlight (Mopper and Zhou, 1990;

Zepp et al., 1987). The addition of DFOM reduced the •OH formation rate by about 90% during an 8 h irradiation, thus confirming the initial importance of Fenton chemistry in •OH photoproduction in the DS sample. Between day 4 to day 7, $H_2O_2$was again photoproduced (Figure 6c, d), but a sharp decrease in DFe was also observed during this period, which 26likely decreased the importance of Fenton chemistry relative to OH photoproduction from other sources, in particular DOM photoreactions (Helms et al., 2013a). The reasons for the reappearance of H_2O_2 after day 4 are not known, but may be related to photochemically-induced changes in DOM composition and structure (Gonsior et al., 2009) and to the initialization of DOM photoflocculation (Helms et al., 2013a; Helms et al., 2013b). The latter is supported by the inverse relation (R^2=0.97) between the DOC-normalized •OH production rate and the DOC-normalized DFe concentration, particularly after day 4 (Figure 6b), i.e., the onset of photoflocculation. To our knowledge, this behavior of H_2O_2 photoproduction has not been previously observed and, thus, warrants further study. After day 10, as most of the DOM had been degraded or mineralized, •OH formation decreased again. DOC decreased about 75 % after 15 days irradiation, in agreement with Helms et al. (Helms et al., 2013b). Also, the DOM showed a loss of aromatic (unsaturated) carbon and a relative rise of carboxyl and O-alkyl carbon (Chen et al., 2014). These results indicate that, •OH is likely produced mainly from the Fenton and photo-Fenton reactions initially, but after that, •OH appears to be produced mainly by other pathways, in particular DOM photoreactions.
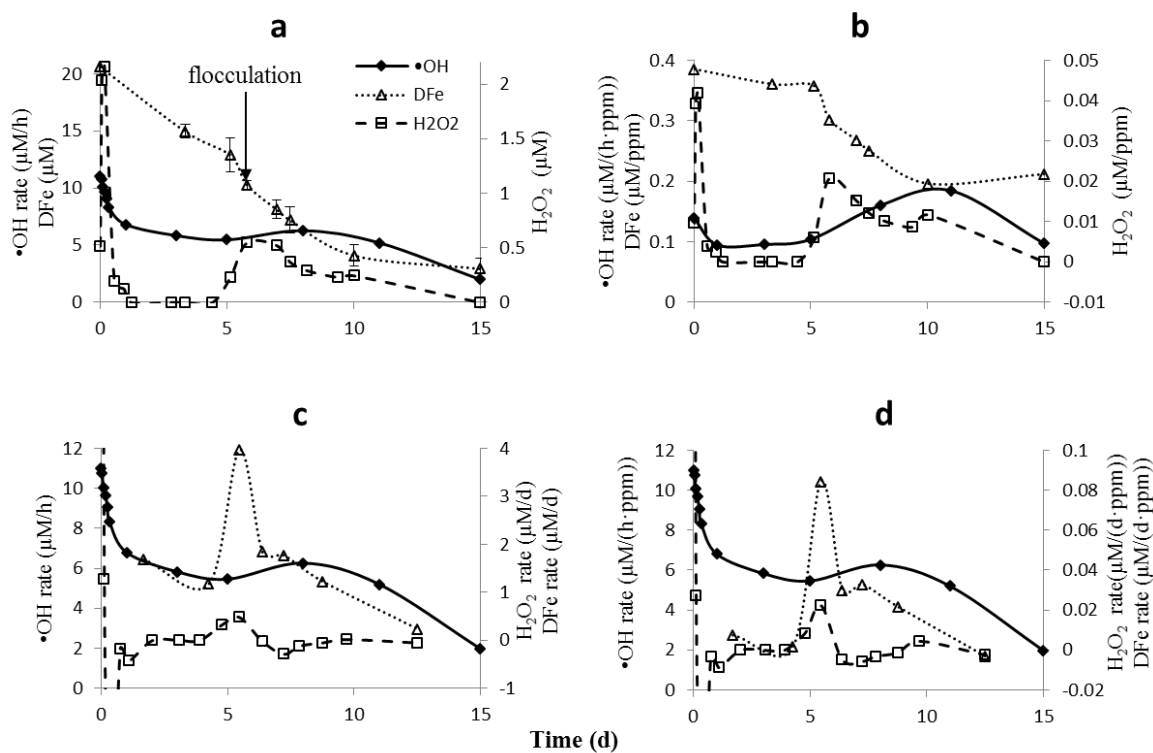
Figure 6. (a) •OH formation rate, DFe and H₂O₂ concentration; (b) •OH formation rate, DFe and H₂O₂ concentration normalized to DOC; (c) •OH formation rate, DFe loss rate and H₂O₂ formation rate; (d) •OH formation rate, DFe loss rate, and H₂O₂ formation rate normalized to DOC during irradiation. •OH (◆), H₂O₂ (□), and DFe (△). Equivalent time points for Fe and H₂O₂ were calibrated based on measured DOC in photodegraded subsamples relative to the original sample (DOC as %).

3.2 •OH formation in the aqueous wood extract sample

To further examine the importance of Fe and DOM on •OH formation, •OH formation rates, DOC, S_R, SUVA$_{254}$ and EEMS were measured in the aqueous extract of the degraded wood sample. Moreover, Fe speciation (PTFe, OFe(II), OFe(III), FFe(II), FFe(III)) was measured in Fe amended sample. Degraded wood is a major source of humic substances in DS water and contains undetectable Fe. During irradiation, flocculation was observed only in the Fe amended sample.

•OH formed in both original and Fe amended wood extracted sample (Figure 7). The •OH formation rate was initially markedly higher in the presence of Fe. During the first hour, the •OH formation rate reached 1.3 μM/h in the Fe amended sample, which was about five times that of the original sample (0.25 μM/h). However, in the Fe amended sample, the •OH formation rates dropped quickly, with the occurrence of flocculation. After the first day, the •OH formation rates were similar and low in the original and Fe amended samples.

During the irradiation, DOC decreased faster in Fe amended sample than in the original sample. The DOC dropped by 23 % in original sample but 53 % in Fe amended sample after 10 d (Figure 8a), which suggests that •OH assists the mineralization and transformation of DOM (Molot et al., 2005; Pullin et al., 2004). Despite this large difference, there was essentially no difference in the absorbance slope ratio (S_R) between the Fe amended sample and original sample (Figure 9b); S_R increased from 0.73 to 0.97 in original sample, and from 0.76 to 1.02 in the Fe amended sample. The decrease in DOC and increase in S_R during irradiation are consistent with the results of Helms et al. (Helms et al., 2008) and may indicate a decrease of molecular weight, a decrease in DOM

aromaticity, a loss of charge transfer between donor and acceptors (Del Vecchio and Blough, 2004), and/or degradation of lignin phenolic chromophores (Fichot and Benner, 2012).
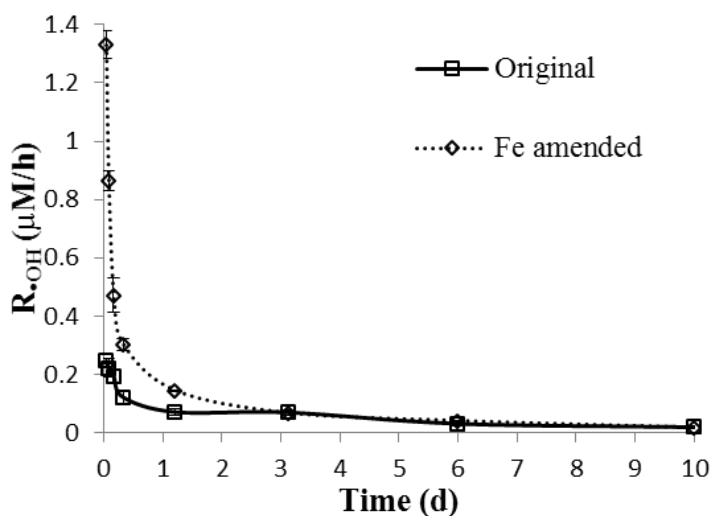
Figure 7. •OH formation rate in original and Fe amended aqueous wood extract.
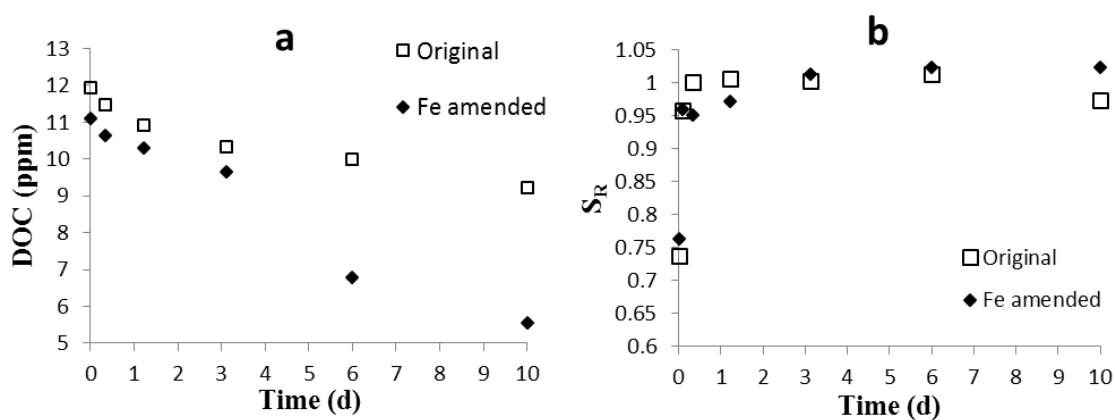
Figure 8. (a) Dissolved organic carbon (DOC); (b) Spectral slope ratio (S_R) in original and Fe amended aqueous wood extract.

In the Fe amended sample, Fe was mainly present as organic complexed Fe(III) in the aqueous phase initially (Figure 9a) (Powell and Wilson-Finelli, 2003; Pozdnyakov et al., 2015; Rue and Bruland, 1995), because the total Fe concentration (~14 μM), greatly exceeded the Fe(III) maximum soluble concentration of Fe(III) (i.e., solubility constant (K_{sp}) of Fe(OH)$_3$ is reported as 2.8×10^{-39}~6×10^{-38} in the pH range 4~5). During the initial 2 h of the irradiation, the OFe(III) was partially converted to FFe(II), as the OFe(III) fraction of TFe dropped from 64% to 38% while FFe(II) fraction rose from 6% to 41 % (Figure 9b). These results indicate a reduction of Fe, probably through charge transfer reactions (LMCT) with DOM (Barbeau, 2006; Klapper et al., 2002), and through the reduction by HO$_2$/O$_2^-$ (Voelker et al., 1997). After 2 h, the high •OH formation rate in conjunction with the changes in the FFe(II) fraction indicate that Fe(II) was oxidized to Fe(III), probably via the Fenton reaction. Because the DOM in the degraded wood extract contained a high concentration of hydroxyl and carboxyl groups (Sleighter and Hatcher, 2008; Waggoner et al., 2015), which can form strong complexes with Fe, the Fenton reaction may have involved mainly organic-complexed Fe, rather than free inorganic Fe. Thus, Fe was rapidly cycling between Fe(II) and Fe(III) (Shiller et al., 2006) during the irradiation.
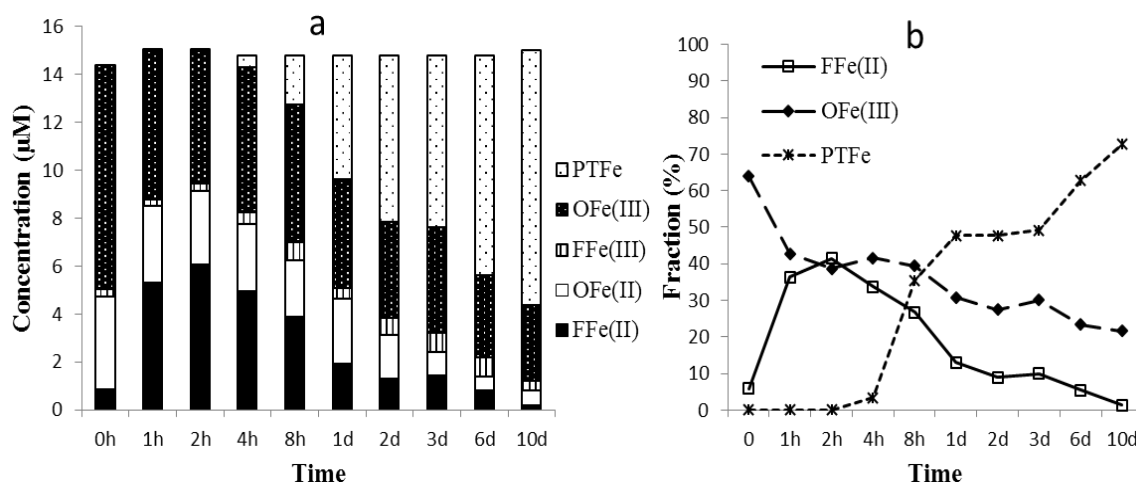
Figure 9. (a) Particle total Fe (PTFe), DOM-complexed Fe(II) (OFe(II)), DOM-complexed Fe(III) (OFe(III)), free Fe(II) (FFe(II)), free Fe(III) (FFe(III); (b) FFe(II) and OFe(III), and PTFe fraction of TFe (%) in Fe amended aqueous wood extract during irradiation. Note non-linearity of the time axis.

Because the iron complexed organic ligands were continuously degraded during the irradiation, when the FFe(III) concentration exceeded the maximum soluble concentration, insoluble $Fe(OH)_3$ formed, which coprecipitated with or adsorbed organic matter. One may argue that the precipitation was mainly due to an increase of pH during the irradiation. The system initially was buffered by carboxylates but was later buffered by bicarbonate because carboxylates degraded while CO_2 accumulated under UV light. Thus, the pH increased and the K_{sp} of $Fe(OH)_3$ decreased, making the Fe less soluble. However, in our experiment, the pH did not significantly change during the first few hours and thus, initially, it would have had little effect on the observed flocculation (Figure 10). Therefore, it appears that the degradation of iron complexing ligands is more important than the pH effect. This conclusion is further supported by Chen et al. (2014),

who found the Fe/carbon molar ratios of DOM decreased while this ratio increased for

POM using X-ray absorption spectra, and Waggoner et al (2015), who showed that the

flocculation occurred with addition of Fe.

To summarize the above results, Fe participates in the Fenton reaction to form •OH,

and continuing irradiation reduces Fe(III) to Fe(II) probably through LMCT reactions and

reduction by HO_2/O_2^-. Moreover, Fe appears to plays a critical role in the

photoflocculation process as virtually no flocculation occurred in the original (low iron)

sample during 10 d.

45
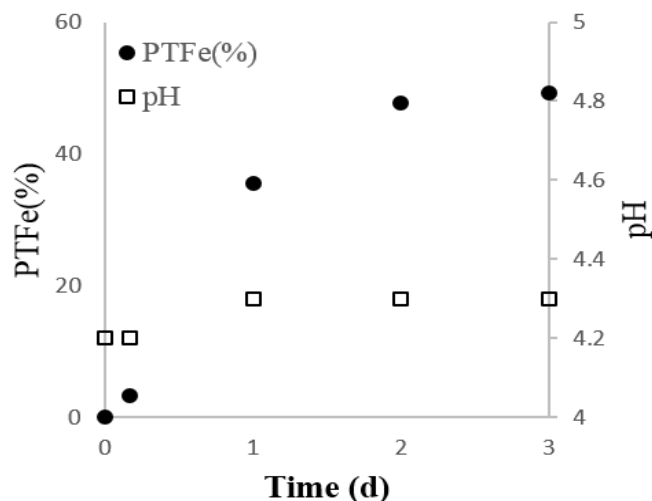
Figure 10. PTFe fraction of TFe (%) and pH in Fe amended aqueous wood extract during 3 d irradiation.

In absence of Fe, •OH also formed and the DOM could be the only source, as nitrate and nitrite concentrations were negligible. •OH formation rate decreased with decreasing DOC during irradiation (Figure 7). Moreover, the •OH formation rates normalized to DOC and SUVA$_{254}$, which is positively correlated to DOM aromaticity (Weishaar et al. 2003; Helms et al. 2008), decreased (Figure 11). The latter results indicate that the non-irradiated original sample has the highest capability to produce •OH, and the chromophoric sites within DOM responsible for •OH production were transformed and/or degraded during irradiation.
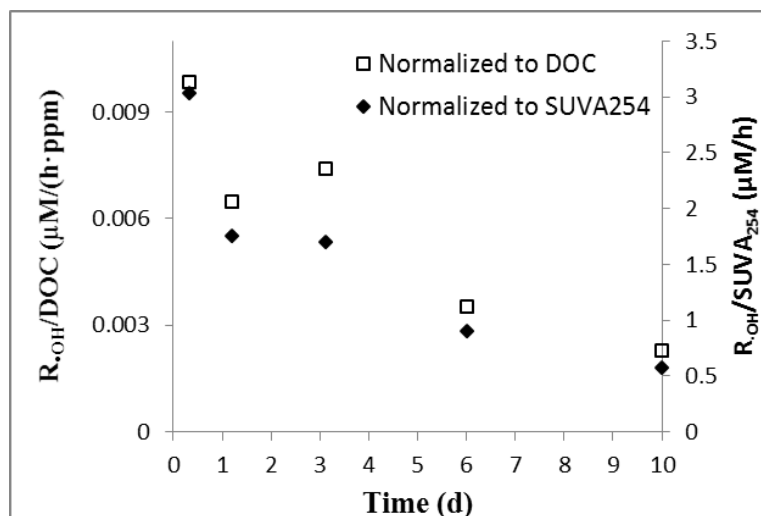
Figure 11. •OH formation rate normalized to DOC and SUVA$_{254}$ in aqueous wood extract.

Fluorescence EEMS showed the overall fluorescent intensity of the aqueous wood extract sample (non-Fe amended) decreased markedly during irradiation (Figure 12). The fluorescence EEMS was not measured in the Fe amended sample because Fe has significant quenching effect on the fluorescence intensity (Cabaniss, 1992; Manciulea et al., 2009; Pullin et al., 2007). Three main components were identified in all non-Fe-amended samples by EEMS coupled with PARAFAC analysis (Figure 13): components 1 and 2 are characterized as humic-like DOM, since they display broad emission spectra around and above 400 nm; components 3 is characterized as tryptophan-like DOM (Fellman et al., 2010; Guo et al., 2011; Yamashita et al., 2008). Components 1 and 2 decreased while component 3 did not change significantly during 10 day irradiation (Figure 14). The decrease of humic-like components during irradiation is consistent with past studies (Ishii and Boyer, 2012; Xu and Jiang, 2013). Also, the result is consistent to

the past studies that showed that aromatic carbons were preferentially removed while amide/peptide-like carbons were preserved during UV exposure (Helms et al., 2014).
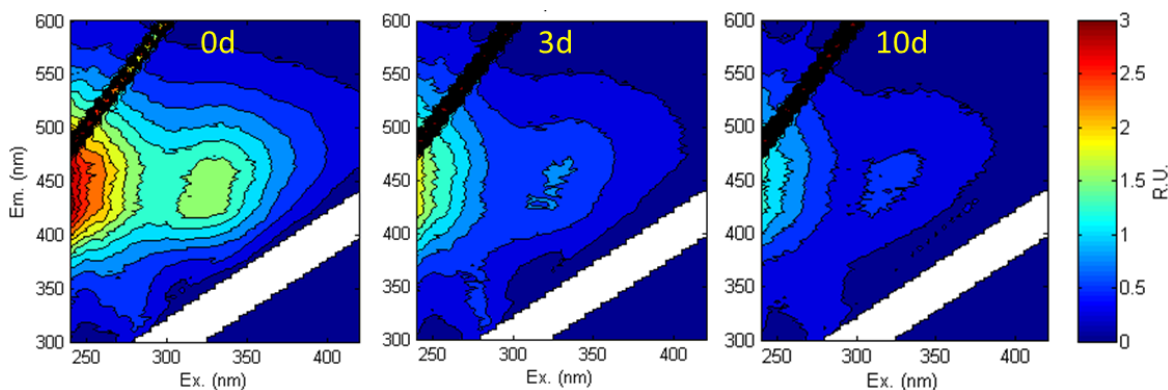
Figure 12. Fluorescence EEMS of the aqueous wood extract sample at 0 d, 3 d, and 10 d irradiation.
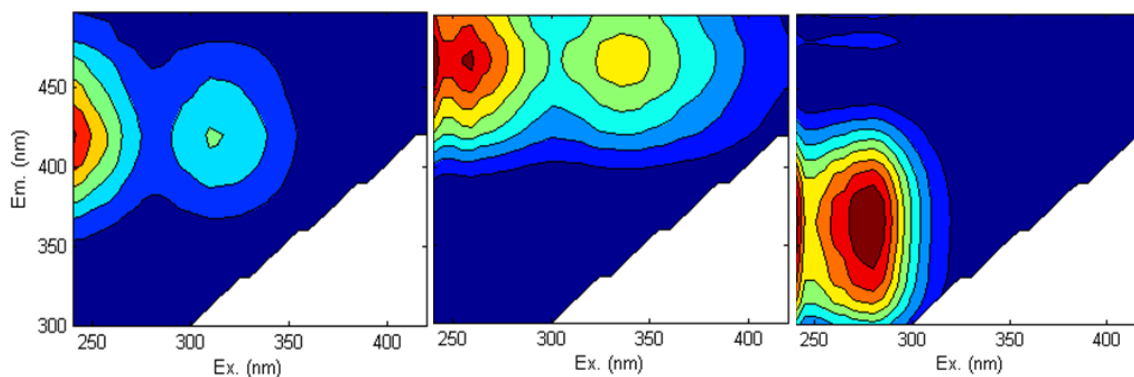
Figure 13. Three components identified by PARAFAC analysis in all non-Fe-amended samples. Components 1 and 2 are humic-like DOM, and component 3 is tryptophan-like DOM.
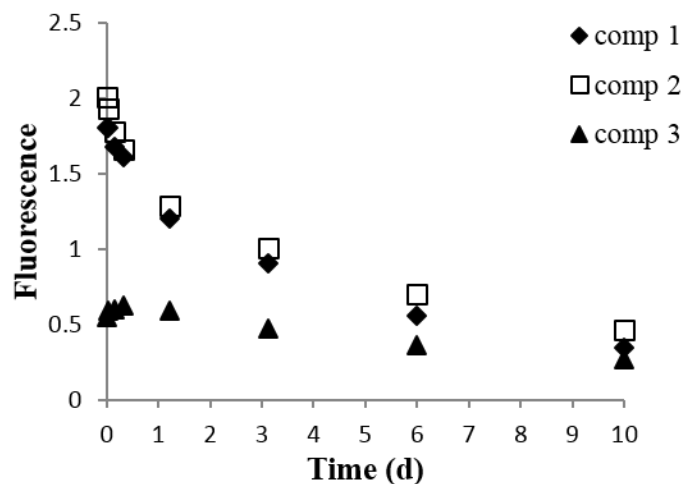
Figure 14. Components 1 and 2 (humic-like DOM), and component 3 (tryptophan-like DOM) during irradiation.

From above results, the decrease of •OH formation rates normalized to DOC and SUVA$_{254}$, and decrease of humic-substance components fluorescence intensity indicate that •OH photochemical formation in natural waters is strongly related to humic substances, which are known to contain aromatic moieties with mainly carboxyl and hydroxyl functionalities (McDonald et al., 2004). The likely phenolic moieties within humic substances that can produce •OH are discussed in Chapter IV by using model compounds.

CHAPTER IV

INSIGHTS INTO THE PHOTOCHEMICAL FORMATION OF THE

HYDROXYL RADICAL FROM DISSOLVED ORGANIC MATTER USING

PHENOLIC ACIDS AS MODEL COMPOUNDS

1. INTRODUCTION

The hydroxyl radical ($\bullet OH$) is one of the most reactive species in natural waters. Dissolved organic matter (DOM) photolysis is an important source for $\bullet OH$ production in many natural waters. There are two main $\bullet OH$ production pathways from DOM: a hydrogen peroxide (H_2O_2) dependent pathway, where the H_2O_2 is formed from DOM (Vione et al., 2006), and an H_2O_2 independent pathway (Page et al., 2011). In the latter pathway, the $\bullet OH$ production sites have been speculated to be quinone moieties within humic substances (Page et al., 2011; Vaughan and Blough, 1998) based on the fact that quinone model compounds take part in the $\bullet OH$ probe trapping reactions (Alegría et al., 1999; Ononye and Bolton, 1986; Pochon et al., 2002; Gan et al., 2008). In the early studies (Ononye and Bolton, 1986), it was hypothesized that excited triplets of quinone abstract a H-atom from water to produce free $\bullet OH$ and a semiquinone. However, several studies have questioned the importance of quinones in the production of $\bullet OH$. Firstly, the quinone concentration within DOM is too low in most instances (Sharpless and Blough, 2014). Secondly, but most importantly, there is strong evidence against the production of *free* $\bullet OH$ by benzoquinone; instead, the evidence supports the formation of a reactive oxidizing intermediate, which is less reactive and more kinetically selective than the free $\bullet OH$, is responsible for the observed $\bullet OH$ trapping reactions (Clark and Stonehill, 1972;

Phillips et al., 1986; Pochon et al., 2002; Gan et al., 2008). Thus, the sources and the mechanisms of the •OH formation from DOM are essentially unknown (Sharpless and Blough, 2014).

This chapter focuses on •OH formation and quantum yields from phenolic acids. We chose to study these compounds because aromatic compounds or moieties within DOM contain mainly carboxyl and hydroxyl functionalities, especially humic acid, lignin and tannin derived phenolics (Hayes et al., 1989). Secondly, an excited quinoid enol tautomer, similar to quinone structure, has been observed in several hydroxyphenacyl compounds by laser flash spectroscopy (Klíčová et al., 2012; Vulpius et al., 2010). Since the excited state quinone is stronger oxidants than ketones (Pochon et al., 2002), this tautomer may take part in the •OH probe reactions. Surprisingly, we found that aromatic compounds with para hydroxyl and carboxyl groups, particularly the 2,4-dihydroxybenzoic and 4-hydroxybenzoic acids, exhibit high •OH photoproduction. We conducted methane trapping and competition kinetics experiments to evaluate the relative importance of free •OH vs. less reactive oxidative species. Moreover, we hypothesize a mechanism for •OH formation from these compounds, and examined pH effects with respect to this mechanism.

2. EXPERIMENTAL

2.1 Chemicals and materials

The following chemicals were used: phenol (purity grade >99 %, Sigma), benzene (HPLC grade, Sigma), sodium benzoate (99.5 %, Sigma), salicylic acid (99%, Fisher), 3-hydroxybenzoic acid (99%, Acros), 4-hydroxybenzoic acid (99%, Sigma), 2,3-

dihydroxybenzoic acid (99%, Sigma), 1,4-benzoquinone (99%, Sigma), 2,6-dihydroxybenzoic acid (98%, Aldrich), 2,4-dihydroxybenzaldehyde (98 %, Aldrich), 2,5-dihydroxybenzoic acid (99%, Fluka), 2,4-dihydroxybenzoic acid (98%, TCI), ferric chloride (99%, Sigma), 1,10-phenanthroline (99%, Aldrich), potassium oxalate (99%, Baker), 3-Amino-2,2,5,5,-tetramethyl-1-pyrrolidinyloxy free radical (3-ap) (Sigma), fluorescamine (99%, Fisher), sodium nitrite (99.7%, Fischer), methane (UHP grade, Matheson), H_2O_2 (35 % w/w, Acros), dimethyl sulfoxide (B&J), methanol (HPLC grade, Acros) and acetonitrile (HPLC grade, EMD). The acetonitrile was dried with anhydrous sodium sulfate (99%, Sigma), which was dried at 200 ℃ about 4 hours prior to use. Ultra-pure water (Milli-Q water, >18 MΩcm^{-1}, Millipore) was used for solution preparation. The buffer solutions were as follows: pH 4.5~5.5 (5 mM acetate buffer), pH 6~7 (5 mM phosphate buffer), pH 8~9 (5 mM borate buffer). Potassium ferrioxalate used for actinometry was prepared by adding three parts potassium oxalate (1.5 M) to one part ferric chloride (1 M). The resulting precipitate was recrystallized three times with Milli-Q water and dried in a vacuum oven.

2.2 Irradiation system and actinometry

All quantum yield (Φs) measurements were carried out using a 3 cm cuvette and an Oriel tunable light source (10 nm bandwidth wavelength) with 1000 W xenon lamp and grating monochromator (Model 77200). The light flux was determined by the potassium ferrioxalate actinometer (Murov et al., 1993).The light flux, P_λ (einstein L^{-1}h^{-1}), was calculated as followed:

$$P_{\lambda=} \frac{\Delta n}{\Phi_\lambda t(1-10^{-A})} \tag{1}$$

Where Δn is ferrous iron photo-generated (moles per unit volume), which is obtained from the trisphenanthroline complex concentration, t is the irradiation time (h), A is the absorbance in a 3 cm cuvette, and Φ_λ is potassium ferrioxalate quantum yields, which were obtained from the *Murov's Handbook of Photochemistry* (Murov et al., 1993). The value of 1.24 was used for Φ_λ in the wavelength rage 280~310 nm.

Methane trapping experiment, competition kinetics experiment, and model compounds degradation experiment were conducted by using a simulator containing UVA340 bulbs (Q-Panel). These lamps have a spectral output nearly identical to natural sunlight from ~295 to ~360 nm (http://www.solarsys.biz/0103.shtml). In a comparison of the light output from the solar simulator to natural sunlight, the solar simulator provided 127% of the photobleaching occurring under winter mid-day sunlight at 36.89 °N latitude (Helms et al., 2008).

2.3 •OH formation rate (R_{OH})

•OH photoproduction from model compounds was determined using 1 mM benzene as the probe. The relative high concentration is used because it can outcompete any other reactions. Production rates of phenol (from benzene) were measured by HPLC (Sun et al., 2014). R_{OH} (M h^{-1}) was calculated as followed:

$$R_{OH} = \frac{R_{ph}}{Y_{ph}} \tag{2}$$

Where R_{ph} is the photo-formation rate of phenol, and Y_{ph} is the yield of photoproduct formed for each probe by •OH, the value is 0.69 (Sun et al., 2014).

2.4 •OH quantum yields (Φs)

For most model compounds, Φs were measured at wavelengths 290~340 nm, unless otherwise indicated. These wavelengths were selected because the natural sunlight

cutoff is ~290 nm and most compounds studied have negligible absorption above 350 nm. Φs were determined from:

$$\Phi = \frac{R_{OH}}{P_\lambda (1 - 10^{-A})} \tag{4}$$

Where P_λ (einstein L^{-1}h^{-1}) is the light flux, which was determined by the potassium ferrioxalate actinometer (Murov et al., 1993). A is the absorbance of the model compounds in a 3 cm cuvette. Φs were examined in buffer solutions and dry acetonitrile.

2.5 Methane trapping reaction

3-Amino-2,2,5,5,-tetramethyl-1-pyrrolidinyloxy free radical (3-ap) was added to the samples (model phenolic chromophore or sodium nitrite in 20 mM borate buffer at pH 8) in a 4 mL septum vial to a final concentration of 100 μM. The mixture was flushed with nitrogen for 5 min to remove oxygen, and then methane for 10 min. The vial was then irradiated in the solar simulator. After 2 h irradiation, 1 mL of the solution was mixed with 200 μL 2.5 mM fluorescamine and analyzed by HPLC (Vaughan and Blough, 1998). Nitrite was selected as a free •OH source because it has absorbance above 290 nm, which is the cut-off for the glass vial.

2.6 Competition kinetics experiments

A series of concentrations (0.5 mM to 3 mM) of competitor formate or DMSO was added to solutions with probes (1 mM benzene or 1 mM benzoate). Formate, benzene, DMSO, and benzoate react with •OH at reaction rates of k_f (3.2×10^9), k_{be} (7.8×10^9), k_{DMSO} (7.0×10^9), and k_{ba} (4.3×10^9) respectively (Buxton et. al., 1987). The experimental rate constant ratios (k_f/k_{be}, k_f/k_{ba}, and k_{DMSO}/k_{ba}) were compared for irradiated solutions of 20 μM 2,4-DHBA and 100 μM H_2O_2, the latter being a pure free •OH source.

3. RESULTS AND DISCUSSIONS

3.1 Benzene trapped-OH Φs from model compounds

We examined eleven model compounds including five dihydroxybenzoic acids (DHBA), three hydroxybenzoic acids (HBA), two resorcinols (RS), and one dihydroxybenzaldehyde (DHA) (Figure 15). The concentration of model compounds used was 20 μM. The absorbance spectra of these compounds at pH ~7, which were measured by an Agilent 8453 diode array spectrophotometer with a 3 cm quartz cuvette, are shown in Figure 16.
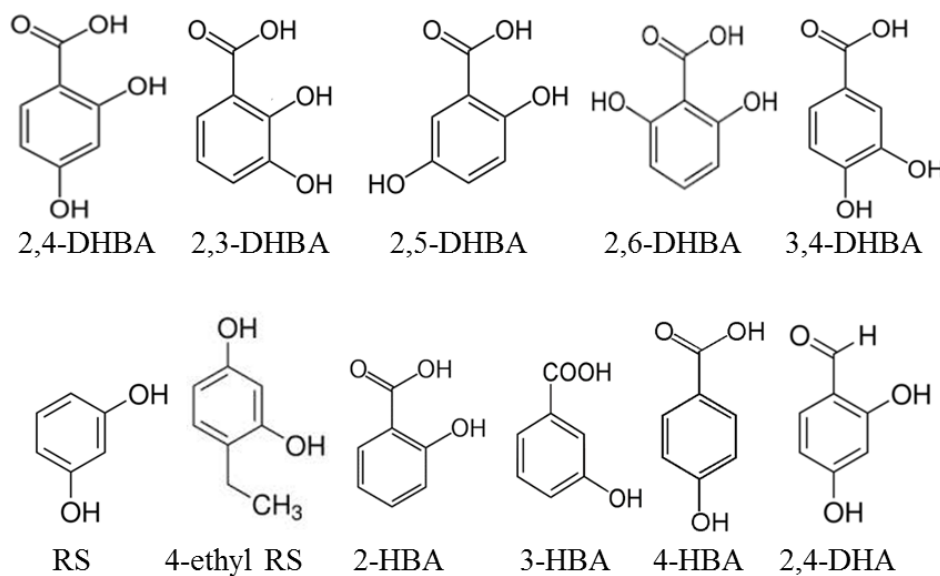
Figure 15. Structure of eleven model compounds. NOTATION: DHBA-dihydroxybenzoic acid, HBA - hydroxybenzoic acid, DHA – dihydroxybenzaldehyde, RS-resorcinol.
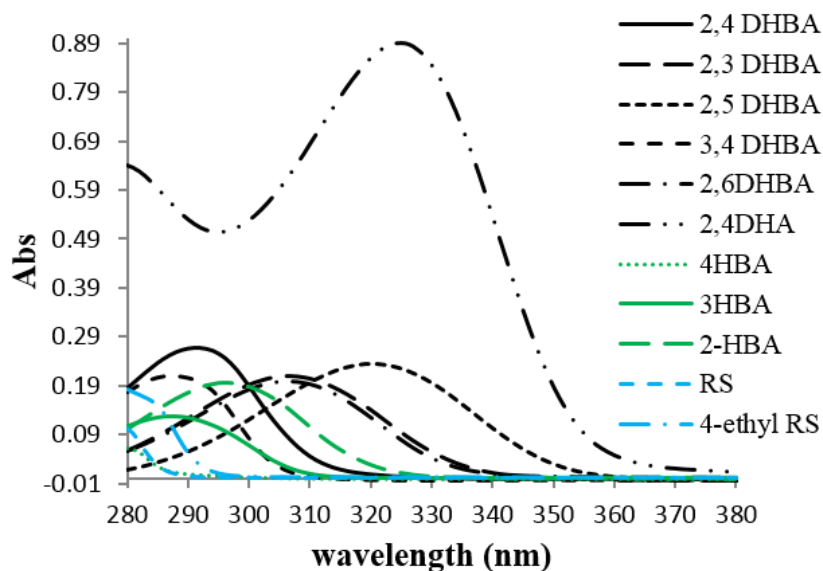
Figure 16. Absorbance spectra of 20 μM model compounds at pH ~7.

•OH Φs of these model compounds using the benzene probe are shown in Table 3, whereas the spectral dependence of the phenolic acids are shown in Figure 17 (Φs were only shown for the wavelengths where the compounds have detectable absorbance ($>5 \times 10^{-3}$). Of the five DHBAs, 2,4-DHBA had the highest •OH Φs (Figure 17a); the Φ at 310 nm is $(12.9 \pm 0.4) \times 10^{-3}$, which is about an order-of-magnitude greater than all other DHBA isomers except 3,4-DHBA. Φs for 4-HBA are similar to 2,4-DHBA, and are much higher than 3-HBA and 2-HBA (Figure 17b). These results show that many phenolic acids are capable of producing •OH, and the ones with para hydroxyl and carboxyl groups (4-HBA and 2,4-DHBA) have the highest •OH Φs.

Table 3.

Quantum yields (Φs) of 20 μM model compounds using benzene as the probe at wavelengths 280-340 nm at pH 7.

	$\Phi s \times 10^3$ at each wavelength					
	290 nm	300 nm	310 nm	320 nm	330 nm	340 nm
2,4-DHBA*	9.8±0.1	8.0±0.1	12.9±0.4	8.9±1.2	/[a]	/
3,4-DHBA	0.7±0.1	0.7±0.1	2.5±0.2	1.0±0.3	/	/
2,5-DHBA	1.4±0.1	1.1±0.1	0.4±0.1	0.2±0.03	0.08±0.02	N/A[b]
2,3-DHBA	0.8±0.2	0.4±0.1	0.3±0.1	0.1	N/A	N/A
2,6-DHBA	N/A	N/A	N/A	N/A	N/A	N/A
2,4-DHA	0.8±0.04	0.5±0.02	0.8±0.02	0.1±0.01	0.1±0.01	0.08
	280 nm	285 nm	290 nm	300 nm	310 nm	
4-HBA	10.0±0.4	10.3±0.6	11.3±1.2	/	/	
2-HBA	0.6±0.1	0.4±0.1	0.5±0.1	0.2±0.1	N/A	
3-HBA	N/A	N/A	N/A	/	/	
RS	2.1±0.3	1.9±0.4	/	/	/	
4-Ethyl-RS	2.1±0.3	1.5±0.2	2.2±0.4	/	/	

*DHBA-dihydroxybenzoic acid, HBA-hydroxybenzoic acid, DHA-dihydroxybenzaldehyde, RS-resorcinol

[a] The symbol / means Φs is not measured due to low absorbance ($<5 \times 10^{-3}$).

[b] The symbol N/A means •OH production is below detection limit (1.2 nM).
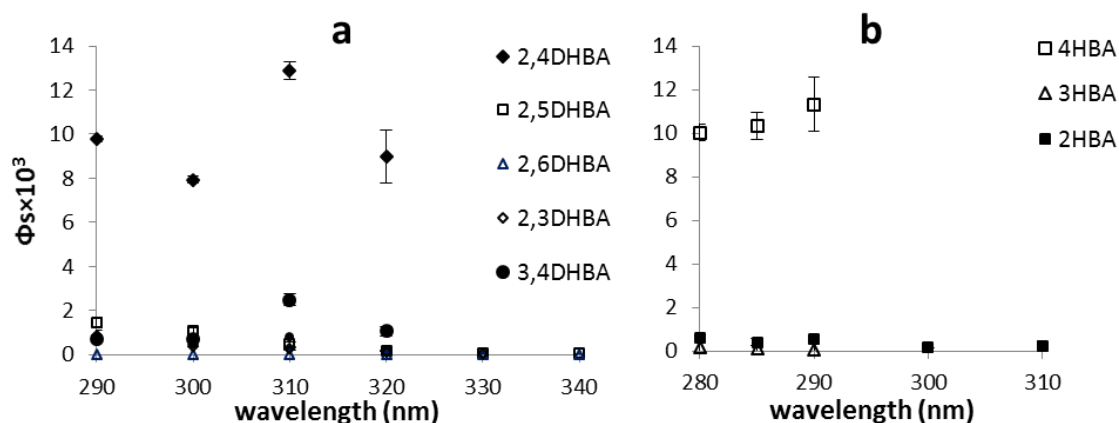
Figure 17. Quantum yields (Φs) of 20 μM phenolic acids model compounds using benzene as the probe at wavelengths 290-340 nm at pH 7. NOTATION: DHBA-dihydroxybenzoic acid, HBA - hydroxybenzoic acid. Large error bars in the case of 2,4DHBA and 4HBA were due to low absorbance at the longer wavelengths.

Due to its high •OH production, 2,4-DHBA was selected for further experimentation. The degradation rate of 2,4-DHBA was measured in the absence of probes by HPLC, and compared with the benzene trapped •OH production rate. In Figure 18, the slopes are the degradation/formation rates (μMh^{-1}). It shows that the formation of •OH appeared to arise from a primary reaction, as suggested by the 4:1 correspondence of the degradation rate of 2,4-DHBA vs. benzene trapped-OH rate.

The absorbance of 2,4-DHBA was measured after 2h irradiation. The result (Figure 19) shows that absorbance centered at 290 nm was lost while peaks at 266, 312 and 490 nm formed. Interestingly, the latter is similar to the absorbance of hydroxybenzoquinone that is produced from 1,4-benzoquinone (Q) photodegradation (Gan et al., 2008). However, 2,4-DHBA is much more stable than 1,4-Q, the absorbance of the latter one

changed dramatically during the 2 h irradiation. The photoproducts from 2,4-DHBA will be examined by mass spectroscopy in a future study.
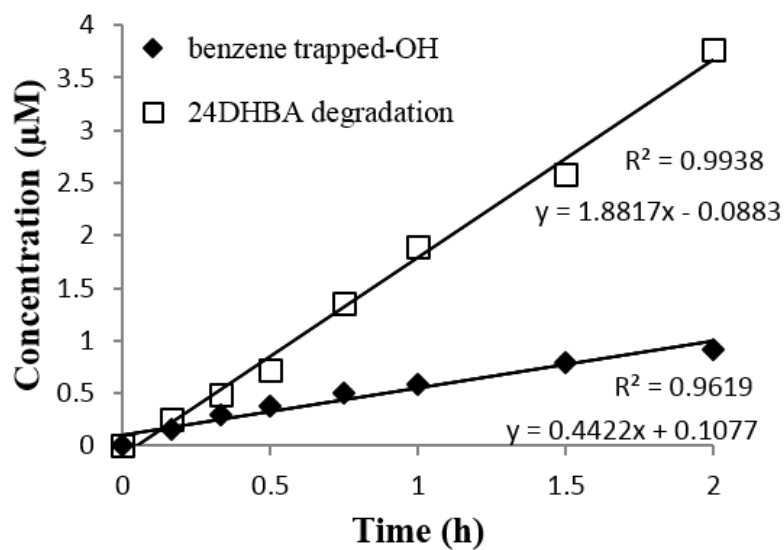
Figure 18. 2,4-DHBA degradation vs. benzene trapped-OH during a 2 h irradiation. The degradation concentration was obtained by HPLC.
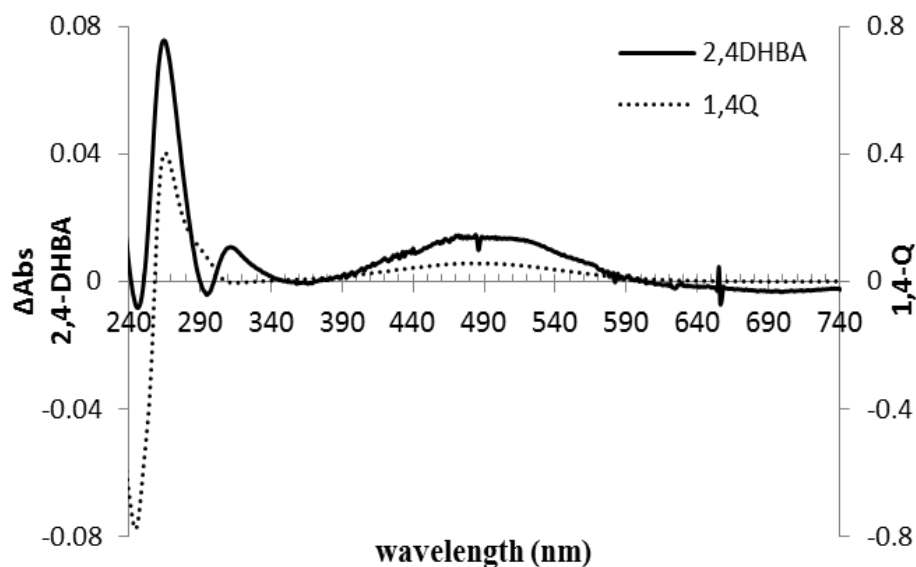
Figure 19. Subtraction of absorbance (2h - 0h) of 2,4-DHBA and 1,4-benzoquinone (Q). Positive absorbance indicates production while negative absorbance indicates loss. Notice difference in the scale range.

3.2 Free •OH vs. less reactive oxidative species

Published quinone studies have shown that a reactive intermediate, perhaps a triplex (or exciplex) containing bound water (Gan et al., 2008; Pochon et al., 2002), rather than free •OH (Ononye and Bolton, 1986), takes part in probe trapping reactions and results in the observed "•OH" production. In order to determine whether free •OH is formed by phenolic model compounds, we conducted methane trapping and competition kinetics experiments using 2,4-DHBA. Free •OH reacts with methane to form the methyl radical (k=1.2×10^{8}M^{-1}s^{-1}); however, the oxidative species are not sufficient reactive to abstract an H atom from methane (Gan et al. 2008 ; Zhu et al. 2008; Page et al., 2011). The methyl radical can be trapped by the nitroxyl radical 3-ap and the product can be converted to a fluorescent derivative by reaction with fluorescamine, which can be

measured by HPLC (Kieber and Blough, 1990; Pochon et al., 2002). In Figure 20, the

methyl peak identity was verified by irradiation of 10 μM nitrite in the presence of 10

mM dimethyl sulfoxide (DMSO) (k=6.6×10^{9}M-^{1}s-^{1}) (Vaughan and Blough, 1998), which

can outcompete nitrite quenching of •OH (k=1.1×10^{10}M-^{1}s-^{1}); the "2,4-DHBA blank" is

irradiation 2,4-DHBA and 3-ap without methane. Our results show that irradiation of 2,4-

DHBA produces this fluorescent methyl radical derivative, like nitrite photolysis, which

is a known source of free •OH (Page et al., 2011). Thus, it can be concluded that

irradiation of 2,4-DHBA produces free •OH.
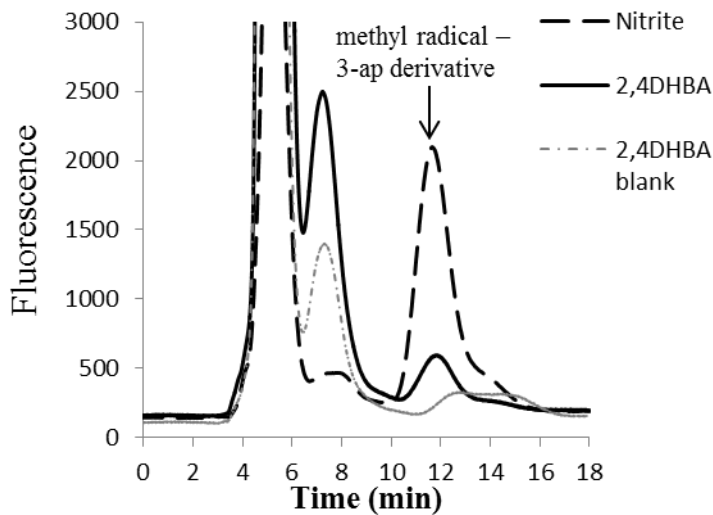
Figure 20. HPLC chromatogram showing the production of the fluorescent methyl

radical – 3-ap fluorescamine derivative from reaction of 20 μM 2,4-DHBA or10 μM

nitrite with methane after 2 h irradiation at pH 8 (50 mM borate buffer).

In the competition kinetics experiments, the formation rates of the photoproduct (phenol or SA) were obtained at different formate concentrations. Formate, benzene, and benzoate react with •OH at a constant reaction rate k_f, k_{be}, and k_{ba}, respectively. From the equation (Zhou and Mopper, 1990):

$$R_n = R_0 \times \frac{k_p[\text{Probe}]}{k_c[\text{Competitor}] + k_p[\text{Probe}]}$$

Where [Probe] is the concentration of probe; [Competitor] is the concentration of competitor; R_n is the photoproduct formation rate at different competitor concentrations of formate or DMSO; R_0 is the photoproduct formation rate with no competitor added. The ratios of the rates are:

$$\frac{R_0}{R_n} = (k_c/k_p)([\text{Competitor}]/[\text{Probe}]) + 1$$

Plotting R_0/R_n against [Competitor]/[Probe], a straight line was obtained (Figure 21, Figure 22, and Figure 23, right panels). The rate constant ratios (k_f/k_{be}, k_f/k_{ba}, and k_{DMSO}/k_{ba}) were calculated from the slopes. The experimental rate constant ratios were compared for irradiated solutions of 20 μM 2,4-DHBA and 100 μM H_2O_2, the latter being a pure free •OH source.
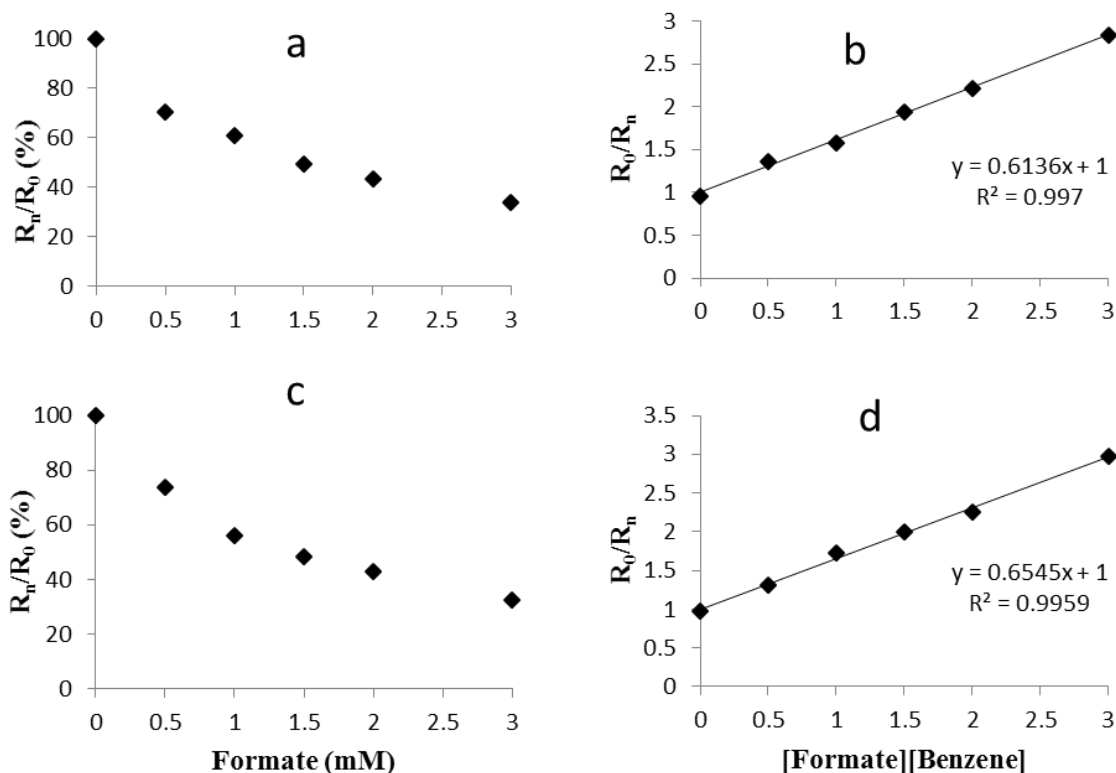
Figure 21. (a) The effect of formate concentration on phenol relative formation rate R_n/R_0 (%); (b) R_0/R_n vs [Formate]/[Benzene] using 2,4- DHBA as the •OH source and benzene as the probe; (c) The effect of different formate concentration on phenol relative formation rate R_n/R_0 (%); (d) R_0/R_n vs [Formate]/[Benzene]) using H_2O_2 as the •OH source and benzene as the probe. R_n is the photoproduct formation rate at a given competitor concentration; R_0 is the photoproduct formation rate with no competitor added.
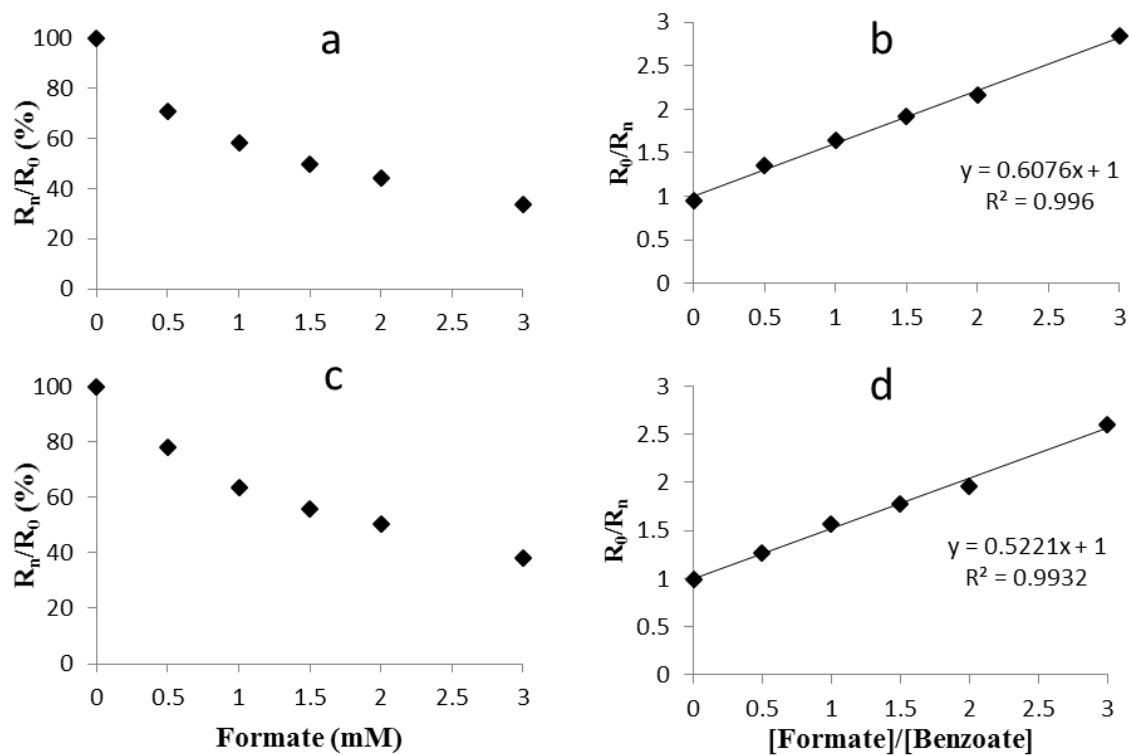
Figure 22. (a) The effect of formate concentration on SA relative formation rate R_n/R_0 (%); (b) R_0/R_n vs [Formate]/[Benzoate] using 2,4- DHBA as the •OH source and benzoate as the probe; (c) The effect of formate concentration on SA relative formation rate R_n/R_0 (%); (d) R_n/R_0 vs [Formate]/[Benzoate]) using H_2O_2 as the •OH source and benzoate as the probe.
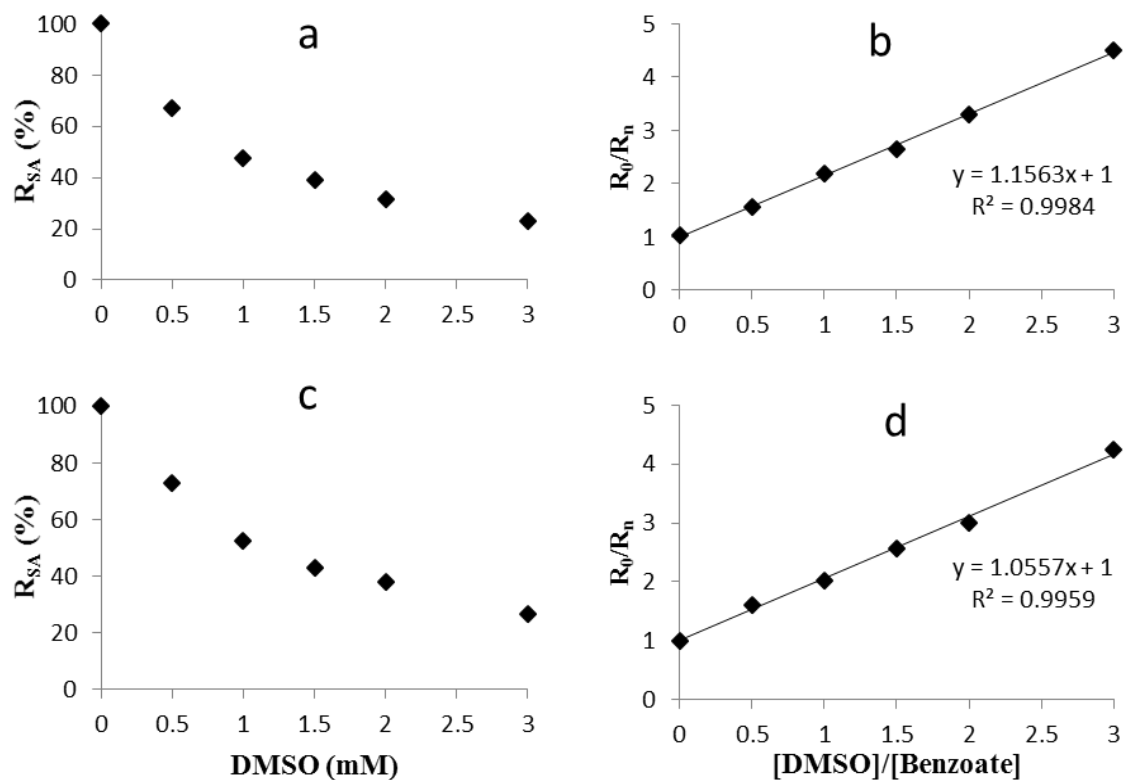
Figure 23. (a) The effect of DMSO concentration on SA relative formation rate R_n/R_0 (%); (b) R_0/R_n vs [Formate]/[Benzoate] using 2,4-DHBA as the •OH source and benzoate as the probe; (c) The effect of DMSO concentration on SA relative formation rate R_n/R_0 (%); (d) R_n/R_0 vs [Formate]/[Benzoate]) using H_2O_2 as the •OH source and benzoate as the probe.

Our results (Table 4) show that k_f/k_{be}, k_f/k_{ba}, and k_{DMSO}/k_{ba} measured using 2,4-DHBA as the OH source were consistent with that measured in irradiated H_2O_2. The slightly higher experimental k_f/k_{be} ratio in H_2O_2 than the literature values may be due to minor differences in •OH method calibration.

From the above results, it may be concluded that free •OH is formed from 2,4-DHBA. This conclusion is consistent with a study of natural DOM that free •OH was produced from irradiated DOM (Page et al., 2011).

Table 4.

Rate constant ratios formate to benzene (k_f/k_{be}), formate to benzoate (k_f/k_{ba}) and DMSO to benzoate (k_{DMSO}/k_{ba}).

	2,4 DHBA as OH source	H_2O_2 as OH source	Value calculated from the literature (Buxton et al., 1988)
k_f/k_{be}	0.62±0.01*	0.64±0.04	0.41~0.56
k_f/k_{ba}	0.60±0.01	0.55±0.03	0.45~0.56
k_{DMSO}/k_{ba}	1.00±0.06	1.11±0.06	1.12~1.23

*: The error is calculated from duplicate measurements.

3.3 Importance of phenolic acids in DOM

The apparent Φs from DOM $(0.08\sim0.6) \times 10^{-3}$ (Vaughan and Blough, 1998; White et al., 2003b) are much lower than the Φs of most of the model phenolic acids. In the case of DOM, the specific chromophore (or chromophores) giving rise to a specific phototransient (e.g., •OH) or product is (are) not known for either indirect photochemical processes or direct photochemical reactions. Therefore, for environmental photochemical studies, the photoefficiency is calculated using the total number of photons absorbed by all DOM chromophores (i.e., as opposed to the actual DOM chromophores giving rise to the photoproduct of interest, e.g., •OH), and the term *apparent* Φ is applied. Therefore, apparent Φs are always less (typically much less) than *true* Φs for pure compounds.

Our results suggest that phenolic acids are important sources of photochemically formed •OH within DOM. These phenolic acids can be originally present in humic substances (Hayes et al., 1989), or formed through photochemical processes, e.g. the acid–to-aldehyde ratio of lignin phenolic compounds increases during irradiation indicating oxidative conversion to phenolic acids (Spencer et al., 2009). In addition, ring hydroxylation of phenols by •OH is well documented (e.g., benzoic acid hydroxylation (Zhou and Mopper, 1990)) and undoubtedly occurs to DOM phenolic moieties during solar irradiation.

3.4 Hypothesized mechanism of •OH production from phenolic model compounds

The phenolic model compounds with para hydroxyl and carboxyl groups have high •OH Φs. We speculate that a triplet state quinoid enol tautomer ($^3Q^*$) is responsible for this high photoproduction (Figure 24). In this scheme, $^3Q^*$ is formed following fast intersystem crossing (ISC) to the triplet state, and then triplet proton transfer through

bound solvent water (Klíčová et al., 2012; Vulpius et al., 2010). In the latter process, water molecules that are hydrogen bonded to the compounds facilitate the transfer of the para phenolic proton to the carbonyl oxygen in the excited triplet. Thus, the $^3Q^*$ is speculated to be present as a water cluster (Klíčová et al., 2012). The hydrogen bond between the tautomer and the bound water may induce H-OH bond cleavage by lowering the activation energy needed for bond dissociation. In agreement with a water dependent mechanism, we found no •OH formation from 2,4-DHBA in dry acetonitrile. In addition, in support of the tautomer hypothesis, substituting either a proton or ethyl group for the carboxyl group greatly decreased the •OH Φs (RS and 4-Ethyl-RS in Table 3). In future research, the tautomer pathway needs to be confirmed, e.g. by using laser flash spectroscopy (Klíčová et al., 2012) and product analyses, e.g., via mass spectrometry.
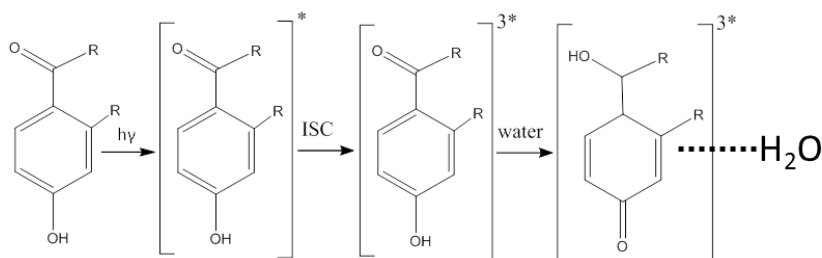
Figure 24. Formation of excited triplet tautomer cluster ($^3Q^*$) through intersystem crossing (ISC) and excited proton transfer. R=H, OH

3.5 Substituent group and pH effects

3,4-DHBA also contains a hydroxyl group para to the carboxyl group but has lower •OH QYs than 2,4-DHBA (Figure 17 and Table 3). The lower QY of 3,4-DHBA may be due to intramolecular hydrogen bonding between the carbonyl (at the 4 position) and

hydroxyl group (at the 3 position) in the tautomer intermediate, which would inhibit or slow photoreduction of this compound (Alegría et al., 1999). Moreover, substituting an aldehyde group for the carboxyl group of 2,4-DHBA to become 2,4-DHA decreased the •OH Φs (Table 3), though 2,4-DHA should also form the excited state tautomer as hypothesized. The reason for the decrease is unknown but may be due to the strong electron withdrawing effect of the carbonyl group. More tests need to be conducted in a future study.

Figure 25 shows that •OH Φ decreased with increasing pH after certain pH values; for 4-HBA the pH value was 7, while for 2,4-DHBA the pH was 9. If both 4-HBA and 2,4-DHBA undergo the $^3Q^*$ pathway to produce •OH, the $^3Q^*$ is in equilibrium with its dianion (Figure 26), as is shown in past studies (Klíčová et al., 2012; Vulpius et al., 2010). Low pH (below the excited state pK_a^* of the $^3Q^*$) favors the $^3Q^*$, while high pH favors its divalent anion. Since proposed •OH formation mechanism requires the presence of $^3Q^*$ (Figure 24), increasing the pH above the pK_a^* would be expected to lead to decreased •OH production. The observation that •OH production decreased with increasing pH after a certain pH supports this $^3Q^*$ hypothesis. However, there is a large discrepancy of the certain pH values between the 4-HBA and 2,4-DHBA. (i.e., pH 7 vs. pH 9).. The higher pH value for 2,4-DHBA suggests that the pK_a^* of the 2,4-DHBA $^3Q^*$ is higher than that of 4-HBA. The reason for the discrepancy is unknown, but may be because hydrogen bonding between ortho carboxyl and hydroxyl groups stabilizes the $^3Q^*$ for 2,4-DHBA. To testify this hypothesis, the pK_a^* values will be measured in a future study using spectrophotometric titration (Klíčová et al., 2012). On the other hand, increasing pH favors the oxidation of water by excited triplets because a decrease in the

redox potential of the reaction •OH + H⁺+e⁻→ H₂O makes the oxidation of water more

exergonic (Ononye and Bolton, 1986). Thus, the Φs of 2,4-DHBA and 4-HBA increased

with increasing pH up to certain pH values. Therefore, pH apparently has opposing

effects on the quantum yields, resulting in the observed maxima.
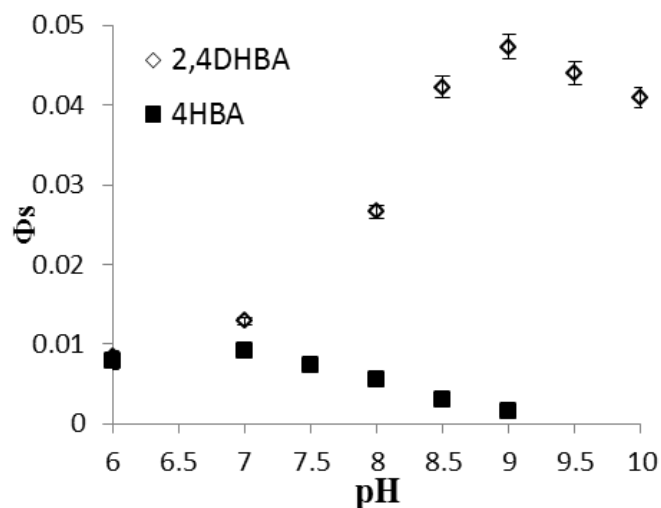
Figure 25. •OH Φs by using benzene of 2,4-DHBA at 310 nm and 4-HBA at 280 nm in

pH range 6~10. The buffer solutions were as follows: pH 6~7 (5 mM phosphate buffer),

pH 8~10 (5 mM borate buffer).
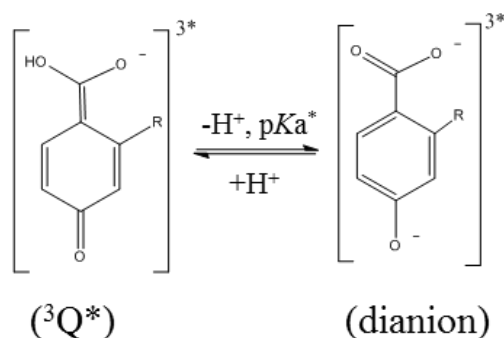
Figure 26. Equilibrium between the quinoid enol tautomer ($^3Q^*$) and its dianion

This study provides new insights into •OH photoproduction pathways from DOM and supports the approach of Stubbins et al. (2008), who showed that model phenolic DOM chromophores can be used to gain insights into DOM photochemical mechanisms and photoreaction sites. However, there are still many important open questions, such as what are the mechanistic details involved in the photoproduction •OH from these model compounds, especially the ones with para hydroxyl and carboxyl groups? Other questions include the effect of pH and different ring functional groups on the photoproduction of •OH. Finally, phenolic acids can readily photoionize via electron ejection (Feitelson et al., 1973); so the question arises as to what role (if any) the resulting excited DOM radical cation plays in the production of •OH? These questions will be the focus of our future studies on the DOM photochemistry.

CHAPTER V

A COMPARISON OF A SIMPLIFIED CUPRIC OXIDE HPLC METHOD

WITH THE TRADITIONAL GC-MS METHOD FOR CHARACTERIZATION

OF LIGNIN PHENOLICS IN ENVIRONMENTAL SAMPLES

PREFACE

The content of this chapter was published in 2015 in Limnology and

Oceanography: Methods, and below is the full citation. See Appendix A for the copyright

permission.

Sun, L, Spencer, R. G. M., Hernes, P. J., Dyda, R. Y., and Mopper, K. (2015)

Interlaboratory comparison of a simplified CuO oxidation/HPLC Method with the

traditional GC method for characterization of lignin phenolics in environmental samples.

Limnology and Oceanography: Methods. 13:1-8

1. INTRODUCTION

Lignin is a major and unique structural polymer of vascular plants. The

composition of its phenols provides information about plant tissues (angiosperm vs.

gymnosperm, woody vs. nonwoody) and the diagenetic state of terrigenous organic

matter (Hedges and Mann, 1979; Opsahl and Benner, 1995). Lignin carbon-normalized

yields in many environments provide quantitative information as to the proportion of

either vascular plant carbon (freshwaters) or terrigenous carbon (marine water) (Hernes

and Benner, 2002; Spencer et al., 2008; Spencer et al., 2009).

The traditional alkaline CuO oxidation method originally developed by Hedges and Ertel (1982) is commonly used to analyze the composition of lignin in complex environmental samples. The procedure has been optimized and modified by several groups. For oxidation, some groups (Knuutinen and Mannila, 1991; Lobbes et al., 2000) utilized up to twenty reaction vessels simultaneously to improve sample throughput; Goñi and Montgomery (2000) employed a microwave digestion system that shortened oxidation time; many groups (Kaiser and Benner, 2011; Kaiser et al., 2001; Louchouarn et al., 2000) add glucose to low carbon sample to prevent losses of lignin phenols by superoxidation. For extraction, ethyl acetate has been used instead of ethyl ether in order to minimize destruction of oxidation products (Goñi and Montgomery, 2000; Kaiser and Benner, 2011; Kögel and Bochter, 1985). Some groups (Amelung et al., 1999; Kaiser and Benner, 2011; Kögel and Bochter, 1985) employed solid phase extraction (SPE) in order to overcome the inefficiency of liquid-liquid extraction and to reduce labor intensity. However, despite these improvements, there are still some major drawbacks. Many groups use Teflon-lined stainless steel or Monel reaction vessels, which are expensive and difficult to obtain. Moreover, the sample throughput (e.g., 10-30 samples per week) remains a limiting factor when a large number of samples need to be analyzed. Finally, GC-MS instrumentation is relatively expensive and the derivatization steps complicate compound-specific isotopic analyses (^{13}C or ^{14}C) since final values need to be corrected for the isotopic contribution of the derivatizing agent. The last drawback can be addressed by employing high performance liquid chromatography (HPLC) (Knuutinen and Mannila, 1991; Lobbes et al., 1999; Steinberg et al., 1984). HPLC is simpler and less expensive, it does not require strict sample dehydration and derivatization steps, and

diode array UV-visible detection, as employed by Lobbes et al. (1999), facilitates reliable quantification of small amounts of lignin phenolics. Unfortunately, there are no published interlaborarory comparisons, and the only intralaboratory comparison (Lobbes et al. 1999) showed poor agreement between the HPLC method and the "standard" GC method. Furthermore, that study did not discuss possible causes for the differences.

For these reasons, we compared the lignin phenolic composition based on a simple HPLC method to that obtained by the conventional high pressure reaction vessel GC-MS procedure (Hernes et al., 2007; Spencer et al., 2010) for a large variety of sample types, including freshwaters, soils, DOM, sediments, isolated aquatic humic substances and plant tissues. In the HPLC method, we employed inexpensive, commercially available thick-walled Teflon vials, and we simplified and optimized sample oxidation and work-up procedures by using milder oxidation conditions followed by SPE. The goal of this study is to determine whether these steps can improve the comparison between the HPLC and GC techniques and whether the HPLC approach provides a viable and reliable alternative to the more labor intensive GC-MS approach for many environmental sample types.

2. EXPERIMENTAL SECTION

2.1 Chemicals and materials

The following chemicals and materials were used: p-hydroxybenzoic acid (99%, Sigma), p-hydroxybenzaldehyde (98%, Sigma), vanillic acid (98%, Alfa Aesar), syringic acid (98% Sigma), vanillin (99%, Sigma), p-hydroxyacetophenone (99%, Sigma), syringaldehyde (98%, Sigma); acetovanillone (98%, Sigma), acetosyringone (97%,

Sigma), *p*-coumaric acid (98%, Sigma), and ferulic acid (98%, Spectrum), ethyl vanillin (98%, Sigma), glucose (99.5%, Sigma), $Fe(NH_4)_2(SO_4)_2.6\ H_2O$ (99%, Fisher), CuO (99%, Wako), ethyl acetate(HPLC grade, B&J), NaOH (50% w/w, VWR), Na_2HPO_4 (99.9%, Mallinckrodt), methanol (HPLC grade, Acros), acetonitrile (HPLC grade), EMD Ar gas (UHP grade, Airgas), and C18 cartridges (300 mg, Analtech Corp.). Ultra-pure water (Milli-Q water, >18 $M\Omega cm^{-1}$) was used for preparation.

2.2 Sample descriptions

Live oak litter (*Quercus wislizeni*), purple needle grass tissue (*Nassella pulchra*), and loblolly pine litter (*Pinus taeda*) were collected at the Sierra Foothills Research and Extension Center, at the UC Davis arboretum, and the Duke Experimental Forest, respectively (Hernes et al., 2007). Three California series soils were bleach-cleaned, then sorbed with leachates from these three litters, and three representative samples included in this study were loblolly leachate sorbed to the Aiken series (an ultisol rich in kaolinite and Fe-oxides), live oak leachate sorbed to the McCarthy series (an andisol rich in amorphic phases, allophane and Fe-oxides), and purple needlegrass leachate sorbed to the Ione series (an oxisol rich in kaolinite and Fe-oxide) (Hernes et al., 2007). Although unaltered soils would also have been a reasonable alternative for comparison, untreated soils have the disadvantage of including discrete organic particles—and heterogeneity in general—that can confound reproducibility. The Congo River was sampled near Maluku (04 °05'02"S; 15 °31'36"E) in January 2008 upstream from Kinshasa at a point just above where the river widens to form Pool Malebo, and filtered through 0.3 μm glass fiber filters (Advantech GF-75) (Spencer et al., 2009); 1 L of the river water was dried on a rotary evaporator followed by either vacuum evaporation (Hernes laboratory) or freeze

drying (Mopper laboratory). Surface sediment from Dabob Bay, Washington (a marine embayment off of Hood Canal) has a long history of use as a lignin phenol reference material (Hedges et al., 1988) and is routinely used for quality control in the Aquatic Organic Geochemistry laboratory at UC Davis. Suwannee River fulvic acid reference standard 1R101F was obtained from the International Humic Substances Society (IHSS).

2.3 Lignin oxidation

Before oxidation, a freshly prepared 2 M NaOH (8%, w/w) solution was sparged with Ar while sonicating for 30 min to remove O_2; Samples (1-100 mg) were weighed into 6 mL square Teflon vials (Savillex Corp.) followed by 0.5 g CuO and 0.1 g $Fe(NH_4)_2(SO_4)_2.6\ H_2O$. 10 mg glucose was added to low organic carbon samples (Kaiser and Benner 2012). 5 mL of 2 M NaOH was added to each vial. A needle was used in the reaction mixture to further sparge with Ar for about 30 min. Ar was used because it is heavier than air. With the cap loosely in place, the sparging needle was slowly withdrawn and the cap screw was immediately closed to minimize the introduction of air. By using a modified evaporation unit (Model 18780, Pierce Chemical Corp.), six vials can be sparged at the same time. The Teflon vials were sealed tightly, shaken vigorously, and put in an oven for 3 h at 150 °C. After cooling, ethyl vanillin was added as internal standard.

2.4 Extraction of phenolic compounds

The oxidized sample was centrifuged at 2500 rpm (Model CL, IEC International) to remove unreacted CuO and other particles. The supernatant was saved and the sediment was washed with 5 mL water and re-centrifuged. The combined supernatant was acidified to pH 2 by adding 12 N HCl and held at room temperature in the dark for 1 h to let any

precipitate settle out. The acidified sample was then re-centrifuged and the supernatant was saved.

C18 cartridges were pre-conditioned with 3mL methanol and 10 mL mili-Q water. The acidified samples were pushed through the column at a flow rate of 4-5 mL/min. After drying the column with a stream of high purity nitrogen for 5 minutes, lignin oxidation products were eluted with 2.0 mL ethyl acetate.

The ethyl acetate was evaporated using a Pierce evaporation unit in a 45 °C water bath under a gentle stream of nitrogen. Immediately after the solvent was evaporated, the samples were re-dissolved in 0.2 mL methanol, sonicated for 1 min, and then diluted to 10% (v:v) methanol: water. The solutions were either analyzed by HPLC or immediately sealed and stored at -20 °C. Most samples were run in duplicate, while low organic carbon samples were run once due to limited material.

2.5 HPLC analysis

A home-made HPLC system was used, consisting of an E-Lab Model 2020 gradient programmer and data acquisition system (OMS Tech, Miami, FL) installed on an IBM-compatible PC, an Eldex Model AA pump (Eldex Laboratories, Menlo Park, CA), a six-port Valco injector (Valco Instruments, Houston, TX) and either a Model 785 A absorbance detector (Applied Biosystem Corp.) or an Agilent photodiode array detector (Model SPD-M20A).

The separation was carried out on a Phenomenex C18 column (5 μm, 250 mm×4.6 mm) with an Alltech 5 μm pre-column at room temperature (~22 °C). The injection volume was 150 μL. The separation was performed by gradient elution at a flow rate of 1.0 mL/min; the gradient program is shown in Table 5. Peaks were detected at 280 nm

wavelength and data was collected by the E-Lab data system. For peak verification,

several samples were also run using photodiode array detection. Spectra were collected

for standards and samples from 200-500 nm. The conditions of our HPLC method are

similar to those in past studies (Lobbes et al., 1999).

Table 5.

HPLC gradient program

Time (min)	% B
0	0
6	0
7	8
27	10
32	22
42	24
43	60
49	100
54	100
55	0

phase A: 50 mM phosphate buffer (pH=2) /methanol (v:v=85:15); phase

B: 50 mM phosphate buffer (pH=2)/methanol/acetonitrile (v:v:v=4:3:3)

2.6 Conventional method (modified from Hedges and Ertel, 1982 steel reaction vessel/GC method)

The lignin phenolic composition of the samples was analyzed using the CuO oxidation and extraction scheme with modifications summarized by Spencer et al (2010). Monel reaction vessels and solvents were sparged and purged with Ar prior to oxidation, while glucose was included in all oxidations in order to eliminate superoxidation effects. Samples were weighed directly into the reaction vessels, separation of lignin-derived phenols was achieved using an Agilent 6890 gas chromatograph fitted with a DB5-MS capillary column (30 m, 0.25 mm inner diameter, J&W Scientific) and equipped with an Agilent 5973 mass selective detector. Quantification was achieved using selected ion monitoring with cinnamic acid as an internal standard following the calibration scheme of Hernes and Benner (2002). All samples were blank-corrected due to the presence of trace amounts of contamination in the NaOH reagent. The blank averaged ~30 ng (<2% of total lignin phenols) per sample.

3. RESULTS AND DISCUSSIONS

3.1 HPLC chromatogram

Eleven oxidation products (Figure 27): *p*-hydroxybenzoic acid (PAD), *p*-hydroxybenzaldehyde (PAL), vanillic acid (VAD), syringic acid (SAD), vanillin (VAL), *p*-hydroxyacetophenone (PON), syringaldehyde (SAL); acetovanillone (VON), acetosyringone (SON), *p*-coumaric acid (CAD), and ferulic acid (FAD) were identified in natural samples including plant tissues, humic substance extracts, soils, sediments and freshwater DOM.
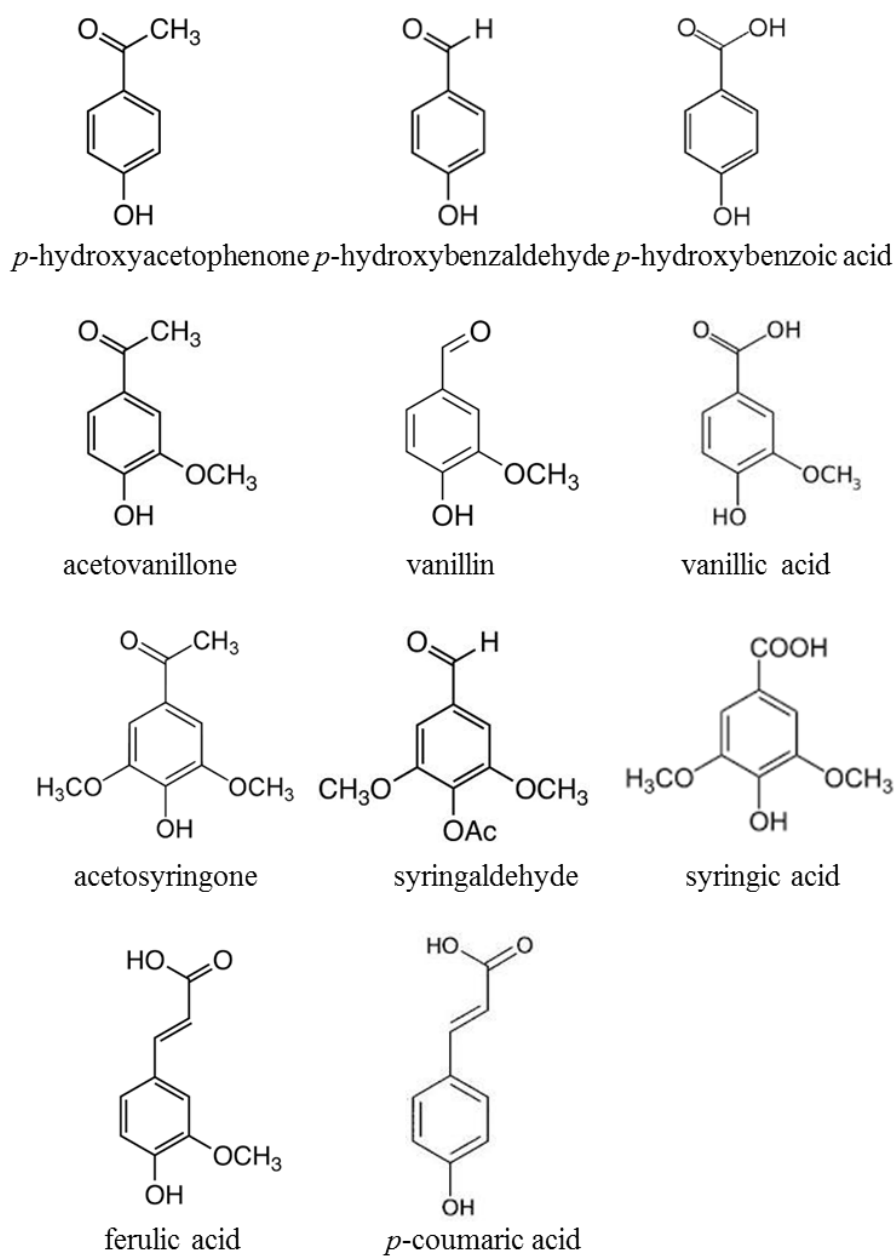
Figure 27. The structures of eleven oxidation products.

Figure. 28 shows representative HPLC chromatograms of Dabob Bay (DB) sediment and Congo River DOM. Using UV detection at 280 nm, interfering peaks were observed for the relatively low lignin-containing Congo River sample, which made quantification difficult for several phenols (PAD, SON, and FAD). However, the interferences could be selectively excluded by diode array detection at multiple wavelengths. Alternatively, for low lignin-containing samples, quantification of the phenols can naturally be improved by use of larger starting amounts of sample. Only one peak, corresponding to PAL, was detected in the procedural blank; the blank averaged 25±4.1 ng (<2% of total lignin phenols, n=5) per sample. Concentrations were calculated using the internal standard ethyl vanillin. The lignin oxidation product compositions of nine natural samples are listed in Table 6. *p*-Hydroxyl phenols are not listed because they can also be derived from non-lignin sources (Hedges and Parker 1976).
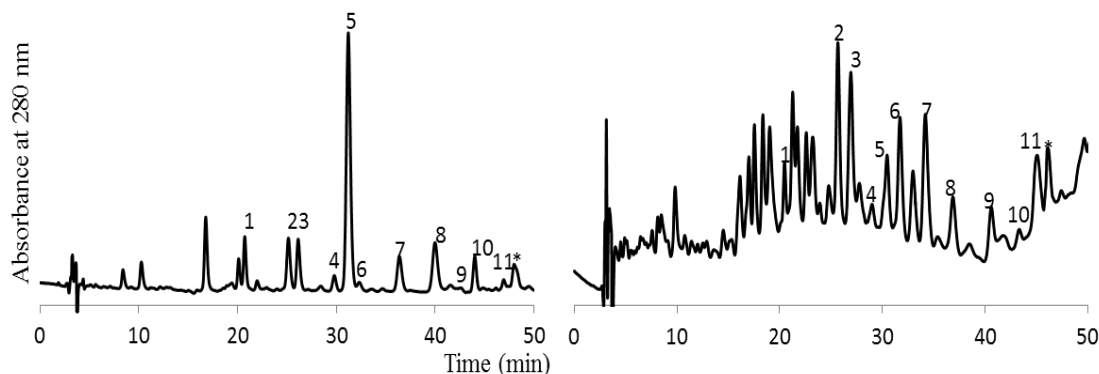
Figure 28. Chromatogram of Dabob Bay (DB) sediment and Congo River sample. 1. *p*-hydroxybenzoic acid (PAD); 2. *p*-hydroxybenzaldehyde (PAL); 3. vanillic acid (VAD); 4. syringic acid (SAD); 5.vanillin (VAL); 6. *p*-hydroxyacetophenone (PON); 7. syringaldehyde (SAL); 8. acetovanillone (VON); 9. acetosyringone (SON); 10. *p*-coumaric acid (CAD); 11. ferulic acid (FAD); *. Ethyl vanillin (EVAL).

Table 6.

Concentrations of CuO oxidation products[a] (μg/g Sed or μg/L) of nine natural samples

	OC (%)	VAL	VAD	VON	SAL	SAD	SON	FAD	CAD	Σ8	C/V[b]	S/V[c]	(Ad/Al)v[d]	(Ad/Al)s[e]
Aiken Loblolly	0.985	9.5	9.0	2.7	0.0	0.2	0.0	1.5	1.9	24.9	0.16	0.01	0.94	/
Loblolly Pine Litter	51.7	9133±553	2452±4	2183±152	40	0	172±34	1223±34	1618±184	16821±960	0.21	0.02	0.27	0.00
Purple Needlegrass	39.9	12491±610	2170±16	2404±53	11336±728	2726±305	3566±254	5391±226	3725±38	43809±2232	0.51	0.98	0.16	0.24
Ione Needlegrass	0.427	7.5	6.5	3.1	5.0	3.0	1.4	3.0	2.1	31.5	0.30	0.55	0.87	0.61
Live Oak litter	42.8	10850±566	2581±365	2669±20	12315±1293	1979±144	1346±37	592±7	3663±327	35995±2880	0.26	0.97	0.24	0.16
McCarthy Live Oak	3.84	7.4	9.1	0.7	12.5	4.3	1.4	2.4	2.4	22.6	0.28	1.06	1.24	0.34
DB sediment	2.5	382±27.1	127±5.5	87±20.2	120±6.7	22±1.2	20	13±0.9	31±1.5	801±57.8	0.07	0.27	0.33	0.19
IHSS	53	165±7.1	261±4.6	57±5.1	194	178±27.6	37±1.8	24±3.6	72	988±49.9	0.20	0.85	1.59	0.92
Congo River[f]		10.1	12.4	6.2	10.3	6.9	5.1	4.2	2.3	57.5	0.22	0.77	1.22	0.67

[a] Errors are standard deviations for the duplicates [b] C=FAD+CAD, V=VAL+VAD+VON. [c] S=SAL+SAD+SON. [d] Ratio of VAD/VAL. [e] Ratio of SAD/SAL. [f] 890.92 μM DOC for Congo river sample.

3.2 Optimizations and recoveries for the simplified HPLC procedure

During the development of the simplified HPLC method, we adapted and modified improvements made by previous studies. These improvements include adding glucose to low carbon samples to prevent superoxidation of the lignin polymer (Kaiser and Benner, 2011; Louchouarn et al., 2000), using ethyl acetate instead of ethyl ether to avoid destruction of oxidation products and using SPE to improve extraction efficiency (Goñi and Montgomery, 2000; Kaiser and Benner, 2011; Kögel and Bochter, 1985). Furthermore, we employed commercially available 6 mL square Teflon vials (Savillex Corp.), which unlike some commonly used Teflon vials, are leak-proof up to at least 170 °C. With these vials, we can readily oxidize more than twenty samples at the same time, which significantly reduced labor intensity and cost, and improved sample throughput.

In the original method (Hedges and Ertel, 1982), the external temperature for oxidation was 170 °C. Subsequently, several groups used lower temperatures when it was discovered that the actual internal temperature was ~15 °C lower (Lobbes et al., 2000; Standley and Kaplan, 1998). Therefore, we examined lignin phenol yields for two samples (purple needle grass and oak litter) at 170 °C for 2 h and 150 °C for 3 h. In general, the agreement between the two oxidation conditions was good; the average difference of total phenols was 6 % (Figure 29). However, we observed on higher acid to aldehyde ratios (Ad/Al) at 170 °C (Table 7), indicating acids are preferentially formed over corresponding aldehydes from the lignin polymer at higher temperature (Hedges and Ertel, 1982; Standley and Kaplan, 1998). Therefore, we used 150 °C as the external temperature for 3 h in our oxidation procedure to avoid "over-oxidation".

Table 7

Lignin phenol concentrations (µg/g) by Teflon vial/HPLC method at different

temperatures.

	Temperature	$\sum_8$	(Ad/Al)v	(Ad/Al)s
Purple Needle Grass	150 ℃	43809 ±2232	0.16	0.24
	170 ℃	38845 ±2013	0.29	0.36
Live Oak Litter	150 ℃	35995 ±2880	0.24	0.16
	170 ℃	36047 ±1875	0.27	0.17
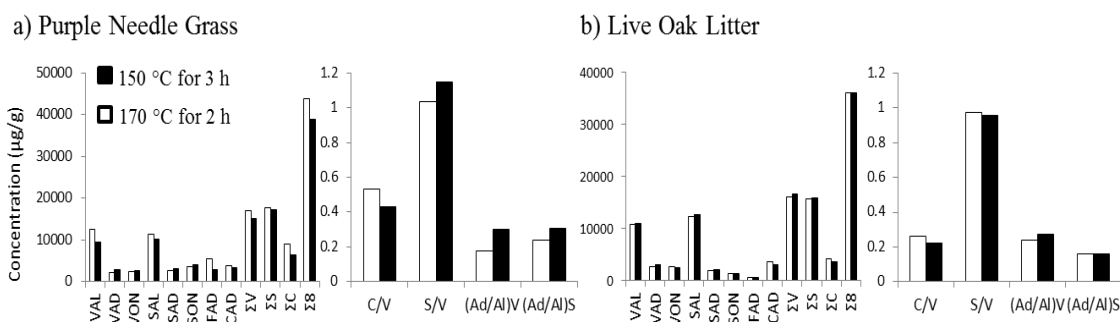
Figure 29. Lignin phenol concentrations (µg/g) by Teflon vial/HPLC method at different

temperatures.

The role of $Fe(NH_4)_2(SO_4)_2.6\ H_2O$ during oxidation was tested using a mixture of

standards and three samples (live oak litter, purple needle grass, and loblolly pine litter).

It was observed that cinnamyl and syringyl phenols were lost by more than 50 % in

mixtures of pure standards without $Fe(NH_4)_2(SO_4)_2.6H_2O$. However, the differences

between natural samples with and without the reagent were small. The samples without

reagent had ≤7% lower total cinnamyl (C), vanillyl (V) and syringyl (S) phenols, ~5-18% lower C/V and S/V ratios, and ~4-13% higher acid/aldehyde ratios than those with the reagent. Therefore, $Fe(NH_4)_2(SO_4)_2.6H_2O$ appears to prevent "over-oxidation" of natural samples to some extent, but may not be significant for samples with a high organic carbon content.

Recoveries were determined by spiking standards (4 nmol) into samples prior to CuO oxidation or SPE steps. Recoveries of eleven phenols were 93 ± 3 % for the SPE step and 88 ± 6 % for the overall procedure including oxidation, centrifugation, SPE and drying (Table 8). Liquid-liquid (ethyl-acetate) extraction was tested for two samples, but did not show better recovery than SPE and was found to be more time-consuming. For the overall procedure, recoveries of <80 % for SON, CAD, and FAD indicate losses of these compounds under our oxidation conditions. Average recoveries of phenolic acids were higher than the other phenolic compounds, indicating that acids are more stable or conversion of aldehydes to acids during the oxidation step. Moreover, total syringyl phenols and cinnamyl phenols had lower recoveries than vanillyl phenols and p-hydroxyphenols, indicating that the former two phenols are less stable under our reaction conditions. The limit of detection (LOD) for the HPLC/UV system was low (1.1 ± 0.7 ng of an individual phenol); however, it can be estimated from the overall reproducibility that, in environmental samples, at least ~130 ng for each phenol (1500 ng for the total eleven phenols) per sample was required for quantitative measurement.

Table 8
Recoveries of lignin phenols[a]

							Compounds											
Recoveries %	VAL	VAD	SAL	SAD	FAD	CAD	PAD	PON	SON	VON	PAL	Ad[b]	Al[c]	Kt[d]	C[e]	S[f]	V[g]	P[h]
SPE	92.9±3.9	99.4±2.5	91.7±3.1	85.2±4.1	90.9±2.7	95.6±4.1	96.0±2.8	96.2±2.9	90.0±3.3	88.1±4.9	91.3±2.9	93.5	91.9	92.8	93.5	88.9	94.8	94.5
Overall	85.2±5.9	99.8±3.1	92.8±1.9	81.3±3.7	73.2±8.7	77.4±5.1	103.9±3.6	90.9±2.5	79.7±7.6	86.4±7.6	86.1±2.3	94.7	91.0	85.2	75.4	85.1	92.6	93.2

[a]See Fig.1 for notations. [b]Ad=VAD+SAD+PAD. [c]Al=VAL+SAL+PAL. [d]Kt=PON+SON+VON. [e]C=FAD+CAD. [f]V=VAL+VAD+VON. [g]S=SAL+SAD+SON. [h]P=PAD+PAL+PON.

3.3 Methods comparison

The lignin oxidation product composition of nine natural samples determined by HPLC/UV absorption are compared to the results obtained by the modified reaction vessel/GC method of Ertel and Hedges (1982) (Figure 29). Since most samples were only measured in duplicates due to limited sample amount, the pooled relative standard errors (PRSE) for individual phenols and total eight phenols ($\sum_8$) were used, which were calculated from:

$$\text{PRSE} = \frac{PRSD}{\sqrt{PN}}$$

Where the PN is the pooled number; the PRSD is the pooled relative standard deviation, which is calculated from relative standard deviation (RSD):

$$\text{PRSD} = \sqrt{\frac{(n_1-1)RSD_1^2 + (n_2-1)RSD_2^2 + \cdots (n_k-1)RSD_k^2}{n_1+n_2+\cdots n_k - PN}}$$

Where the n is the number of times each sample was measured. The PN is 6 for VAL, VAD, VON, and FAD, and 4-5 for the individual phenols with non-detectable concentrations or lack of duplicates for some samples. PRSE did not exceed 5 % and averaged 2.7±1.2 %. PRSE and PN were used to run t-test for all samples. Based on this analysis, $\sum_8$ is indistinguishable between the two methods for Aiken loblolly, loblolly pine litter, live oak litter, and IHSS samples, but different for McCarthy live oak, Ione needle grass, purple needle grass, Dabob Bay sediment, and Congo River ($p<0.001$) samples. The Dabob Bay sediment sample had low organic carbon (Table 6), which possibly resulted in loss or over-oxidation for some phenols during the reaction procedure. Alternatively, the differences may have been due to differences between the two procedures or to procedural artifacts (e.g., the Congo River water sample required pre-drying steps in two laboratories that could introduce additional errors; also, the purple

needle grass tended to float on the solution surface, which may have led to variable extraction efficiencies). Overall, the differences for a total of eight oxidation products ($\sum_8$) relative to the conventional method did not exceed 38 % and averaged 4.5±23 %, and the difference between two methods is insignificant according to a paired a t-test (t=0.5765). The strong agreement between the two independent sets of analyses (particularly for the sub-set of samples where the concentrations of the lignin phenols were not at or near the detection limit or where sample inhomogeneity problems were not evident) indicates that the methods are relatively robust, i.e., relatively insensitive to minor to modest variations in the sample work up steps.

The HPLC/UV method generally yielded lower acid: aldehyde ratios for syringyl phenols (Figure 30), which can be explained by the lower temperature (150 °C) used for the HPLC method. The most divergent results were observed in low organic carbon samples for syringyl and cinnamyl phenols, calculated as S/V and C/V ratios. These phenols are most sensitive to oxidation conditions (Kaiser and Benner 2012), e.g., the destruction of syringyl compounds and the transformation of *p*-coumaric acid into *p*-hydroxybenzoic acid have been reported as side reactions (Standley and Kaplan 1998). Different amounts of glucose addition might have also contributed to the observed differences in the ratios between the methods. In the HPLC method, a 10 mg glucose addition was used, while in the GC method, a 75 mg addition was used (Spencer et al., 2010). It is possible that 10 mg glucose was not enough to minimize these side reactions(Amelung et al., 1999; Kaiser et al., 2001). The level of glucose added to samples, especially low carbon samples, needs to be systematically studied.
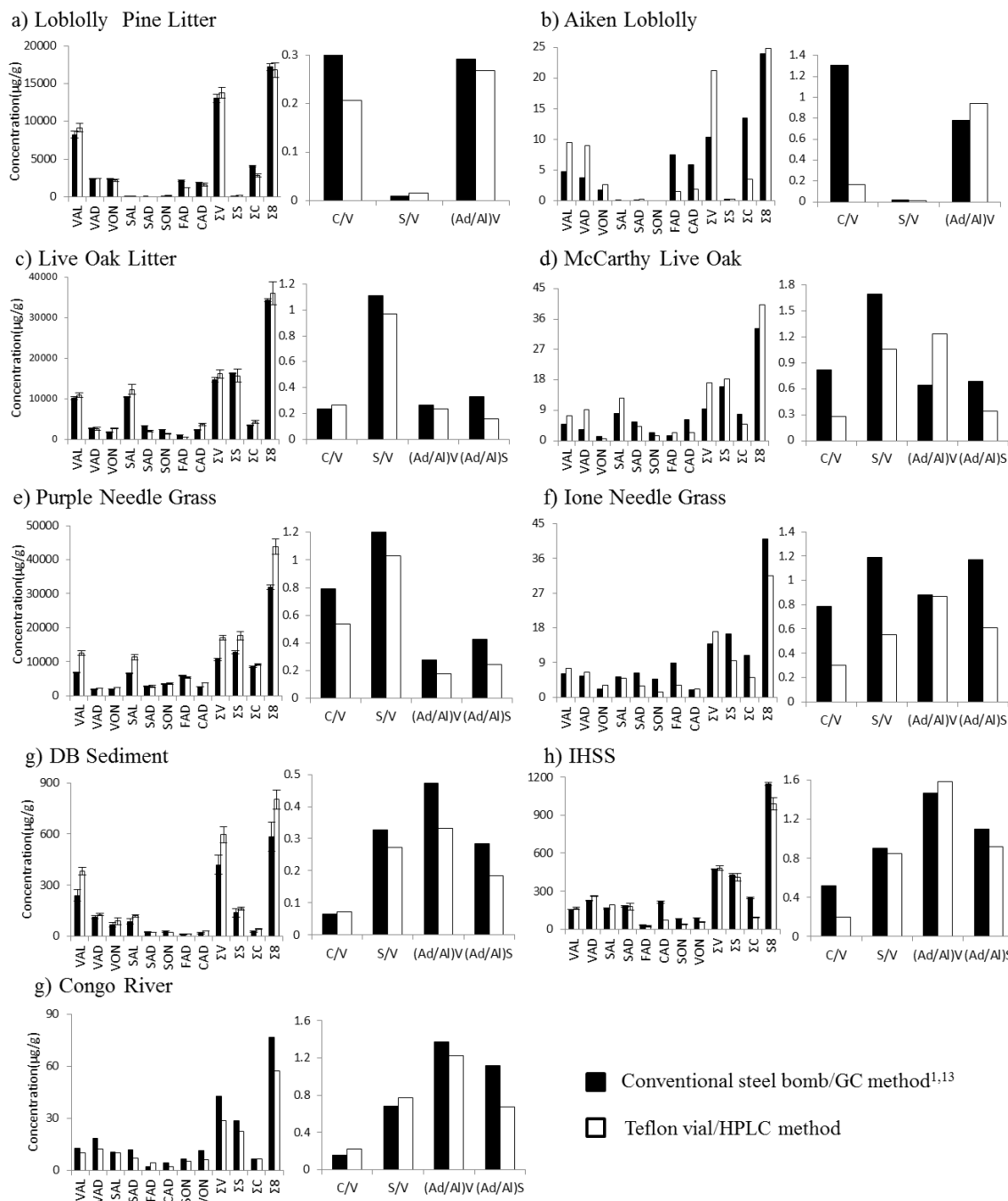
Figure 30. Lignin phenol concentrations (μg/g, Congo River sample is μg/L) by Teflon vial/HPLC method were compared to the modified conventional reaction vessel/GC method. Error bars are pooled standard errors

Despite general good agreement obtained in this comparison, it should be pointed out that the process of extracting, oxidizing, and analyzing lignin components of aqueous and solid biogeochemical samples involves many procedural steps in which subtle operational differences can lead to significant differences in the lignin phenol fingerprint (Lobbes et al., 2000). For example, evaporation under a stream of nitrogen can preferentially volatilize the aldehydes and possibly the ketones as well, relative to the acids. This loss can impact individual ratios, or if the ethyl vanillin internal standard is preferentially lost, calculated totals for compounds with different volatility would be affected. Moreover, in the oxidizing step for solid samples, differences can arise during the release of organic matter from mineral matrices due to different extraction efficiencies (Hernes et al., 2013; Kaiser et al., 1996), if this process is different between two different oxidation setups, the results will naturally be somewhat different. Therefore, it is recommended that well-characterized standards, such as the Suwannee River reference standard from IHSS, be run and reported as part of any sample run in order to facilitate comparison between laboratories or published results.

3.4 Lignin phenol composition of different samples

Both methods clearly show gymnosperm samples (Loblolly pine litter and Aiken Loblolly) contain few syringyl phenols, which is consistent to the past studies (Hedges and Mann, 1979; Lobbes et al., 1999; Opsahl and Benner, 1995). Lignin acids (VAD, SAD), which contain para-carboxyl and hydroxyl groups, could be important photochemical sources for hydroxyl radical ($\cdot$OH) formation in natural waters (see Chapter IV). The lignin acid fraction of the total eight lignin phenols ranges from 11 to 44 %. Our results show this fraction is much higher in freshwater samples than in wood

tissue sample;e.g., acid:aldehyde (Ad/Al) ratios for vanillyl phenols are 1.22 and 1.59 in

the Congo River and IHSS samples, respectively, while they are 0.24, 0.16, and 0.27 in

the Live Oak litter, Purple Needle grass, and Loblolly Pine litter respectively (Table 5).

The higher lignin acid content of freshwater samples, compared to wood tissue samples,

indicates a higher degree of lignin oxidation. This result is consistent with our

observation that "over-oxidation" during oxidation leads to an increase in the Ad/Al ratio,

and also consistent with past studies that showed that photodegradation resulted in an in

increase of the Ad/Al ratio (Spencer et al., 2012). The geochemical conversion of

aldehyde to acid through photodegradation and/or oxidation may play an important role

in OH photoformation in natural waters (see Chapter IV).

CHAPTER VI

SUMMARY, CONCLUSIONS AND FUTURE DIRECTIONS

1. Summary and Conclusions

The hydroxyl radical (•OH) is a short-lived reactive species. In natural waters, it is mainly produced from photochemical reactions by three pathways: nitrate and nitrite photolysis, the photo-Fenton reaction, and DOM photoreactions. This dissertation mainly focuses on the source of •OH from DOM photoreactions and the photo-Fenton reaction in natural waters.

The first goal of this study was to develop an accurate method for measuring •OH formation rate during long-term irradiation experiments with natural waters. The •OH production rate is commonly determined indirectly either through the loss of a probe or accumulation of a product from the probe. However, in both DOM-rich and DOM-poor natural waters, we found the previous methods based on measuring sequential cumulative concentrations of photoproducts from probes benzene and benzoic acid underestimated the actual •OH formation rate. The underestimation was mainly due to the degradation of the measured photoproducts phenol (from benzene) and salicylic acid (from benzoic acid) during the prolonged irradiation; the degradation rates followed pseudo first order kinetics. Thus, to avoid this underestimation, I examined time-course •OH formation rates using two approaches: 1) correcting for photoproduct loss, and 2) obtaining near-instantaneous formation rates. The corrected formation rates were obtained by adding the photodegradation rates of corresponding photoproducts to their formation rates, and the instantaneous rates were obtained by measuring the photoproducts formation rates for a

short time ($\leq$ 2h). By performing corrections for probe product degradation, the agreement of corrected •OH formation rates to near-instantaneous formation rates improved. However, for longer irradiation periods (more than 8 h), neither uncorrected nor corrected •OH formation rates agreed well with the near-instantaneous formation rates. The reason for the large discrepancies might be that the added probes changed DOM photodegradation and •OH production pathways, which became significant after long-term irradiations containing the probe. Therefore, it is recommended that only the near-instantaneous formation rates are used to estimate •OH photochemical formation rates during long-term irradiation experiments, regardless of the probes used. Moreover, the observed "•OH" measured by these probes (as well as most other commonly used •OH probes) may include both free •OH and other highly reactive oxidative species, which can also participate in the probe trapping reactions.

By employing the near-instantaneous formation rate method, •OH formation rates were measured to study the source of •OH during photoflocculation, which may be an important in the transformation and transport of DOM and particulate organic matter (POM) to the ocean. We estimated time-course •OH photo-formation rates in Great Dismal Swamp (DS) and aqueous wood extract samples using near-instantaneous formation rates. During a 15 day irradiation experiment, flocculation was observed after day 4 in the DS water sample, which is an iron- and DOM-rich, but nitrogen-poor freshwater. The results showed that the formation of •OH was highly dependent on the concentration of Fe, hydrogen peroxide (H_2O_2) and DOC. Prior to flocculation (<day 4), Fenton and photo-Fenton reactions were the main sources of •OH. After all H_2O_2 was consumed and most of the Fe was removed by precipitation, •OH appeared to be

produced mainly by DOM photoreactions. Nitrate photolysis was likely a negligible source based on the low total dissolved nitrogen concentration in the DS sample.

To further confirm the importance of Fe and DOM on •OH formation, •OH formation rates, DOM optical properties and Fe speciation were measured in an aqueous extract of a naturally degraded wood sample with and without Fe addition. •OH formed in both original and Fe amended aqueous wood extract samples. The •OH formation rate was initially markedly higher in the Fe amended sample. In this sample, Fe was mainly present as dissolved organic complexed Fe(III) initially. During irradiation, the Fe(III) was reduced to Fe(II), probably through charge transfer reactions with DOM. At the same time, the high •OH formation rate in conjunction with the changes in the free Fe(II) fraction indicate that Fe(II) was oxidized to Fe(III), probably via the Fenton and charge transfer reactions. Moreover, because the iron complexed organic ligands were continuously degraded during the irradiation, when the free Fe(III) concentration exceeded the maximum soluble concentration, insoluble $Fe(OH)_3$ formed, which coprecipitated with or adsorbed organic matter. Therefore, Fe not only participates in the Fenton reaction to form •OH, it appears to play a critical role in the photoflocculation process as virtually no flocculation occurred in the original (low iron) sample during 10 d of irradiation. In the absence of Fe, •OH also formed; therefore the DOM could be the only source, as nitrate and nitrite concentrations were negligible. During the course of the irradiation, •OH formation rates normalized to DOC and $SUVA_{254}$, and humic-substance fluorescence intensity decreased markedly indicating that the chromophoric sites within DOM responsible for •OH production were transformed and/or degraded during irradiation.

Since freshwater DOM (i.e., humic substances) is known to contain aromatic moieties with mainly carboxyl and hydroxyl functionalities, phenolic acids were used as model DOM chromophores to elucidate possible sources of •OH photoformation from DOM. The •OH quantum yields (Φs) at 280~340 nm for eleven model compounds (including five dihydroxybenzoic acids (DHBA), three hydroxybenzoic acids (HBA), two resorcinols, and one dihydroxybenzaldehyde were measured by trapping reaction with benzene. It was found that many phenolic acids are capable of producing •OH, especially those with para hydroxyl and carboxyl groups (especially 2,4-DHBA and 4-HBA), which have markedly high •OH Φs. By conducting methane trapping and competition kinetics experiments, it was confirmed that both free •OH and oxidative intermediates were produced from these compounds. Also, the benzene probe appears to be much more specific to free •OH. The results suggest that hydroxybenzoic acid moieties within DOM play an important role in the photoproduction of •OH and transient oxidative species. It was hypothesized that a quinoid enol tautomer present as a water cluster was responsible for •OH production from phenolic compounds with para hydroxyl and carboxyl groups. The hypothesized mechanism involves the formation of tautomer intermediate following fast intersystem crossing to the triplet state, and then triplet proton transfer through bound solvent water. The hydrogen bond between the tautomer and the bound water may induce H-OH bond cleavage by lowering the activation energy needed for bond dissociation. pH may have opposing effects, resulting in observed maxima •OH quantum yield at a certain pH.

From above results, aromatic compounds with para hydroxyl and carboxyl groups are capable of producing •OH. These structures are commonly present in humic

substances derived from tannin and lignin. In order to examine the lignin phenolic composition of natural samples, a simplified method using alkaline copper oxide oxidation coupled with solid-phase extraction and high performance liquid chromatography (HPLC-UV-vis) was developed. It was found that during the oxidation step, syringyl phenols and cinnamyl phenols were less stable than other phenolics. I found that, to avoid "over-oxidation", milder hydrolysis conditions (150 °C for 3 h) than commonly reported (170 °C for 2 h) should be used. Furthermore, the addition of $Fe(NH_4)_2(SO_4)_2 . 6\ H_2O$ may not be useful for samples with high carbon matrices. The simplified HPLC-UV-vis method showed overall good agreement with the conventional GC-MS method in an interlaboratory comparison; the mean difference of nine environment samples for a total of eight oxidation products was 4.5% with a relative standard deviation of 23 %. Also, for low organic carbon samples, a greater amount of glucose should be added than previously reported. The agreement between the simplified HPLC and conventional GC methods was generally good, a few differences were observed. The discrepancies may have been due to differences between the two procedures or to procedural artifacts (e.g., the river water sample involved different pre-drying steps in the two laboratories that could have introduced additional variability; also, the grass sample tended to float on the solution surface, which may have led to variable extraction efficiencies). The lower costs, higher sample throughput and employment of underivatized samples of the simplified HPLC method should increase the accessibility of lignin analyses, including compound-specific isotope analyses.

The lignin acid content, which contains para-carboxyl and hydroxyl groups (and therefore may be an important source for •OH formation), was found to vary substantially

between these widely different samples. The lignin acid fraction of the total eight lignin phenols ranged from 11 to 44 %. The fraction is much higher in freshwater samples than in wood tissue sample. It may indicate a geochemical conversion of aldehyde to acid through photodegradation and/or oxidation when the wood lignin is transported to freshwaters.

2. Future directions

The probes for measuring •OH are not necessarily specific for free •OH, but are capable of detecting other lower-energy oxidative species to varying degrees. Thus, it is necessary to examine a variety of probes to determine which are specific for free •OH. The probes may be tested by competition kinetics experiments, in which a series of different concentrations of competitors are added to the solutions in the presence of probes. The experimental rate constant ratios of competitor to probe in natural waters should then be compared with known pure free •OH sources, e.g. H_2O_2.

In the Fenton reaction, •OH formation highly depends on H_2O_2 formation and Fe chemistry. In the DS sample, the results show that H_2O_2 was produced dramatically initially, but fell to zero between day 2 and day 4, and then was produced again after day 4 upon the onset of flocculation. The reasons for the reappearance of H_2O_2 after day 4 are not known, but may be related to major photochemically-induced changes in DOM composition and structure (Gonsior et al., 2009) and to the initialization of DOM photoflocculation (Helms et al., 2013a; Helms et al., 2013b). This behavior of H_2O_2 photoproduction from DOM has not been previously observed and, thus, warrants further study.

The photo-Fenton reaction involves the oxidation of Fe(II) to Fe(III). Continuing irradiation cycles Fe(III) to Fe(II), probably through LMCT reactions with DOM. DOM may form surface coatings on Fe-oxide particles and participate in surface reactions or form molecular Fe-DOM complexes. It has been shown that DOM is involved in reduction of Fe as charge-transfer agents during LMCT reactions (Scott et al., 1998; Barbeau, K., 2006; Klapper et al., 2002). Several studies revealed the charge-transfer abilities of quinone moieties within DOM (Scot et al., 1998; Nurmi and Tratnyek, 2002; Ariese et al., 2004). For instance, Fe(III)-reducing microorganisms transfer electrons to quinone moieties in humic substances, and the produced hydroquinone groups can transfer electrons to Fe(III) oxides (Scot et al., 1998). Thus, in the future, the LMCT reactions and the moieties within the DOM that can participate in these reactions may need to be identified and studied, as they play important roles in Fe chemistry.

In the study of •OH from model compounds, i.e., 2,4-dihydroxybenzoic acid (2,4-DHBA), it was found that absorbance centered at 290 nm was lost while peaks at 266, 312 and 490 nm formed upon irradiation. Interestingly, the latter peak is similar to the absorbance of hydroxybenzoquinone that is produced from quinone photodegradation. Thus, mass spectroscopy will be employed to examine the products, which will help our understanding of the detailed mechanism, especially how it is related to the quinone photochemistry. Moreover, as a triplet state quinoid enol tautomer mechanism is proposed to account for high •OH photoproduction from the phenolic acids with para hydroxyl and carboxyl groups, the formation of this tautomer (transient spectrum) needs to be confirmed by using laser flash photolysis spectroscopy (Vulpius et al., 2010).

Furthermore, to elucidate the possible mechanism and the role of O_2, •OH production and the products will be examined under oxic and anoxic conditions.

Lastly, there are many important open questions. For example, can phenolic acids with para hydroxyl and carboxyl groups photoproduce both free •OH and the less reactive oxidative species? It is not known whether the proposed tautomer mechanism can give rise to both products, as benzoquinone does not produce free •OH. Other questions include the effect of pH and different ring functional groups on the photoproduction of •OH, e.g., substituting an aldehyde group for the carboxyl group of 2,4-DHBA decreased the •OH Φs (2,4-DHA). To study the pH effect on the quinoid enol tautomer formation and therefore •OH photoproduction, the excited pKa of the tautomer will be examined by spectrophotometric titration (Klíčová et al., 2012). Finally, phenolic acids can readily photoionize via electron ejection; so the question arises as to what role (if any) the resulting excited DOM radical cation plays in the production of •OH? These questions will be the focus of our future studies on the DOM photochemistry.

REFERENCES

Aeschbacher, M., Sander, M. and Schwarzenbach, R.P., 2009. Novel electrochemical approach to assess the redox properties of humic substances. Environ. Sci. Technol., 44(1): 87-93

al Housari, F., Vione, D., Chiron, S. and Barbati, S., 2010. Reactive photoinduced species in estuarine waters. Characterization of hydroxyl radical, singlet oxygen and dissolved organic matter triplet state in natural oxidation processes. Photochem. Photobiol. Sci., 9(1): 78-86

Alegría, A.E., Ferrer, A., Santiago, G., Sepúlveda, E. and Flores, W., 1999. Photochemistry of water-soluble quinones. Production of the hydroxyl radical, singlet oxygen and the superoxide ion. J. Photochem. Photobiol. A: Chem., 127(1–3): 57-65. http://dx.doi.org/10.1016/S1010-6030(99)00138-0

Amelung, W., Flach, K.-W. and Zech, W., 1999. Lignin in Particle-Size Fractions of Native Grassland Soils as Influenced by Climate. Soil Sci. Soc. Am. J., 63(5): 1222-1228. http://dx.doi.org/10.2136/sssaj1999.6351222x

Anastasio, C. and McGregor, K.G., 2001. Chemistry of fog waters in California's Central Valley: 1. In situ photoformation of hydroxyl radical and singlet molecular oxygen. Atmos. Environ., 35(6): 1079-1089. http://dx.doi.org/10.1016/S1352-2310(00)00281-8

Arakaki, T. and Faust, B.C., 1998. Sources, sinks, and mechanisms of hydroxyl radical (•OH) photoproduction and consumption in authentic acidic continental cloud

waters from Whiteface Mountain, New York: The role of the Fe (r)(r=II, III) photochemical cycle. J. Geophys. Res. Atmos., 103(D3): 3487-3504

Balakrishnan, I. and Reddy, M.P., 1970. Mechanism of reaction of hydroxyl radicals with benzene in the .gamma. radiolysis of the aerated aqueous benzene system. J. Phys. Chem., 74(4): 850-855. http://dx.doi.org/10.1021/j100699a031

Barbeau, K., 2006. Photochemistry of organic iron (III) complexing ligands in oceanic systems. Photochem. Photobiol., 82(6): 1505-1516

Baruah, M.K., Upreti, M.C., Baishya, N.K. and Dutta, S.N., 1981. Interaction of iron with humic acid extracted from lignite. Fuel, 60(10): 971-974

Bassan, A., Blomberg, M.R.A. and Siegbahn, P.E.M., 2003. Mechanism of Aromatic Hydroxylation by an Activated Fe^{IV} O Core in Tetrahydrobiopterin-Dependent Hydroxylases. Chem.-Eur. J., 9(17): 4055-4067. http://dx.doi.org/10.1002/chem.200304768

Baxendale, J. and Magee, J., 1953. The oxidation of benzene by hydrogen peroxide and iron salts. Discuss. Faraday Soc., 14: 160-169

Beltran-Heredia, J., Torregrosa, J., Dominguez, J.R. and Peres, J.A., 2001. Comparison of the degradation of p-hydroxybenzoic acid in aqueous solution by several oxidation processes. Chemos., 42(4): 351-359. http://dx.doi.org/10.1016/S0045-6535(00)00136-3

Bossmann, S.H. et al., 1998. New Evidence against Hydroxyl Radicals as Reactive Intermediates in the Thermal and Photochemically Enhanced Fenton Reactions. J. Phys. Chem. A, 102(28): 5542-5550. http://dx.doi.org/10.1021/jp980129j

Brezonik, P.L. and Fulkerson-Brekken, J., 1998. Nitrate-induced photolysis in natural waters: controls on concentrations of hydroxyl radical photo-intermediates by natural scavenging agents. Environ. Sci. Technol., 32(19): 3004-3010

Burns, J. et al., 2012. Methods for reactive oxygen species (ROS) detection in aqueous environments. Aqua. Sci., 74(4): 683-734.10.1007/s00027-012-0251-x

Buxton, G.V., Greenstock, C.L., Helman, W.P. and Ross, A.B., 1988. Critical review of rate constants for reactions of hydrated electrons, hydrogen atoms and hydroxyl radicals. Phys. Chem. Ref. Data, 17: 513-886

Cabaniss, S.E., 1992. Synchronous Fluorescence Spectra of Metal-Fulvic Acid Complexes. Environ. Sci. Technol., 26(6): 1133-1139. http://dx.doi.org/10.1021/es50002a018

Canonica, S., Jans, U., Stemmler, K. and Hoigne, J., 1995. Transformation kinetics of phenols in water: Photosensitization by dissolved natural organic material and aromatic ketones. Environ. Sci. Technol., 29(7): 1822-1831

Chen, H. et al., 2014. Production of Black Carbon-like and Aliphatic Molecules from Terrestrial Dissolved Organic Matter in the Presence of Sunlight and Iron. Environ. Sci. Technol. Letters, 1(10): 399-404

Clark, K. and Stonehill, H., 1972. Photochemistry and radiation chemistry of anthraquinone-2-sodium-sulphonate in aqueous solution. Part 1.—Photochemical kinetics in aerobic solution. J. Chem. Soc., Faraday Trans. 1, 68: 577-590

Cooper, W.J., Zika, R.G., Petasne, R.G. and Fischer, A.M., 1989. Sunlight-induced photochemistry of humic substances in natural waters: major reactive species. Adv. Chem. Ser, 219: 333-362

Del Vecchio, R. and Blough, N.V., 2004. On the origin of the optical properties of humic substances. Environ. Sci. Technol., 38(14): 3885-3891

Emmenegger, L., Schönenberger, R., Sigg, L. and Sulzberger, B., 2001. Light‑induced redox cycling of iron in circumneutral lakes. Limnol. Oceanogr., 46(1): 49-61

Esplugas, S., Gimenez, J., Contreras, S., Pascual, E. and Rodríguez, M., 2002. Comparison of different advanced oxidation processes for phenol degradation. Water Res., 36(4): 1034-1042

Feitelson, J., Hayon, E. and Treinin, A., 1973. Photoionization of phenols in water. Effects of light intensity, oxygen, pH, and temperature. J. Am. Chem. Soc., 95(4): 1025-1029

Fellman, J.B., Hood, E. and Spencer, R.G., 2010. Fluorescence spectroscopy opens new windows into dissolved organic matter dynamics in freshwater ecosystems: A review. Limnol. Oceanogr., 55(6): 2452-2462

Fichot, C.G. and Benner, R., 2012. The spectral slope coefficient of chromophoric dissolved organic matter (S275‑295) as a tracer of terrigenous dissolved organic carbon in river‑influenced ocean margins. Limnol. Oceanogr., 57(5): 1453-1466

Gan, D., Jia, M., Vaughan, P.P., Falvey, D.E. and Blough, N.V., 2008. Aqueous photochemistry of methyl-benzoquinone. J. Phys. Chem. A, 112(13): 2803-2812

Gao, H. and Zepp, R.G., 1998. Factors influencing photoreactions of dissolved organic matter in a coastal river of the southeastern United States. Environ. Sci. Technol., 32(19): 2940-2946

Geib, S.M. et al., 2008. Lignin degradation in wood-feeding insects. PNAS, 105(35): 12932-12937

Golanoski, K.S., Fang, S., Del Vecchio, R. and Blough, N.V., 2012. Investigating the Mechanism of Phenol Photooxidation by Humic Substances. Environ. Sci. Technol., 46(7): 3912-3920. http://dx.doi.org/10.1021/es300142y

Goñi, M.A. and Montgomery, S., 2000. Alkaline CuO oxidation with a microwave digestion system: Lignin analyses of geochemical samples. Anal. Chem., 72(14): 3116-3121. http://dx.doi.org/10.1021/ac991316w

Gonsior, M. et al., 2009. Photochemically induced changes in dissolved organic matter identified by ultrahigh resolution Fourier transform ion cyclotron resonance mass spectrometry. Environ. Sci. Technol., 43(3): 698-703

Guo, W. et al., 2011. Assessing the dynamics of chromophoric dissolved organic matter in a subtropical estuary using parallel factor analysis. Mar. Chem., 124(1): 125-133

Haag, W.R. and Hoigné, J., 1985. Photo-sensitized oxidation in natural water via. OH radicals. Chemos., 14(11): 1659-1671

Hayes, M.H.B., MacCarthy, P., Malcolm, R.L. and Swift, R.S., 1989. Humic substances II. In search of structure. John Wiley & Sons Ltd

Hedges, J.I., Clark, W.A. and Cowie, G.L., 1988. Organic matter sources to the water column and surficial sediments of a marine bay. Limnol. Oceanogr., 33(5): 1116-1136

Hedges, J.I. and Ertel, J.R., 1982. Characterization of lignin by gas capillary chromatography of cupric oxide oxidation products. Anal. Chem., 54(2): 174-178. http://dx.doi.org/10.1021/ac202004r

Hedges, J.I. and Mann, D.C., 1979. The characterization of plant tissues by their lignin oxidation products. Geochim. Cosmochim. Acta, 43(11): 1803-1807. http://dx.doi.org/10.1016/0016-7037(79)90028-0

Heitner, C., Dimmel, D. and Schmidt, J., 2010. Lignin and lignans: advances in chemistry. CRC press

Helms, J.R., Mao, J., Schmidt-Rohr, K., Abdulla, H. and Mopper, K., 2013a. Photochemical flocculation of terrestrial dissolved organic matter and iron. Geochim. Cosmochim. Acta, 121(0): 398-413. http://dx.doi.org/10.1016/j.gca.2013.07.025

Helms, J.R., Mao, J., Schmidt-Rohr, K., Abdulla, H. and Mopper, K., 2013b. Photochemical flocculation of terrestrial dissolved organic matter and iron. Geochim. Cosmochim. Acta, 121(0): 398-413. http://dx.doi.org/10.1016/j.gca.2013.07.025

Helms, J.R. et al., 2014. Loss of optical and molecular indicators of terrigenous dissolved organic matter during long-term photobleaching. Aqua. Sci., 76(3): 353-373

Helms, J.R. et al., 2013c. Photochemical bleaching of oceanic dissolved organic matter and its effect on absorption spectral slope and fluorescence. Mar. Chem., 155: 81-91

Helms, J.R. et al., 2008. Absorption spectral slopes and slope ratios as indicators of molecular weight, source, and photobleaching of chromophoric dissolved organic matter. Limnol. Oceanogr., 53(3): 955

Hernes, P.J. and Benner, R., 2002. Transport and diagenesis of dissolved and particulate terrigenous organic matter in the North Pacific Ocean. Deep-Sea Res. Part I –

Oceanogr. Res. Papers, 49(12): 2119-2132. http://dx.doi.org/10.1016/S0967-0637(02)00128-0

Hernes, P.J., Kaiser, K., Dyda, R.Y. and Cerli, C., 2013. Molecular Trickery in Soil Organic Matter: Hidden Lignin. Environ. Sci. Technol., 47(16): 9077-9085. http://dx.doi.org/10.1021/es401019n

Hernes, P.J., Robinson, A.C. and Aufdenkampe, A.K., 2007. Fractionation of lignin during leaching and sorption and implications for organic matter "freshness". Geophys. Res. Letters, 34(17)

Hoigné, J., Faust Bruce, C., Haag Werner, R., Scully Frank, E. and Zepp Richard, G., 1988. Aquatic Humic Substances as Sources and Sinks of Photochemically Produced Transient Reactants, Aquatic Humic Substances. Advances in Chemistry. American Chemical Society, pp. 363-381. http://dx.doi.org/10.1021/ba-1988-0219.ch023

Ishii, S.K.L. and Boyer, T.H., 2012. Behavior of Reoccurring PARAFAC Components in Fluorescent Dissolved Organic Matter in Natural and Engineered Systems: A Critical Review. Environ. Sci. Technol., 46(4): 2006-2017. http://dx.doi.org/10.1021/es2043504

Kaiser, K. and Benner, R., 2011. Characterization of lignin by gas chromatography and mass spectrometry using a simplified CuO oxidation method. Anal. Chem., 84(1): 459-464. http://dx.doi.org/10.1021/ac202004r

Kaiser, K., Guggenberger, G., Haumaier, L. and Zech, W., 2001. Seasonal variations in the chemical composition of dissolved organic matter in organic forest floor layer leachates of old-growth Scots pine (Pinus sylvestris L.) and European beech

(Fagus sylvatica L.) stands in northeastern Bavaria, Germany. Biogeochem., 55(2): 103-143. http://dx.doi.org/10.1023/A:1010694032121

Kaiser, K., Guggenberger, G. and Zech, W., 1996. Sorption of DOM and DOM fractions to forest soils. Geoderma, 74(3–4): 281-303. http://dx.doi.org/10.1016/S0016-7061(96)00071-7

Klapper, L. et al., 2002. Fulvic acid oxidation state detection using fluorescence spectroscopy. Environ. Sci. Technol., 36(14): 3170-3175

Klíčová, Ĺ. et al., 2012. Adiabatic Triplet State Tautomerization of p-Hydroxyacetophenone in Aqueous Solution. J. Phys. Chem. A, 116(11): 2935-2944. http://dx.doi.org/10.1021/jp3011469

Knuutinen, J. and Mannila, J., 1991. High-performance liquid chromatographic study on oxidation products of lignin and humic substances. Water Sci. Technol., 24(3-4): 437-440

Kögel, I. and Bochter, R., 1985. Characterization of lignin in forest humus layers by high-performance liquid chromatography of cupric oxide oxidation products. Soil Biol. Biochem., 17(5): 637-640. http://dx.doi.org/10.1016/0038-0717(85)90040-9

Koppenol, W. and Liebman, J.F., 1984. The oxidizing nature of the hydroxyl radical. A comparison with the ferryl ion (FeO2+). J. Phys. Chem., 88(1): 99-101

Lobbes, J.M., Fitznar, H.P. and Kattner, G., 2000. Biogeochemical characteristics of dissolved and particulate organic matter in Russian rivers entering the Arctic Ocean. Geochim. Cosmochim. Acta, 64(17): 2973-2983. http://dx.doi.org/10.1016/S0016-7037(00)00409-9

Lobbes, J.r.M., Fitznar, H.P. and Kattner, G., 1999. High-performance liquid chromatography of lignin-derived phenols in environmental samples with diode array detection. Anal. Chem., 71(15): 3008-3012

Loeff, I. and Stein, G., 1963. The radiation and photochemistry of aqueous solutions of benzene. J. Chem. Soc. 489: 2623-2633

Louchouarn, P., Opsahl, S. and Benner, R., 2000. Isolation and Quantification of Dissolved Lignin from Natural Waters Using Solid-Phase Extraction and GC/MS. Anal. Chem., 72(13): 2780-2787. http://dx.doi.org/10.1021/ac9912552

Mack, J. and Bolton, J.R., 1999. Photochemistry of nitrite and nitrate in aqueous solution: a review. J. Photochem. Photobiol. A Chem., 128(1): 1-13

Mague, T., Friberg, E., Hughes, D. and Morris, I., 1980. Extracellular release of carbon by marine phytoplankton; a physiological approach. Limnol. Oceanogr., 25(2): 262-279

Manciulea, A., Baker, A. and Lead, J.R., 2009. A fluorescence quenching study of the interaction of Suwannee River fulvic acid with iron oxide nanoparticles. Chemos., 76(8): 1023-1027

Matthews, R. and Sangster, D., 1965. Measurement by benzoate radiolytic decarboxylation of relative rate constants for hydroxyl radical reactions. J. Phys. Chem., 69(6): 1938-1946

Maurino, V., Borghesi, D., Vione, D. and Minero, C., 2008. Transformation of phenolic compounds upon UVA irradiation of anthraquinone-2-sulfonate. Photochem. Photobiol. Sci., 7(3): 321-327

McDonald, S., Bishop, A.G., Prenzler, P.D. and Robards, K., 2004. Analytical chemistry of freshwater humic substances. Anal. Chim. Acta., 527(2): 105-124

Mezyk, S.P., Neubauer, T.J., Cooper, W.J. and Peller, J.R., 2007. Free-radical-induced oxidative and reductive degradation of sulfa drugs in water: absolute kinetics and efficiencies of hydroxyl radical and hydrated electron reactions. J. Phys. Chem. A, 111(37): 9019-9024

Miller, C.J., Rose, A.L. and Waite, T.D., 2012. Hydroxyl radical production by H2O2-mediated oxidation of Fe (II) complexed by Suwannee River fulvic acid under circumneutral freshwater conditions. Environ. Sci. Technol., 47(2): 829-835

Miller, W.L. and Kester, D.R., 1988. Hydrogen peroxide measurement in seawater by (p-hydroxyphenyl) acetic acid dimerization. Anal. Chem., 60(24): 2711-2715

Minero, C. et al., 2007. Photochemincal processes involving nitrite in surface water samples. Aqua. Sci., 69(1): 71-85. http://dx.doi.org/10.1007/s00027-007-0881-6

Minor, E., Dalzell, B., Stubbins, A. and Mopper, K., 2007. Evaluating the photoalteration of estuarine dissolved organic matter using direct temperature-resolved mass spectrometry and UV-visible spectroscopy. Aqua. Sci., 69(4): 440-455. http://dx.doi.org/10.1007/s00027-007-0897-y

Molot, L.A., Hudson, J.J., Dillon, P.J. and Miller, S.A., 2005. Effect of pH on photo-oxidation of dissolved organic carbon by hydroxyl radicals in a coloured, softwater stream. Aqua. Sci., 67(2): 189-195

Mopper, K. and Kieber, D.J., 2000. Marine photochemistry and its impact on carbon cycling in: Mora, S., Demers, S., Vernet. M (Eds), The Effects of UV Radiation in the Marine Environment. Cambridge University, pp 101-129

Mopper, K. and Zhou, X., 1990. Hydroxyl Radical Photoproduction in the Sea and Its Potential Impact on Marine Processes. Science, 250(4981): 661-664. http://dx.doi.org/10.1126/science.250.4981.661

Mopper, K. et al., 1991. Photochemical degradation of dissolved organic carbon and its impact on the oceanic carbon cycle. Nature, 353(6339): 60-62

Moran, M.A. and Zepp, R.G., 1997. Role of photoreactions in the formation of biologically labile compounds from dissolved organic matter. Limnol. Oceanogr., 42(6): 1307-1316

Mostofa, K.G. et al., 2013. Photoinduced Generation of Hydroxyl Radical in Natural Waters. In: K.M.G. Mostofa, T. Yoshioka, A. Mottaleb and D. Vione (Eds), Photobiogeochemistry of Organic Matter. Environmental Science and Engineering. Springer Berlin Heidelberg, pp. 209-272. http://dx.doi.org/10.1007/978-3-642-32223-5_3

Murov, S.L., Carmichael, I. and Hug, G.L., 1993. Handbook of photochemistry. CRC Press

Murphy, K.R. et al., 2010. Measurement of dissolved organic matter fluorescence in aquatic environments: an interlaboratory comparison. Environ. Sci. Technol., 44(24): 9405-9412

Nakatani, N., Ueda, M., Shindo, H., Takeda, K. and Sakugawa, H., 2007. Contribution of the photo-Fenton reaction to hydroxyl radical formation rates in river and rain water samples. Anal. Sci., 23(9): 1137-1142

Ononye, A.I. and Bolton, J.R., 1986. Mechanism of the photochemistry of p-benzoquinone in aqueous solutions. 2. Optical flash photolysis studies. J. Phys. Chem., 90(23): 6270-6274

Ononye, A.I., McIntosh, A.R. and Bolton, J.R., 1986. Mechanism of the photochemistry of p-benzoquinone in aqueous solutions. 1. Spin trapping and flash photolysis electron paramagnetic resonance studies. J. Phys. Chem., 90(23): 6266-6270

Opsahl, S. and Benner, R., 1995. Early diagenesis of vascular plant tissues: lignin and cutin decomposition and biogeochemical implications. Geochim. Cosmochim. Acta, 59(23): 4889-4904

Page, S.E., Arnold, W.A. and McNeill, K., 2010. Terephthalate as a probe for photochemically generated hydroxyl radical. J. Environ. Monit., 12(9): 1658-1665

Page, S.E., Arnold, W.A. and McNeill, K., 2011. Assessing the Contribution of Free Hydroxyl Radical in Organic Matter-Sensitized Photohydroxylation Reactions. Environ. Sci. Technol., 45(7): 2818-2825. http://dx.doi.org/10.1021/es2000694

Palmqvist, E. and Hahn-Hägerdal, B., 2000. Fermentation of lignocellulosic hydrolysates. II: inhibitors and mechanisms of inhibition. Bioresour. Technol., 74(1): 25-33

Phillips, D., Moore, J.N. and Hester, R.E., 1986. Time-resolved resonance Raman spectroscopy applied to anthraquinone photochemistry. J. Chem. Soc., Faraday Trans., 82(12): 2093-2104

Pochon, A. et al., 2002. Photochemical Oxidation of Water by 2-Methyl-1,4-benzoquinone: Evidence against the Formation of Free Hydroxyl Radical. J. Phys. Chem. A, 106(12): 2889-2894. http://dx.doi.org/10.1021/jp012856b

Powell, R.T. and Wilson-Finelli, A., 2003. Photochemical degradation of organic iron complexing ligands in seawater. Aqua. Sci., 65(4): 367-374

Pozdnyakov, I.P., Plyusnin, V.F., Grivin, V.P. and Oliveros, E., 2015. photochemistry of Fe (III) complexes with salicylic acid derivatives in aqueous solutions. J. Photochem. and Photobiol. A: Chem., 307: 9-15. http://dx.doi.org/10.1016/j.jphotochem.2015.03.018

Pullin, M.J., Anthony, C. and Maurice, P.A., 2007. Effects of iron on the molecular weight distribution, light absorption, and fluorescence properties of natural organic matter. Environ. Engi. Sci., 24(8): 987-997

Pullin, M.J., Bertilsson, S., Goldstone, J.V. and Voelker, B.M., 2004. Effects of sunlight and hydroxyl radical on dissolved organic matter: Bacterial growth efficiency and production of carboxylic acids and other substrates. Limnol. Oceanogr., 49(6): 2011-2022

Qian, J., Mopper, K. and Kieber, D.J., 2001. Photochemical production of the hydroxyl radical in Antarctic waters. Deep Sea Res. Part I: Oceanogr. Res. Papers,, 48(3): 741-759. http://dx.doi.org/10.1016/S0967-0637(00)00068-6

Rue, E.L. and Bruland, K.W., 1995. Complexation of iron (III) by natural organic ligands in the Central North Pacific as determined by a new competitive ligand equilibration/adsorptive cathodic stripping voltammetric method. Mar. Chem., 50(1): 117-138

Sharpless, C.M. and Blough, N.V., 2014. The importance of charge-transfer interactions in determining chromophoric dissolved organic matter (CDOM) optical and photochemical properties. Environ. Sci. Processes Impacts, 16(4): 654-671

Shiller, A.M., Duan, S., van Erp, P. and Bianchi, T.S., 2006. Photo‐oxidation of dissolved organic matter in river water and its effect on trace element speciation. Limnol. Oceanogr., 51(4): 1716-1728

Sleighter, R.L. and Hatcher, P.G., 2008. Molecular characterization of dissolved organic matter (DOM) along a river to ocean transect of the lower Chesapeake Bay by ultrahigh resolution electrospray ionization Fourier transform ion cyclotron resonance mass spectrometry. Mar. Chem., 110(3): 140-152

Southworth, B.A. and Voelker, B.M., 2003. Hydroxyl Radical Production via the Photo-Fenton Reaction in the Presence of Fulvic Acid. Environ. Sci. Technol., 37(6): 1130-1136. http://dx.doi.org/10.1021/es020757l

Spencer, R.G. et al., 2010. Comparison of XAD with other dissolved lignin isolation techniques and a compilation of analytical improvements for the analysis of lignin in aquatic settings. Org. Geochem., 41(5): 445-453

Spencer, R.G., Aiken, G.R., Wickland, K.P., Striegl, R.G. and Hernes, P.J., 2008. Seasonal and spatial variability in dissolved organic matter quantity and composition from the Yukon River basin, Alaska. Global Biogeochem. Cycles, 22(4)

Spencer, R.G. et al., 2009a. Photochemical degradation of dissolved organic matter and dissolved lignin phenols from the Congo River. J.Geophys. Res. Biogeosci (2005–2012), 114(G3)

Spencer, R.G.M. et al., 2012. An initial investigation into the organic matter biogeochemistry of the Congo River. Geochimica et Cosmochimica Acta, 84(0): 614-627.http://dx.doi.org/10.1016/j.gca.2012.01.013

Spencer, R.G.M. et al., 2009b. Photochemical degradation of dissolved organic matter and dissolved lignin phenols from the Congo River. J. Geophys. Res. Biogeosci., 114(G3): G03010. http://dx.doi.org/10.1029/2009JG000968

Standley, L.J. and Kaplan, L.A., 1998. Isolation and analysis of lignin-derived phenols in aquatic humic substances: improvements on the procedures. Organic Geochem., 28(11): 689-697. http://dx.doi.org/10.1016/S0146-6380(98)00041-2

Stedmon, C.A. and Bro, R., 2008. Characterizing dissolved organic matter fluorescence with parallel factor analysis: a tutorial. Limnol. Oceanogr. Methods, 6: 572-579

Steinberg, S., Venkatesan, M. and Kaplan, I., 1984. Analysis of the products of the oxidation of lignin by CuO in biological and geological samples by reversed-phase high-performance liquid chromatography. J. Chromatogr. A, 298: 427-434. http://dx.doi.org/10.1016/S0021-9673(01)92740-2

Stubbins, A. et al., 2008. Relating carbon monoxide photoproduction to dissolved organic matter functionality. Environ. Sci. Technol., 42(9): 3271-3276

Sun, L., Chen, H., Abdulla, H.A. and Mopper, K., 2014. Estimating hydroxyl radical photochemical formation rates in natural waters during long-term laboratory irradiation experiments. Environ. Sci. Processes Impacts, 16(4): 757-763. http://dx.doi.org/10.1039/C3EM00587A

Takeda, K., Takedoi, H., Yamaji, S., Ohta, K. and Sakugawa, H., 2004. Determination of hydroxyl radical photoproduction rates in natural waters. Anal. Sci., 20(1): 153-158

Tangen, G., Wickstrøm, T., Lierhagen, S., Vogt, R. and Lund, W., 2002. Fractionation and determination of aluminum and iron in soil water samples using SPE cartridges and ICP-AES. Environ. Sci. Technol., 36(24): 5421-5425

Vaughan, P.P. and Blough, N.V., 1998. Photochemical Formation of Hydroxyl Radical by Constituents of Natural Waters. Environ. Sci. Technol., 32(19): 2947-2953. http://dx.doi.org/10.1021/es9710417

Vermilyea, A.W. and Voelker, B.M., 2009. Photo-Fenton reaction at near neutral pH. Environ. Sci. Technol., 43(18): 6927-6933

Viollier, E., Inglett, P., Hunter, K., Roychoudhury, A. and Van Cappellen, P., 2000. The ferrozine method revisited: Fe (II)/Fe (III) determination in natural waters. Appl. Geochem., 15(6): 785-790

Vione, D. et al., 2006. Sources and sinks of hydroxyl radicals upon irradiation of natural water samples. Environ. Sci. Technol., 40(12): 3775-3781

Vione, D. et al., 2010. Comparison of different probe molecules for the quantification of hydroxyl radicals in aqueous solution. Environ. Chem. Letters, 8(1): 95-100. http://dx.doi.org/10.1007/s10311-008-0197-3

Voelker, B.M., Morel, F.M. and Sulzberger, B., 1997. Iron redox cycling in surface waters: effects of humic substances and light. Environ. Sci. Technol., 31(4): 1004-1011

Vulpius, D., Geipel, G. and Bernhard, G., 2010. Excited-state proton transfer of 3-hydroxybenzoic acid and 4-hydroxybenzoic acid. Spectrochim. Acta, Part A, 75(2): 558-562

Waggoner, D.C., Chen, H., Willoughby, A.S. and Hatcher, P.G., 2015. Formation of black carbon-like and alicyclic aliphatic compounds by hydroxyl radical initiated degradation of lignin. Organic Geochem., 82: 69-76

Weishaar, J.L. et al., 2003. Evaluation of specific ultraviolet absorbance as an indicator of the chemical composition and reactivity of dissolved organic carbon. Environ. Sci. Technol., 37(20): 4702-4708. http://dx.doi.org/10.1021/es030360x

White, E., Vaughan, P. and Zepp, R., 2003. Role of the photo-Fenton reaction in the production of hydroxyl radicals and photobleaching of colored dissolved organic matter in a coastal river of the southeastern United States. Aqua. Sci., 65(4): 402-414. http://dx.doi.org/10.1007/s00027-003-0675-4

Wilkinson, F., Helman, W.P. and Ross, A.B., 1995. Rate constants for the decay and reactions of the lowest electronically excited singlet state of molecular oxygen in solution. An expanded and revised compilation. J. Phys. Chem. Ref. Data, 24: 663

Xu, H. and Jiang, H., 2013. UV-induced photochemical heterogeneity of dissolved and attached organic matter associated with cyanobacterial blooms in a eutrophic freshwater lake. Water Res., 47(17): 6506-6515. http://dx.doi.org/10.1016/j.watres.2013.08.021

Yamashita, Y., Jaffé, R., Maie, N. and Tanoue, E., 2008. Assessing the dynamics of dissolved organic matter (DOM) in coastal environments by excitation emission matrix fluorescence and parallel factor analysis (EEM‐PARAFAC). Limnol. Oceanogr., 53(5): 1900-1908

Yoshizawa, K., Shiota, Y. and Yamabe, T., 1998. Methane−Methanol Conversion by
     MnO+, FeO+, and CoO+: A Theoretical Study of Catalytic Selectivity. JACS,
     120(3): 564-572. http://dx.doi.org/10.1021/ja971723u

Zepp, R.G., Faust, B.C. and Hoigne, J., 1992. Hydroxyl radical formation in aqueous
     reactions (pH 3-8) of iron (II) with hydrogen peroxide: the photo-Fenton reaction.
     Environ. Sci. Technol., 26(2): 313-319

Zepp, R.G., Hoigne, J. and Bader, H., 1987. Nitrate-induced photooxidation of trace
     organic chemicals in water. Environ. Sci. Technol., 21(5): 443-450.
     http://dx.doi.org/10.1021/es00159a004

Zhou, X. and Mopper, K., 1990. Determination of photochemically produced hydroxyl
     radicals in seawater and freshwater. Mar. Chem., 30(0): 71-
     88.http://dx.doi.org/10.1016/0304-4203(90)90062-H

Zlotnik, I. and Dubinsky, Z., 1989. The effect of light and temperature on DOC excretion
     by phytoplankton. Limnol. Oceanogr., 34(5): 831-839

APPENDIX A

COPYRIGHTS PERMISSIONS

Permission for Chapter II and Chapter III part 1, which contain the Environmental Science: Processes & Impacts article, published by Royal Society of Chemistry

Authors of articles in our journals or chapters in our books do not need to formally request permission to reproduce their article or book chapter in their thesis or dissertation. For all cases of reproduction the correct acknowledgement should be given in the caption of the reproduced material. The acknowledgement depends on the publication in which the material was published. The form of the acknowledgement to be included in the caption can be found on the page entitled *Acknowledgements to be used by RSC authors*.

(see http://www.rsc.org/Publishing/copyright/permission-requests.asp)

Permission for Chapter V, which contain the Limnology and Oceanography: Methods article, published by Wiley Online Library

Details and publisher terms and conditions are available by the link below:

http://s100.copyright.com/CustomerAdmin/PLF.jsp?ref=9f3e9ae6-d70f-41f7-a37e-1b3bff7080a8

This Agreement between luni sun ("You") and John Wiley and Sons ("John Wiley and Sons") consists of your license details and the terms and conditions provided by John Wiley and Sons and Copyright Clearance Center.

License Number	3634331279152
License date	May 22, 2015

Licensed Content Publisher	John Wiley and Sons
Licensed Content Publication	Limnology and Oceanography: Methods
Licensed Content Title	A comparison of a simplified cupric oxide oxidation HPLC method with the traditional GC-MS method for characterization of lignin phenolics in environmental samples
Licensed Content Author	Luni Sun,Robert G. M. Spencer,Peter J. Hernes,Rachael Y. Dyda,Kenneth Mopper
Licensed Content Date	Jan 28, 2015
Pages	8
Type of use	Dissertation/Thesis
Requestor type	Author of this Wiley article
Format	Electronic
Portion	Full article
Will you be translating?	No
Title of your thesis / dissertation	STUDY OF PHOTOCHEMICAL FORMATION OF HYDROXYL RADICAL IN NATURAL WATERS
Expected completion date	Aug 2015
Expected size (number of pages)	120

APPENDIX B

ABBREVIATIONS AND ACRONYMS USED

Ad/Al: acid to aldehyde ratios

Ar: argon

C: carbon

CAD: *p*-coumaric acid

Cu: copper

C/V: cinnamyl to vanillyl phenols ratio

d: day

DB: Dabob Bay

DFOM: desferrioxamine mesylate

DHBA: dihydroxybenzoic acid

DOC: dissolved organic carbon

DOI: digital object indentifier

DOM: dissolved organic matter

DS; Dismal Swamp

EEMS: excitation-emission matrix fluorescence

EPR: electron paramagnetic resonance

EVAL: Ethyl vanillin

FAD: ferulic acid

Fe: iron

FFe: free Fe

GC: gas chromatography

h: hour

H: hydrogen

H_2O_2: hydrogen peroxide

HBA: hydroxybenzoic acid

HPLC: high performance liquid chromatography

IHSS: Suwannee River fulvic acid reference standard

KHP: Potassium hydrogen phthalate

$K_{sp:}$ solubility constant

LMCT: ligand to metal charge transfer

LOD: limit of detection

min: minute

MS: mass spectroscopy

N: nitrogen

O: oxygen

•OH: hydroxyl radical

$O^{•-}$: superoxide ion

OFe: organically-complexed Fe

PAD: *p*-hydroxybenzoic acid

PAL: *p*-hydroxybenzaldehyde

PARAFAC: parallel factor analysis

PFe: particulate Fe

PN: pooled number

POM: particulate organic matter

PON: p-hydroxyacetophenone

PRSE: pooled relative standard errors

RS: resorcinol

SA: salicylic acid

SAD: syringic acid

SAL: syringaldehyde

SON: acetosyringone

SPE: solid phase extraction

S_R: slope ratio

S/V: syringyl to vanillyl phenols ratio

$\sum_8$: total eight phenols

TDN: total dissolved nitrogen

TOC: total organic carbon

v: volume

VAD: vanillic acid

VAL: vanillin

VON: acetovanillone

VITA

LUNI SUN

Department of Chemistry and Biochemistry

Old Dominion University

Norfolk

VA23529

EDUCATION

Ph.D., Chemistry,   Old Dominion University, Norfolk, USA   08/2009-present

M.S., Marine Chemistry, Ocean University of China, Qingdao, China   09/2006-06/2009

B.S., Chemistry,   Ocean University of China, Qingdao, China   09/2002-06/2006

PRESENTATIONS

(1)Poster: Determination of Ammonium in Natural Waters in Gordon Conference, NH, 2011

(2)Poster: A Simplified CuO Oxidation Method for Characterization of Lignin Phenolics in Environmental Samplesin ASLO Conference, LA, 2013

(3)Oral: High Precision TOC/DOC Analyzer with a NM Detection Limit in ASLO Conference, LA, 2013

(4)Poster: Estimating hydroxyl radical photochemical formation rates in natural waters during long-term laboratory irradiation experimentsin GRAD day event, Norfolk, 2014